DECIPHERING THE "POLARITY CODE": THE MECHANISM OF PAR COMPLEX SUBSTRATE POLARIZATION

by

MATTHEW JOHNSON BAILEY

A DISSERTATION

Presented to the Department of Chemistry and Biochemistry
and the Graduate School of the University of Oregon
in partial fulfillment of the requirements
for the degree of
Doctor of Philosophy

March 2017

DISSERTATION APPROVAL PAGE

Student: Matthew Johnson Bailey

Title: Deciphering the "Polarity Code": the Mechanism of Par Complex Substrate Polarization

This dissertation has been accepted and approved in partial fulfillment of the requirements for the Doctor of Philosophy degree in the Department of Chemistry and Biochemistry by:

Tom Stevens	Chairperson
Kenneth Prehoda	Advisor
Bruce Bowerman	Core Member
Bradley Nolen	Core Member
Victoria Herman	Institutional Representative

and

Scott L. Pratt	Dean of the Graduate School

Original approval signatures are on file with the University of Oregon Graduate School.

Degree awarded March 2017

DISSERTATION ABSTRACT

Matthew Johnson Bailey

Doctor of Philosophy

Department of Chemistry and Biochemistry

March 2017

Title: Deciphering the "Polarity Code": The Mechanism of Par Complex Substrate Polarization

Animal cells, as distinct as epithelia and migratory cells, have cell polarity that is defined by a common set of molecules. The Par complex polarizes the cortex of animal cells through the activity of atypical protein kinase C (aPKC). In this work, I aimed to determine the mechanism of aPKC substrate polarization and identify common characteristics of aPKC substrates that are polarized by phosphorylation. I found that several diverse Par-polarized proteins contain short highly basic and hydrophobic motifs that overlap with their aPKC phosphorylation sites. These Phospho-Regulated Basic and Hydrophobic (PRBH) motifs mediate plasma membrane localization by electrostatics-based phospholipid binding when unphosphorylated but are displaced into the cytoplasm when phosphorylated. To assess whether the Par complex polarizes other proteins by this mechanism, I developed an algorithm to identify potential PRBH motifs and score these linear motifs for basic and hydrophobic character, as well as the quality and number of aPKC phosphorylation sites. Using this algorithm, I identified numerous putative PRBH candidates in the fruit fly proteome and performed two screens of these candidates for Par-polarized proteins. The first screen focused on determining whether aPKC regulates cortical targeting of proteins that are reported to be polarized. This screen identified the

Rho GAP crossveinless-c (cv-c) to be a novel aPKC substrate and found that aPKC is sufficient to polarize cv-c in a reconstituted polarity assay. The second screen characterized the localization of putative PRBH motif-containing proteins *in vivo*. This screen identified a previously uncharacterized protein, CG6454, to be basolateral in epithelia; however, *ex vivo* experiments found it to have a Ca^{2+}-dependent and aPKC-independent membrane targeting mechanism. Overall this work identified a common mechanism for Par substrate polarization and used knowledge of this mechanism to identify a novel Par effector.

This dissertation contains previously published and unpublished co-authored material.

CURRICULUM VITAE

NAME OF AUTHOR: Matthew Johnson Bailey

GRADUATE AND UNDERGRADUATE SCHOOLS ATTENDED:

University of Oregon, Eugene
Juniata College, Huntingdon
University of Leeds, Leeds

DEGREES AWARDED:

Doctor of Philosophy, Chemistry and Biochemistry, 2017, University of Oregon
Master of Science, Chemistry, 2014, University of Oregon
Bachelor of Science, Biochemistry with a Secondary Emphasis in Philosophy, 2010, Juniata College

AREAS OF SPECIAL INTEREST:

Molecular Biology
Cell Biology
Biochemistry

PROFESSIONAL EXPERIENCE:

Graduate Research Fellow, Department of Chemistry and Biochemistry, University of Oregon, Eugene, Oregon, 2010-2017

Graduate Teaching Fellow, Department of Chemistry and Biochemistry, University of Oregon, Eugene, 2010-2011

GRANTS, AWARDS, AND HONORS:

Pete von Hippel Graduate Scholar Award, University of Oregon, 2015

Best Poster Award, Institute of Molecular Biology, University of Oregon, 2014

National Institutes of Health Molecular Biology and Biophysics Training Grant, University of Oregon, 2011-2014

PUBLICATIONS:

Bailey, M.J., and Prehoda, K.E. (2015). Establishment of Par-Polarized Cortical Domains via Phosphoregulated Membrane Motifs. Dev. Cell 35, 199–210.

Bailey, M.J., and Prehoda, K.E. The Par Complex Polarizes the RhoGAP Crossveinless-C by Phosphorylation. In Preparation.

Bailey, M.J., Estrella, A.M., and Prehoda, K.E. Drosophila CG6454 is a Calcium-Dependent Basolateral Protein. In Preparation.

ACKNOWLEDGMENTS

I would like to thank Dr. Ken Prehoda for his continual support through my graduate work. In many ways, Ken trained me to be a scientist and I am extremely grateful that he taught me to be think critically and to keep searching for big and interesting questions. Thank you to my committee for of Dr. Tom Stevens, Dr. Brad Nolen, Dr. Bruce Bowerman, and Dr. Tory Herman for their guidance and feedback through my graduate work. I must additionally thank Dr. Tom Stevens and the Molecular Biology and Biophysics Training Grant for funding several years of my graduate work. I never would have made it through graduate school without the amazing team of people in the Prehoda Lab. Specifically, I must thank Chiharu Graybill, Kimmy Jones, Michael Drummond, Ryan Holly, Oggie Golub, Michelle Lu, and Nicole Paterson. I had two excellent undergraduates, Alaní Estrella and Robert Lyle McPherson, who I must thank for their enthusiasm and assistance. Thanks to the members of the IMB community for being friendly and maintaining a supportive environment. Thanks to the friends I've had in Eugene, especially Andrew Wagner for being a total brah and spotting me, and Nicole Paterson for surrounding me with all the cats, chickens, and goats. Thank you, Sir Kinkytail McCuddlebottom, for cuddles, purrs, and for not eating my face when I was asleep. Thank you, Zack Thill, for his love and helping me become happier. My sister, Liz Gee, as well as Kevin Gee and their family for always being there for me. Lastly, I need to thank my parents, Rick and Janet Bailey for their endless enthusiasm and support.

To my family for their endless love and support

TABLE OF CONTENTS

Chapter Page

Chapter Page

Chapter Page

Chapter Page

LIST OF FIGURES

CHAPTER I

CELL POLARITY AND THE PAR COMPLEX: PARTITIONING OF THE CELL CORTEX IN ANIMALS

This chapter contains unpublished co-authored material with K.E. Prehoda. I wrote the manuscript and K.E. Prehoda provided editorial comments.

INTRODUCTION

The typical eukaryotic cell shown in Biology textbooks is symmetric, with little organization beyond the partitioning of components into organelles. However, many are characterized by an asymmetric distribution of specific molecules, a feature known as cell polarity (Goldstein and Macara, 2007; Knust and Bossinger, 2002). A few examples of polarized cells include epithelial cells, neural stem cells (neuroblasts), neurons, migratory cells, and some zygotes (Figure 1). The asymmetric distribution of proteins, lipids, and RNA defines the shapes of these cells, and in many cases, serves an important function. For instance, epithelial cells form an adherent sheet with their luminal and basal sides functionalized for distinct purposes (Rodriguez-Boulan and Macara, 2014) (Figure 2). The apical membrane of the gut epithelium is specialized for mucous secretion while the basal side has connections to the basement membrane. Neuroblasts polarize during mitosis to produce daughter cells with different molecular identities, directing one daughter cell to differentiate and the other to remain a neural stem cell (Fuerstenberg et

al., 2002). Migratory cells, such as the leukocytes of the immune system polarize to define their direction of motion (Mayor and Etienne-Manneville, 2016). These examples highlight some of the important functions of cell polarity that are unique to animals and function in dissimilar cell types.

Loss of cell polarity can have devastating effects during development and tissue maintenance, and these roles have been extensively reviewed elsewhere (Goldstein and Macara, 2007; Macara and McCaffrey, 2013). Previous studies have emphasized that a loss of cell polarity can cause dramatic developmental defects including embryonic lethality. In adults, loss of cell polarity can lead to tissue disorganization, resulting in loss of function and an increased risk of cancer (Lee and Vasioukhin, 2008). Due to the

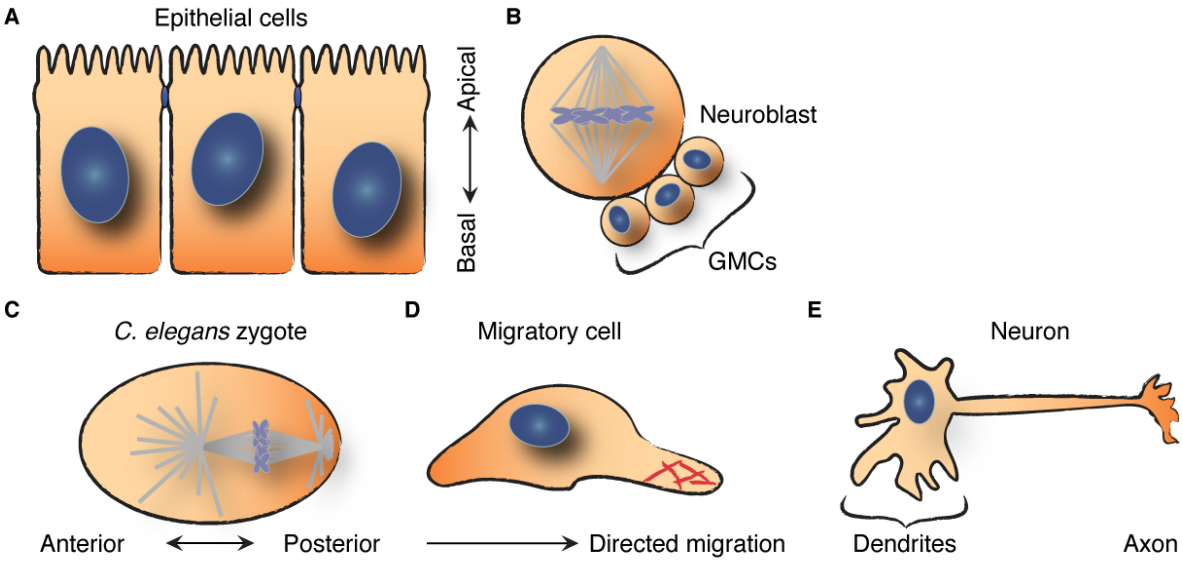

Figure 1. Polarized cells in animals. (A) Epithelial cells form a sheet that is selectively permeable. (B) *Drosophila* neuroblasts establish apical-basal polarity during mitosis such that on daughter cell remains a neuroblast while the other differentiates to a neuronal precursor cell, or a ganglion mother cell (GMC). (C) The *C. elegans* zygote establishes anterior-posterior polarity during the first cellular division. This causes the resulting daughter cells to have distinct identities. (D) Migratory cells, such as astrocytes polarize to use their cytoskeleton (red) for directed migration. (E) Neurons have axonal-dendritic polarity.

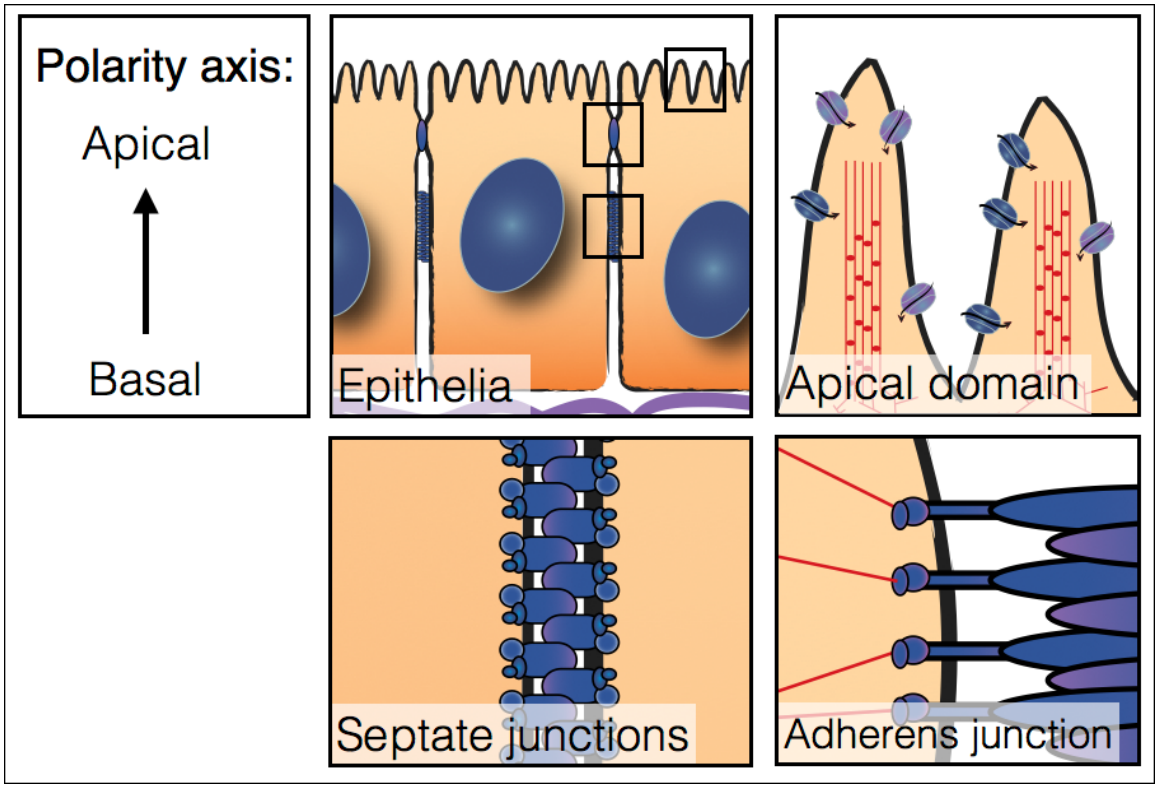

Figure 2. Cell polarity allows cortical domains to perform specialized functions. Polarization of molecules in epithelial cells serves functions such as forming a barrier that is only permeable to small molecules (septate junctions), selective ion transport (apical domain) and cell-cell adhesion (adherens junctions). F-actin based structures are red.

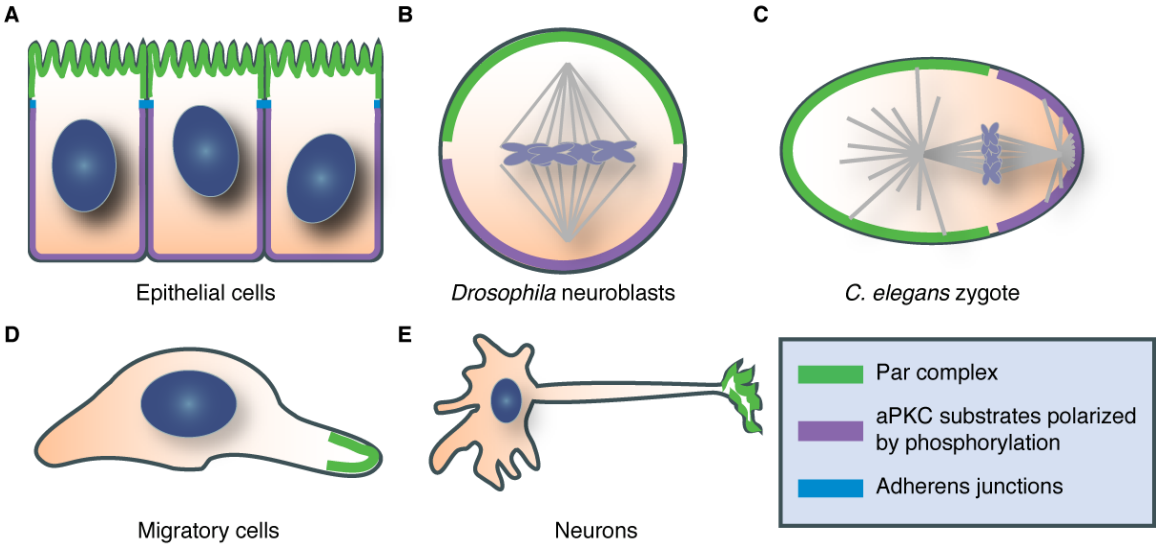

Figure 3. Cortical polarity domains of the Par complex and its substrates. (A-E) Polarized cells have mutually exclusive cortical domains for the Par complex (green) and its substrates (purple). In epithelial cells, these domains are separated by adherens junctions (blue).

associations between the loss of cell polarity and cancer, biopsies often use loss of cell polarity as a biomarker for malignant cancers. The essential role of cell polarity in animal health and viability make it vital to understand its molecular mechanisms.

The metazoan cell cortex is polarized into membrane-associated protein complexes

While polarized cells have widely divergent morphologies, they have many molecular similarities that are likely related to the mechanisms that control animal cell polarity (Goldstein and Macara, 2007; Knust and Bossinger, 2002). The cell cortex of polarized metazoan cells is organized into molecularly distinct domains, which I will refer to as polarity domains (Figure 3). The protein contents of these polarity domains serve important cell type-specific purposes, such as the physical connections between epithelial cells that are formed by adherens and septate junctions. Neuroblasts have a simple two domain polarity system with apical and basal domains occupying opposite and mutually exclusive cortical domains (Prehoda, 2009). In the *C. elegans* zygote and the *Drosophila* oocyte, the two polarity domains are oriented along anterior-posterior axis (2003). Epithelia have a more complex polarity that include apical, basolateral, and junctional domains (Flores-Benitez and Knust, 2016). The apical domain of many epithelial cells, such as a columnar epithelium, is highly ciliated. The lateral region includes junctions, including adherens junctions and septate junctions in *Drosophila.* These junctions connect a cell to its neighbors in the epithelial sheet. The basal region often has connections to the underlying basement membrane. In these polarized cells, loss of specific molecules from a polarity domain can prevent the assembly of a polarity domain and cause the cell to depolarize.

The Partitioning-defective (Par) complex plays an essential role in polarizing many cell types and has conserved importance across metazoa (Knust and Bossinger, 2002; Nance, 2005; Welchman et al., 2007). It does so by localizing to the apical domain of neuroblasts and epithelia, where it directs genetically downstream molecules to their respective polarity domains. Par complex apical localization is essential for many proteins to become polarized to the basal and basolateral domains.

Mechanisms to localize and activate the Par complex

When the Par complex is localized to the apical membrane, it can direct genetically downstream proteins to their proper cortical domain. The Par complex consists of the protein kinase atypical protein kinase C (aPKC), Par-6, and Cdc42. Genetically upstream proteins, including Par-3 (*Drosophila* Bazooka, Baz) recruit the Par complex to the cell cortex (Etemad-Moghadam et al., 1995; Kuchinke et al., 1998). The role of Baz/Par-3 in recruiting the Par complex to the apical domain is of particular importance in *Drosophila* neuroblasts and immature epithelia, where aPKC, Par-6, and Baz/Par-3 colocalize in the apical domain (Wodarz et al., 2000). However, aPKC targets Baz/Par-3 to adherens junctions by phosphorylation in mature epithelia (Hurd et al., 2003; Izumi et al., 1998; Morais-de-Sá et al., 2010). The Rho GTPase, Cdc42, regulates the localization and activity of aPKC through its GTPase activity and protein-protein interactions with Par-6 (Atwood et al., 2007; Joberty et al., 2000; Lin et al., 2000). aPKC and Par-6 are closely associated and colocalize in neuroblasts, epithelia, neurons, and other polarized cell types (Joberty et al., 2000; Lin et al., 2000; Rolls, 2003; Watts et al., 1996). Par-6 serves as an essential link between aPKC and Cdc42. aPKC/Par-6 binds

GTP-bound Cdc42, which activates aPKC kinase activity at the apical membrane. The multiple interactions between aPKC, Par-6 and Cdc42 ensure that aPKC localization is coupled to its activation. It is essential to couple polarized localization on the plasma membrane to activation as ectopic kinase activity can have devastating effects on cell polarity by targeting aPKC substrates to the wrong region of a polarized cell.

The Par complex polarizes substrates by phosphorylation

Once localized and activated, the Par complex is poised to target downstream proteins to their proper polarity domain. Prior studies have emphasized that many proteins polarized by the Par complex are substrates of aPKC, these include Crumbs, Lethal (2) giant larvae (Lgl), Miranda (Mira), Numb, Par-1, PAR-2, and Baz/Par-3 (Atwood and Prehoda, 2009; Betschinger et al., 2003; Hao et al., 2006; Hurov et al., 2004; Smith et al., 2007; Sotillos, 2004; Suzuki et al., 2004). Lgl, Mira, Numb, Par-1, and PAR-2 are excluded from the Par cortical domain by phosphorylation (Figure 4). However, other Par substrates respond differently to phosphorylation. Phosphorylation removes Baz from the apical domain of epithelia, but not neuroblasts

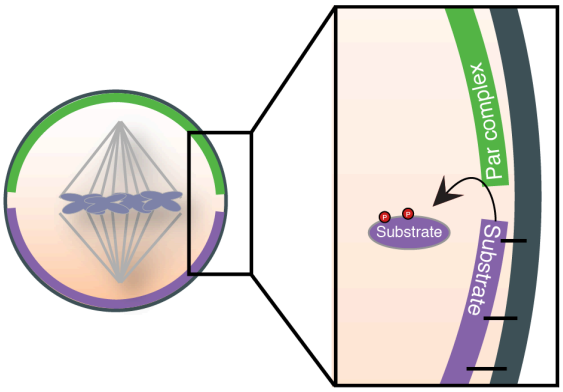

Figure 4. The Par complex polarizes its substrates by phosphorylation-induced cortical displacement. Phosphorylation inhibits localization of these substrates to the apical domain occupied by the Par complex. Substrates polarized by this mechanism include Lgl, Mira, Numb, Par-1, and PAR-2.

(Morais-de-Sá et al., 2010; Wodarz et al., 2000). Alternately, phosphorylation stabilizes Crumbs apical localization (Sotillos, 2004). However, a substrate polarization mechanism that can be generalized to multiple Par substrates has not been identified.

Intriguingly, phosphorylation has been shown to inhibit cortical localization of several aPKC substrates polarized by phosphorylation (Atwood and Prehoda, 2009; Betschinger et al., 2003; Hao et al., 2006; Hurov et al., 2004; Smith et al., 2007; Suzuki et al., 2004). In cell culture experiments with Lgl, Mira, Numb, human Par-1b and PAR-2, the substrate localized to the cell cortex when aPKC was absent, but co-transfection

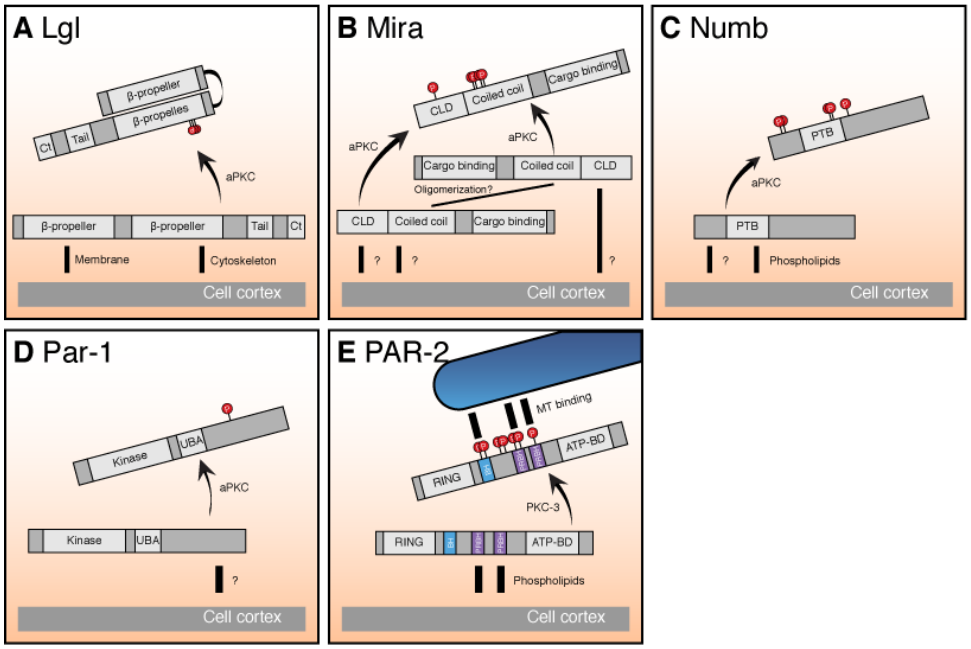

Figure 5. Cortical targeting mechanisms of aPKC substrates. (A) Lgl localizes to the cell cortex by binding the membrane and the actomyosin cytoskeleton. aPKC is proposed to regulate autoinhibition. Ct, COOH-terminus. (B) Mira localizes to the cell cortex by its NH2-terminus, which includes the cortical localization domain (CLD) and part of its coiled coil region. (C) Numb localizeds to the cell cortex by its NH2-terminus and its Phosphotyrosine binding domain (PTB). (D) Par-1 localizes to the cell cortex via its COOH-terminus. UBA, Ubiquitin associated domain. (E) PAR-2 binds membrane phospholipids with its two Phospho-Regulated Basic and Hydrophobic (PRBH, purple) motifs. These PRBH motifs and a Basic and Hydrophobic (BH, blue) motif also bind microtubules (MTs) and PKC-3 phosphorylation does not inhibit MT binding.

with aPKC caused the substrate to localize to the cytoplasm. These studies identified specific non-phosphorylatable (i.e. phosphodead) mutants that aPKC cannot displace from the cell cortex. These studies have also demonstrated that aPKC cannot polarize these phosphodead mutants *in vivo*, suggesting that displacement of a substrate from the cell cortex is an essential step of polarization.

Cortical localization mechanisms of polarized Par substrates

Several findings have implicated the cytoskeleton and membrane lipids in localizing aPKC substrates to the cell cortex (Figure 5). Here I will summarize the literature on the cortical targeting mechanisms of aPKC substrates for which phosphorylation inhibits cortical targeting. This section discusses how each substrate localizes to the cell cortex and the role of phosphorylation in substrate polarization.

Lgl is reported to interact with the actomyosin cytoskeleton

The neoplastic tumor suppressor Lgl has a critical role in cell polarity, but its function and regulation largely remain enigmatic (Vasioukhin, 2006). Early work to characterize the localization mechanism of Lgl focused on its interactions with the cytoskeleton (Figure 5A). Strand *et al*. found Lgl to be a homo-oligomer that binds to non-muscle myosin II and proposed that it regulates the cytoskeleton (NMY-II) (Strand et al., 1994a, 1994b). Conservation of these interactions was later shown by the work of Betschinger *et al*., where experiments with a series of deletion constructs indicated that the COOH-terminus of *Drosophila* Lgl binds NMY-II (Betschinger et al., 2005). They also showed that this interaction is regulated by an intramolecular inhibitory interaction

between the NH2- and COOH-terminus of Lgl. Additionally, aPKC phosphorylation of Lgl was shown to relieve this autoinhibition and allow Lgl to bind myosin. Some results of this study are contested, which have raised doubts that actomyosin mediates Lgl cortical targeting. Recently, Dong *et al*. were unable to reproduce the finding that actin was necessary for Lgl to localize to the cell cortex (Dong et al., 2015). Further studies are needed to verify the cortical targeting mechanism of Lgl.

The cortical targeting mechanism of Mira is uncharacterized

The neuronal fate determinant Mira initiates neuronal fate changes by regulating the localization of its binding partners. Structure-function studies found that the NH2-terminus (residues 1-290) of Mira is necessary and sufficient for its cortical targeting and polarization in metaphase neuroblasts (Fuerstenberg et al., 1998; Shen et al., 1998) (Figure 5B). Sequence analysis of Mira identified a coiled-coil within this region, suggesting that oligomerization is necessary for cortical targeting (Fuerstenberg et al., 1998). Phosphorylation has been found to regulate Mira cortical targeting in several studies (Atwood and Prehoda, 2009; Sousa-Nunes et al., 2009; Zhang et al., 2015). aPKC phosphorylation of the NH2-terminus of Mira is essential for its polarization and cortical displacement (Atwood and Prehoda, 2009). Further studies are needed to identify the cortical targeting mechanism of Mira and determine how this is regulated by Mira.

Numb localizes to the cell cortex through protein and phospholipid binding

Numb is a fate determinant and conserved regulator of Notch signaling. Structure-function studies of Numb were first completed by the lab of Lily and Yuh Nung Jan, where they demonstrated that the NH2-terminus of *Drosophila* Numb, but not the phosphotyrosine binding (PTB) domain, is necessary for cortical targeting and polarization in neuroblasts (Frise et al., 1996; Knoblich et al., 1997) (Figure 5C). However, subsequent studies found Partner of Numb (Pon) binds the PTB domain and is sufficient for Numb polarization in neuroblasts when ectopically expressed in ectodermal cells (Lu et al., 1998). The details of how Numb and Pon regulate each other's polarization remains uncharacterized.

Phospholipids have been implicated in Numb cortical targeting. Characterization of mammalian Numb found that phospholipids mediate cortical targeting (Dho et al., 1999). The authors found that the PTB domain of mammalian Numb binds phospholipids and localizes it to the cell cortex. This study suggested that Numb has phospholipid binding sites outside the PTB domain, however, they have not yet been identified.

The role of aPKC phosphorylation to regulate cortical localization of Numb was first found in *C. elegans.* Zhang *et al*. found that NUM-1 (*C. elegans* Numb homolog) localizes to the cortex of cultured cells, but PKC-3 (*C. elegans* aPKC homolog) inhibits cortical targeting by site-specific phosphorylation (Zhang et al., 2001a, 2001b). A subsequent study found that this was conserved to flies and mammals (Smith et al., 2007). Furthermore, Smith *et al.* found that phosphorylation is necessary for Numb polarization *in vivo*. These studies have provided few mechanistic clues as to how phosphorylation induces Numb polarization.

Cortical targeting of Par-1 requires the actomyosin cytoskeleton

Par-1 is a key regulator of microtubules through phosphorylation of Tau and other microtubule-associated proteins (Drewes et al., 1997). Regulation of microtubules is a key downstream function of Par-1 in the polarization of cells including the *C. elegans* zygote and *Drosophila* oocyte (Doerflinger et al., 2006; Kemphues et al., 1988) but is unnecessary for its localization (Böhm et al., 1997; Vaccari et al., 2005) (Figure 5D). The COOH-terminus has a conserved role in cortical targeting and polarization (Doerflinger et al., 2006; Vaccari et al., 2005). This cortical targeting region contains a single aPKC phosphosite that mediates cortical displacement and polarization of Par-1 in metazoans (Hurov et al., 2004; Suzuki et al., 2004). The mechanism of Par-1 cortical targeting by the COOH-terminus remains uncharacterized, as does a role for phosphorylation in inhibiting cortical targeting.

PAR-2 localizes to the cell cortex by phospholipid binding

PAR-2 is a RING finger domain-containing protein that is unique to *C. elegans* and nematodes. Cortical targeting and polarization of PAR-2 depends on a central region that contains seven PKC-3 phosphorylation sites (Hao et al., 2006) (Figure 5E). Phosphorylation of these sites inhibits cortical displacement in cell culture and mediates posterior polarization of PAR-2 in the zygote (Hao et al., 2006). The cortical targeting region of PAR-2 was found to have multiple polybasic motifs for phospholipid and microtubule binding (Motegi et al., 2011). Interestingly, this study also demonstrated that phosphorylation inhibits phospholipid binding at these sites and that microtubule binding is inhibited to a lesser extent by phosphorylation. Importantly, this study provided the

first mechanistic evidence to demonstrate how aPKC phosphorylation polarizes a substrate on the cell cortex.

Knowledge gap: mechanisms to induce substrate polarization

How phosphorylation alters the activity and localization of aPKC substrates remains largely uncharacterized. Phosphorylation can alter a protein's activity by a variety of mechanisms, including alterations to structure, dynamics, and electrostatics. Prior studies have provided few mechanistic answers regarding how phosphorylation alters the localization of these substrates. Furthermore, it remains unclear why only a subset of aPKC substrates are polarized by phosphorylation (Etemad-Moghadam et al., 1995; Kuchinke et al., 1998; Schober et al., 1999; Wodarz et al., 1999). To identify the mechanisms of Par polarity, it is crucial to understand the principles by which phosphorylation induces substrate polarization.

To better understand the mechanisms of aPKC substrate polarization, I address the following outstanding questions:

- How do Par complex substrates localize to the cell cortex?
- How does the Par complex polarize its substrates?
- Are Par substrates polarized by a common mechanism?

Addressing these questions will provide insights into the molecular mechanisms that allow the Par complex to polarize proteins. I address these questions in Chapter II by finding Phospho-Regulated phospholipid binding sites on Lgl, Mira, and Numb. Chapter

III was published in volume 35 of the journal *Developmental Cell* in October 2015. I was the first author for this paper and I shared authorship with the principle investigator for this work, Ken Prehoda. Chapter III assesses whether aPKC polarizes other proteins to the basal or basolateral domain by phosphorylation of a putative phospholipid binding site and identifies Crossveinless-c (Cv-c) to be an aPKC substrate and Par-polarized protein. I expect that Chapter III will be published later this year. I am the first author for this work and I share authorship with Kenneth Prehoda, who was the principle investigator for this work. In Chapter IV, I describe a screen for basal and basolateral proteins *in vivo*. This work identifies CG6454 to localize to the basolateral domain of epithelial cells, although it has an aPKC-independent polarization mechanism. I expect that Chapter IV will be published later this year. I am the first author for this work, Alaní Estrella is second author, and Kenneth Prehoda was the principle investigator for this work. Chapter V is a summary and discussion of the findings described in this dissertation.

BRIDGE TO CHAPTER II

Above, I discussed the mechanisms of cell polarity and focused on protein polarization by the Par complex. I alluded to a gap in our understanding of how phosphorylation induces polarization of aPKC substrates. In the next chapter, I assess the cortical targeting and polarization mechanisms of the aPKC substrates Lgl, Mira, and Numb. This study determines how phosphorylation regulates cortical targeting of these substrates, and develops a method to identify additional aPKC substrates that are polarized by this mechanism.

CHAPTER II

ESTABLISHMENT OF PAR-POLARIZED CORTICAL DOMAINS VIA PHOSPHOREGULATED MEMBRANE MOTIFS

This work was published in volume 35 of Developmental Cell in 2015. I performed all experimental work. K.E. Prehoda and I performed the computer programming. K.E. Prehoda and I wrote this work. K.E. Prehoda was the principle investigator for this work.

SUMMARY

The Par polarity complex creates mutually exclusive cortical domains in diverse animal cells. Activity of the atypical protein kinase C (aPKC) is a key output of the Par complex as phosphorylation removes substrates from the Par domain. Here, we investigate how diverse, apparently unrelated Par substrates couple phosphorylation to cortical displacement. Each protein contains a basic and hydrophobic (BH) motif that interacts directly with phospholipids and also overlaps with aPKC phosphorylation sites. Phosphorylation alters the electrostatic character of the sequence, inhibiting interaction with phospholipids and the cell cortex. We searched for overlapping BH and aPKC phosphorylation site motifs (i.e., putative phosphoregulated BH motifs) in several animal proteomes. Candidate proteins with strong PRBH signals associated with the cell cortex but were displaced into the cytoplasm by aPKC. These findings demonstrate a potentially

general mechanism for exclusion of proteins from the Par cortical domain in polarized cells.

INTRODUCTION

Animal cells are polarized in remarkably diverse ways, such as the specialized apical cortex of a simple epithelium and the leading edge of motile cells (Knoblich, 2010; Overeem et al., 2015; Tepass, 2012). Although these cells are dramatically different, they are polarized by the same molecular machinery known as the Par complex (Goehring, 2014; Goldstein and Macara, 2007). The capacity of the Par complex to direct diverse cell polarities derives in part from its ability to act on a multitude of downstream proteins. For example, in asymmetrically dividing neural stem cells, the Par complex polarizes fate determinants (Betschinger et al., 2003; Knoblich, 2010), whereas in epithelia it organizes junctional components (Suzuki et al., 2001; Tepass, 2012). The characteristic adaptability of the Par complex to regulate distinct classes of proteins suggests that there may be a common mechanism by which it acts on downstream factors, yet little is known about how Par activity is coupled to substrate polarity. Knowledge of this mechanism is important not only for our basic understanding of Par-mediated polarity, but it might also allow for the identification of novel Par-regulated proteins and provide insight into the evolutionary pathways underlying the wide range of polarities found among metazoa.

The Par complex polarizes cells by creating and maintaining mutually exclusive cortical domains. Upstream factors that can be cell-type-specific define the Par domain (Cuenca et al., 2003; Harris and Peifer, 2005; Martin-Belmonte et al., 2007; Rolls, 2003; Schober et al., 1999; Wodarz et al., 1999), and downstream proteins are excluded from

this cortical area to create the substrate domain. While the Par complex can function through other mechanisms (Cline and Nelson, 2007; Stein et al., 2005; Zhang and Macara, 2006), a key output is the activity of atypical protein kinase C (aPKC). Proteins that are directly downstream of the Par complex are often aPKC substrates, and phosphorylation is both necessary and sufficient for cortical displacement and concomitant removal from the Par domain (Atwood and Prehoda, 2009; Betschinger et al., 2003; Hao et al., 2006; Hurov et al., 2004; Smith et al., 2007; Suzuki et al., 2004; Wirtz-Peitz et al., 2008; Zhang et al., 2001b). For proteins polarized by this mechanism, their phosphorylation must be coupled to release from the cortex. Although phosphorylation-coupled cortical release is critical to Par complex-mediated polarity, very little is known about the mechanisms by which Par substrates associate with the cortex and how phosphorylation is linked to this interaction. The lack of sequence homology or shared globular domain structure among Par substrates has made it difficult to identify a "polarity code."

The Par complex functions at the cell cortex, a complex organelle that includes the phospholipid bilayer and a meshwork of membrane-associated proteins and cytoskeletal elements beneath it (Engelman, 2005; Groves and Kuriyan, 2010; Morone et al., 2006). It has been unclear how these components might contribute to Par-mediated polarity, although actin polymerization is known to be required and protein-protein interactions have been implicated for certain substrates (Betschinger et al., 2005; Dho et al., 1999; Knoblich et al., 1997; Strand et al., 1994a). Direct lipid binding has only been demonstrated for Numb PTB domain, however, this is not sufficient for cortical localization (Dho et al., 1999). Given the complexity of the cell cortex and the potential

for diverse protein-phospholipid and protein-protein interactions, we set out to identify the interactions that retain Par-polarized proteins within their cortical domain and how aPKC phosphorylation regulates these cortical interactions to prevent entry into the Par domain.

RESULTS

Short, charged, hydrophobic motifs target Lgl, Mira, and Numb to the cell cortex

To determine if there might be a general mechanism of Par complex polarization, we selected three substrates with no apparent sequence homology or shared domain structure: Lgl, Mira, and Numb (Figure 6A–1A") (Betschinger et al., 2005; Dho et al., 2006; Fuerstenberg et al., 1998; Matsuzaki et al., 1998). Lgl and Numb each have protein interaction domains: β-propellers, a tomosyn homology region (THR), and a phosphotyrosine-binding (PTB) domain, but they are not sufficient for cortical association in *Drosophila* (Betschinger et al., 2005; Knoblich et al., 1997). Cortical localization of Mira is specified by its NH_2-terminal 1–290 amino acids (Fuerstenberg et al., 1998; Matsuzaki et al., 1998), which does not contain any recognizable globular domains. These three diverse Par complex substrates lack clear globular domains that would mediate interactions with the cortex or membrane (Lemmon, 2008). Short stretches of basic and hydrophobic (BH) amino acids are known to interact with the membrane, so we analyzed the basic and hydrophobic character of the sequences using

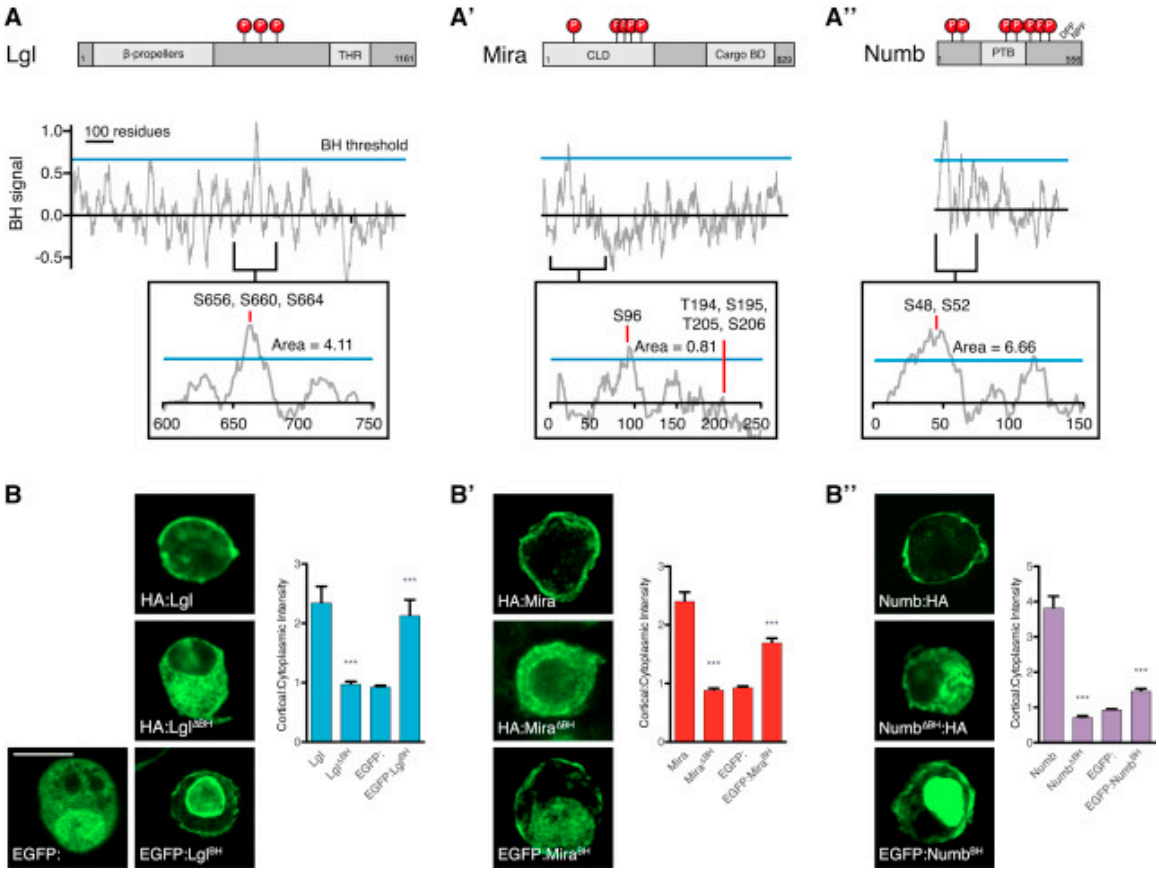

Figure 6. Lgl, Mira, and Numb Localize to the Cell Cortex through BH Motifs. (A–A") Domain architecture and Basic hydrophobic motif signal in Lgl (A), Mira (A'), and Numb (A"). BH motifs are defined by peaks with a BH signal >0.6 (denoted by blue line) and the peak area indicates the strength of the peak's BH character. aPKC phosphorylation sites are labeled. THR, tomosyn homology region; CLD, cortical localization domain; Cargo BD, cargo binding domain; PTB, phosphotyrosine binding domain; DPF, α-adaptin-binding motif; NPF, Eps15-binding motif. (B–B") BH motifs are necessary and sufficient for cortical targeting of Lgl (B), Mira (B'), and Numb (B"). The BH motif of Lgl (B), Mira (B'), and Numb (B") are necessary and sufficient for cortical targeting in S2 cells. Representative images of the localization are and the quantification

of the cortical to cytoplasmic intensity ratio (mean ± SEM). Non-parametric t test: ***p < 0.0001. Scale bar, 10 μm.

the BH scoring algorithm (Brzeska et al., 2010). Sequence windows with BH scores exceeding 0.6 are candidate phospholipid binding motifs and we found that Lgl, Mira, and Numb each contain a single region above this threshold (Figure 6A–1A″). Interestingly, each of these sequences overlaps with a known or predicted aPKC phosphorylation site (Atwood and Prehoda, 2009; Betschinger et al., 2003; Smith et al., 2007). We identified several aPKC sites with BH scores below the threshold, indicating that not all aPKC sites are BH motifs (see below for a more extensive comparison of BH motifs and the aPKC recognition sequence).

Given their short sequences, the BH scoring algorithm could have a high false positive rate, so we investigated whether the Lgl, Mira, and Numb BH motifs mediate cortical localization. Each of these proteins localizes to the cortex of cultured *Drosophila* S2 cells consistent with their ability to interact with the cortex opposite Par domains. Deletion of each protein's candidate BH motif caused a loss of cortical enrichment and strong cytoplasmic signal (Figure 6B–1B″). In some cases, BH motifs often require additional multivalent interactions to associate with the membrane (Papayannopoulos et al., 2005; Swierczynski and Blackshear, 1996; Winters et al., 2005), so we tested whether each could function on their own. When EGFP is attached to stabilize these short, unstructured sequences (~30–70 amino acids), each BH motif was enriched at the S2 cortex (Figure 6B–1B″), although at reduced levels compared to the full-length proteins. These data indicate that cortical localization of Lgl, Mira, and Numb

is mediated by their BH motifs. Although additional interactions are likely needed to reinforce cortical recruitment, this appears to be a common mechanism for BH-mediated membrane association (McLaughlin and Murray, 2005; Rohatgi et al., 2000; Winters et al., 2005).

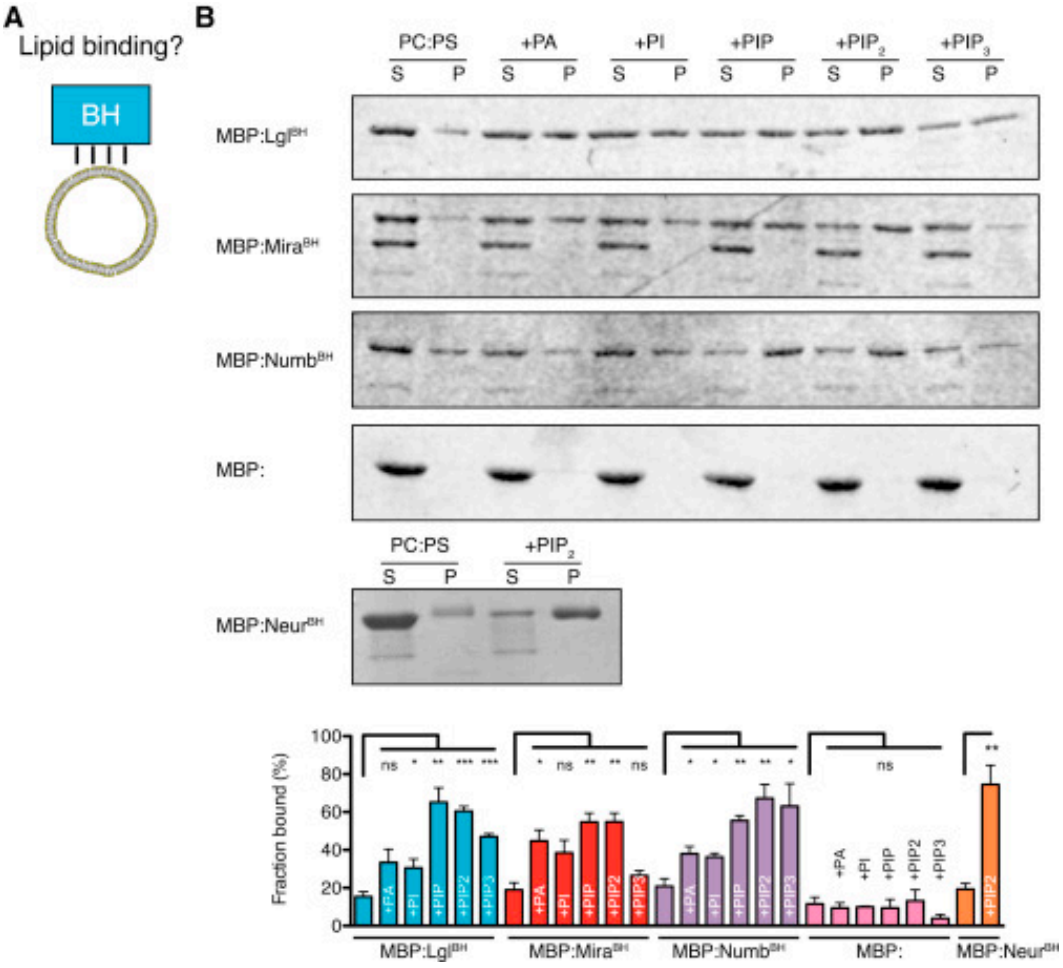

Figure 7. Phospholipid Binding Mediates Localization to the Cell Cortex. (A) BH motif phospholipid binding was tested using a cosedimentation phospholipid binding assay. (B) The BH motifs of Lgl, Mira, and Numb bind directly to phospholipid vesicles. The BH motif from Neuralized (Neur residues 68–88) was used as a positive control. The supernatant (S) and pellet (P) contain the unbound and bound fractions, respectively. All vesicles contained a 4-1 mixture of phosphatidylcholine (PC) to phosphatidylserine (PS), plus 10% of the following: PA, phosphatidic acid; PI, phosphatidylinositol; PI4P, phosphatidylinositol-4-phosphate; PIP_2, phosphatidlyinositol-4,5-bisphosphate; PIP_3, phosphoinositol-3,4,5-trisphosphate. The fraction bound expressed as a percentage is

shown in the bottom panel. Error bars represent SEM from three independent measurements. Significance levels, $^{*}p < 0.05$, $^{**}p < 0.01$, and $^{***}p < 0.001$. See also Supplemental Figure 1 for sequence analysis of Neur BH motif.

Lgl, Mira, and Numb BH motifs bind directly to phospholipids

The key role of the Lgl, Mira, and Numb BH motifs in cortical localization suggests that protein-phospholipid interactions are, at least in part, responsible for the cortical association of Par substrates. To test for direct protein-phospholipid interactions, we purified the BH motifs as maltose-binding protein (MBP) fusions and tested whether they associate with giant unilamellar vesicles (GUVs) of various lipid compositions via a co-sedimentation assay (Figure 7A). Using the BH motif from Neuralized (Neur) as a positive control (Skwarek et al., 2007), we found that each of the BH motifs from Lgl, Mira, and Numb exhibited very little binding to vesicles containing phosphatidylserine and phosphatidylcholine alone, but interacted with these vesicles when they were doped with various negatively charged phospholipids (Figures 7B). Although phosphoinositides with multiple phosphates were slightly preferred over other negatively charged lipids (e.g., phosphatidic acid [PA]), the level of specificity is small enough that we do not expect it to be physiologically relevant.

Par substrate cortical recruitment Is mediated by electrostatic interactions

The BH motifs of Lgl, Mira, and Numb have multiple positively charged residues that may confer favorable electrostatics for binding phospholipids. Polybasic regions can bind negatively charged phospholipids, including PS and phosphoinositides. To investigate the role of charge in cortical targeting, we mutated basic residues within the

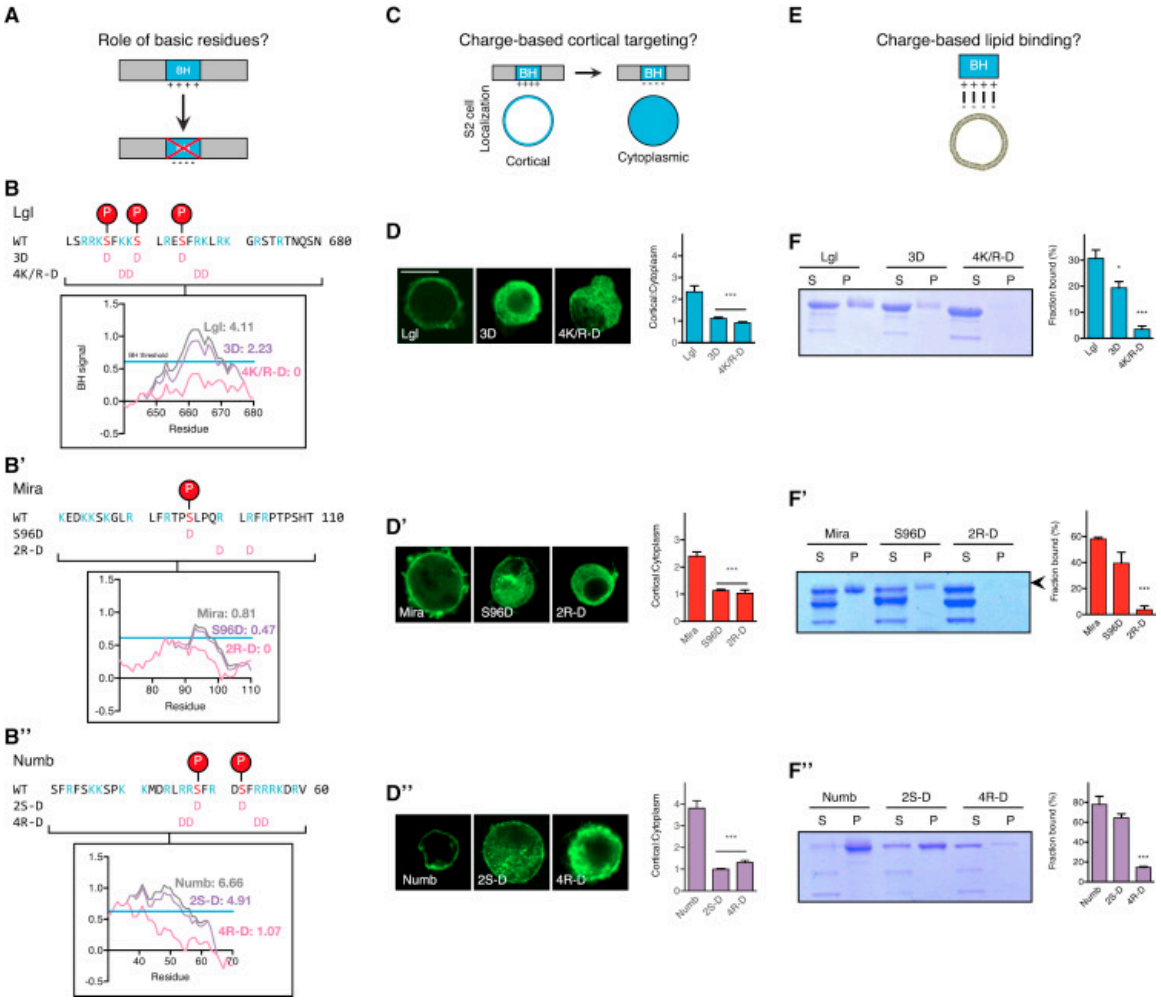

Figure 8. Electrostatic Interactions Mediate Lgl, Mira, and Numb Interactions with Phospholipids and the Cell Cortex. (A) BH motif point mutants test the role for charged residues in cortical localization. (B–B") Charged residues contribute to BH motif of Lgl (B), Mira (B′), and Numb (B"). The sequence of the BH motifs from Lgl, Mira, and Numb are displayed and the mutated residues are indicated. Basic residues (blue) and aPKC phosphosites (red). The inset shows the effect of each mutation on the BH signal and the area of the BH peak, as computed by BH-search. The BH threshold is displayed by a blue line with a BH signal of 0.6. (C) S2 cell localization assay tested if BH motif charge mediates localization to the cell cortex. (D–D") Mutations to acidic residues reduce localization of full-length Lgl, Mira, and Numb to the cell cortex in transiently transfected S2 cells. The localization was quantified as a cortical to cytoplasmic signal intensity ratio for at least 16 cells (mean ± SEM). Scale bar, 10 μm. See also Supplemental Figure 2 for additional point mutants. (E) Lipid binding assays tested if BH motif charge disrupts phospholipid binding. (F–F") Acidic mutations reduce phospholipid binding. A Coomassie-stained gel from lipid vesicle binding sedimentation assays with vesicles of 4:1 PC:PS plus 10% PIP_2 is shown. S indicates supernatant and P the pellet fraction. Arrowheads mark the full MBP-BH protein while other bands are truncation products (e.g., MBP alone). The fraction of protein bound (mean ± SEM) is shown. non-parametric t test relative to the unmutated BH motif: $^{*}p < 0.05$, $^{***}p < 0.0001$.

BH motif to the acidic residue aspartic acid; these mutations reduced the calculated BH signal to often eliminate BH motif identification (Figure 8A–4B″). We found that mutations that acidify the BH motif greatly reduce cortical localization of the full-length protein in S2 cells (Figure 8C–4D″). Further, this effect was not site-specific because mutations at multiple sites along the BH motif caused similar localization phenotypes (Supplemental Figure 2A).

Consistent with their effect on cortical localization, charge swap mutations reduced BH affinity for liposomes (Figures 8E-F"). To further test the role of electrostatics, we measured liposome interactions in the presence of 500 mM KCl, which reduces the entropic cost of displacing ions from the bilayer surface (McLaughlin, 1989). High ionic strength reduced the interaction between phospholipids and each BH motif (Supplemental Figure 2B), supporting the conclusion that direct, electrostatic interactions with phospholipids mediate BH motif cortical enrichment.

aPKC phosphorylation regulates BH cortical targeting and phospholipid binding

The Lgl, Mira, and Numb BH motifs contain verified and/or predicted aPKC phosphorylation sites. As charge swap mutations significantly reduce BH motif phospholipid binding and cortical association, we predicted that Par-induced polarization results when BH and aPKC phosphorylation site motifs are in close enough proximity that the phosphorylation(s) can sufficiently influence BH electrostatics to reduce the

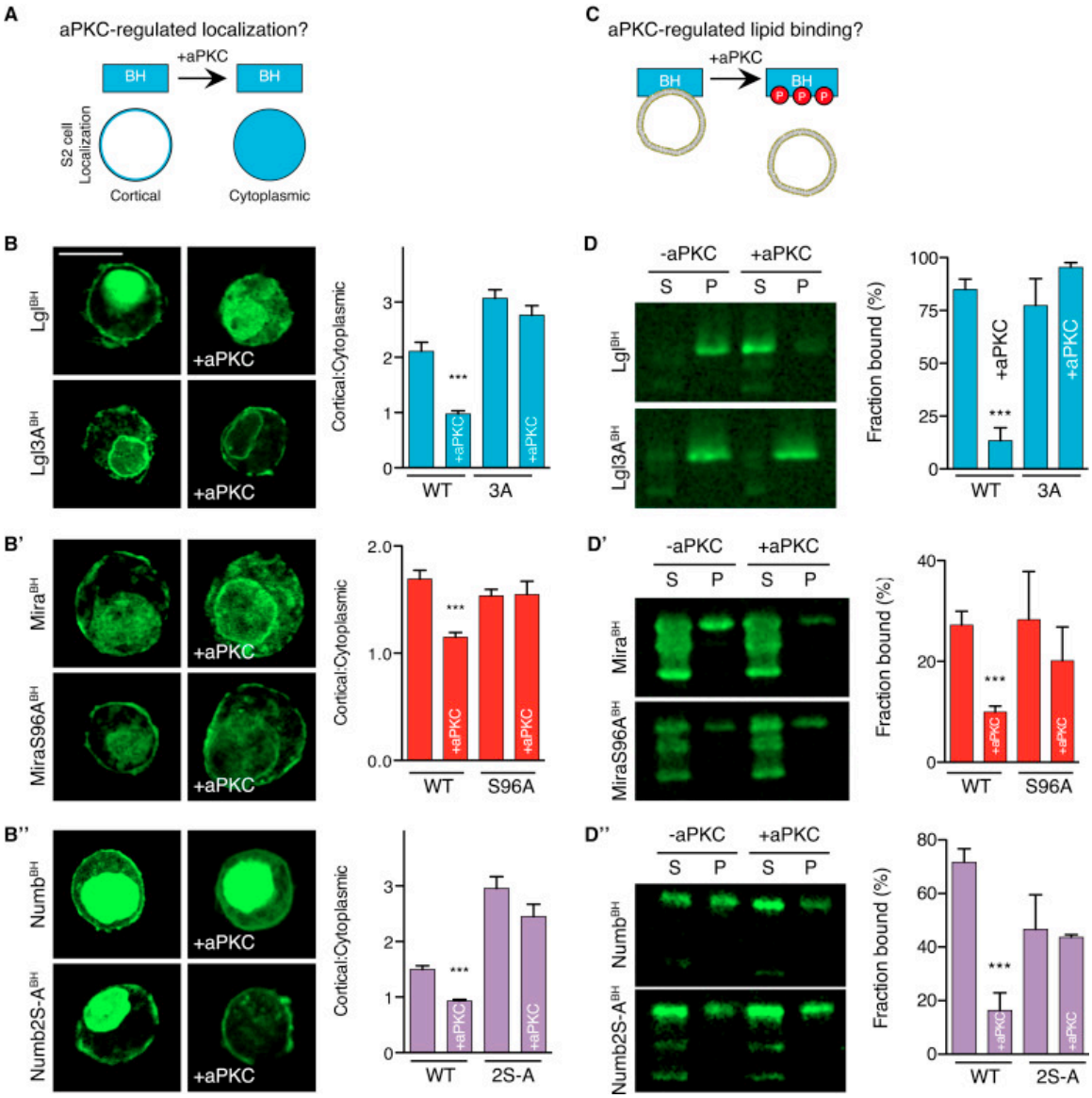

Figure 9. Phosphorylation Directly Inhibits Par Substrate BH Motif Interactions with Phospholipids and the Cell Cortex. (A) Schematic of aPKC regulation of BH motif cortical localization assay. (B–B") Phosphorylation by aPKC disrupts Lgl (B), Mira (B'), and Numb (B") BH motif cortical enrichment. The localization of EGFP fused BH motifs both in the absence and presence (+aPKC) of aPKC is shown, along with that for BH motifs with phosphorylation sites mutated to alanine (3A, S96A, S48AS52A). Cortical-to-cytoplasmic intensity ratios are quantified (mean ± SEM). Non-parametric t test to assess the effect of aPKC cotransfection. ***$p < 0.0001$. Scale bar, 10 μm. See also Supplemental Figure 3. (C) The effect of aPKC phosphorylation on phospholipid binding was tested with lipid cosedimentation assays. (D–D") Effect of aPKC on Par substrate BH motif binding to vesicles (4:1 PC:PS + 10% PIP_2) in ± aPKC conditions. Samples were analyzed by immunoblotting for the MBP tag. S, supernatant; P, pellet. The fraction of protein bound was quantified as an intensity ratio of S-to-P fractions (mean ± SEM). Non-parametric t test to compare ± aPKC conditions. ***$p < 0.0001$.

affinity for the membrane. This would allow Par substrates to associate with the cortex via their BH motif (and any accessory interactions) in regions lacking the Par complex. However, upon entering the Par cortical domain, the BH motif would be phosphorylated by aPKC, altering electrostatic character and reducing membrane affinity. Consistent with this model, we observed that phosphomimetic Lgl BH had reduced PIP_2 binding, although no statistically significant difference was observed for Mira or Numb BH motifs (Figures 8F–3F″). However, expression of aPKC significantly reduced cortical enrichment of the motifs from all three proteins (Figures 9A–4B″), recapitulating the behavior of the full-length proteins. Non-phosphorylatable variants of each BH motif remain localized to the cell cortex when aPKC was expressed (Figures 9B–4B″ and Supplemental Figure 3A), indicating that phosphorylation is required for displacement. Furthermore, we found that aPKC phosphorylation inhibits BH interaction with PIP_2-containing vesicles, suggesting that disruption of this direct interaction is responsible for cortical displacement (Figures 9C–4D″). Addition of aPKC had no effect on non-phosphorylatable BH motif variants Lgl3A, MiraS96A, or NumbS48AS52A, in the absence of ATP, or with aPKC harboring a kinase dead mutation (K293W) (Supplemental Figure 3B-D). The difference between the phosphomimetic and aPKC-phosphorylated proteins in binding PIP_2-containing vesicles likely arises from the higher negative charge density of the phosphorylated proteins. We conclude that aPKC displaces Lgl, Mira, and Numb from the cortex by phosphorylation inhibiting phospholipid binding.

A bioinformatics approach to identifying candidate PRBH motifs

Our analysis of Lgl, Mira, and Numb suggests that phospho-regulated BH (PRBH) motifs mediate Par substrate polarization by coupling phosphorylation to membrane affinity. This coupling derives from the overlap of BH and aPKC phosphorylation motifs, and we used this criterion to search for putative PRBH motifs. We implemented an algorithm in the Python programming language (van Rossum, 2001) using the maximum BH score within a motif (Brzeska et al., 2010) along with a scoring system based on the aPKC phosphorylation site motif consensus sequence (Wang et al., 2012), modified to include Miranda (Figure 10A). We used the maximum BH score rather than the sum of BH scores within a motif to select for short, highly charged sequences like those found in Lgl, Miranda, and Numb. Additionally, to account for the observation that these sequences often contain multiple phosphorylations sites (Graybill and Prehoda, 2014), the PRBH score is increased by 0.2 times the number of

Figure 10 (next page). PRBHscreen Identifies Candidate aPKC-Regulated PRBH Motifs. (A) Schematic representation of bioinformatics identification of PRBH motifs. The BH motif scoring algorithm identifies sequences with strong BH character, scoring residues as previously described (Brzeska et al., 2010). A representative BH plot has been included to how the max BH score is computed. aPKC consensus sites were identified and scored by scanning for S/T residues with preferred residues in the specific NH_2- and COOH-terminal sites and the scale indicates the position-dependent score for each amino acid shows. Unlisted residues have no effect on the overall phosphosite score. An overall PRBH score was assigned to sequences identified in both the BH and aPKC site identifying algorithm. (B and C) PRBH score distribution from in the *Drosophila* and human proteome. Select PRBH motifs from the fly and human proteome are highlighted in (B) and (C), respectively. The number of aPKC sites are labeled in blue, purple and red. Blue lines mark the threshold values. (D) aPKC phosphorylates candidate PRBH motifs. A ^{32}P autoradiograph demonstrates that Amer1^{PRBH}, CKIγ-2^{PRBH}, MPP7^{PRBH}, and PIP82^{PRBH} are phosphorylated by aPKC. A Coomassie-stained loading control gel is displayed. (E–H) aPKC inhibits localization to the cell cortex for several candidate PRBH motifs. Representative images are shown with a quantification of the cortical to cytoplasmic signal intensity ratio as the mean ± SEM. Significance was evaluated using a non-parametric t-test, where ns, not significant; $^{**}p < 0.001$; $^{***}p < 0.0001$.

phosphorylation sites. The weighting factor was set such that the BH and aPKC site score contributions to the overall PRBH score remained balanced. We used this algorithm to identify candidate PRBH motifs in several animal proteomes and numerically describe PRBH motifs by a maximum BH score (a metric of the basic character), aPKC site scores, and the number of aPKC sites identified (Figures 10B-C, 2-9A, and Supplemental Data Table 1). The Lgl PRBH was identified as one of the top scoring motifs in the

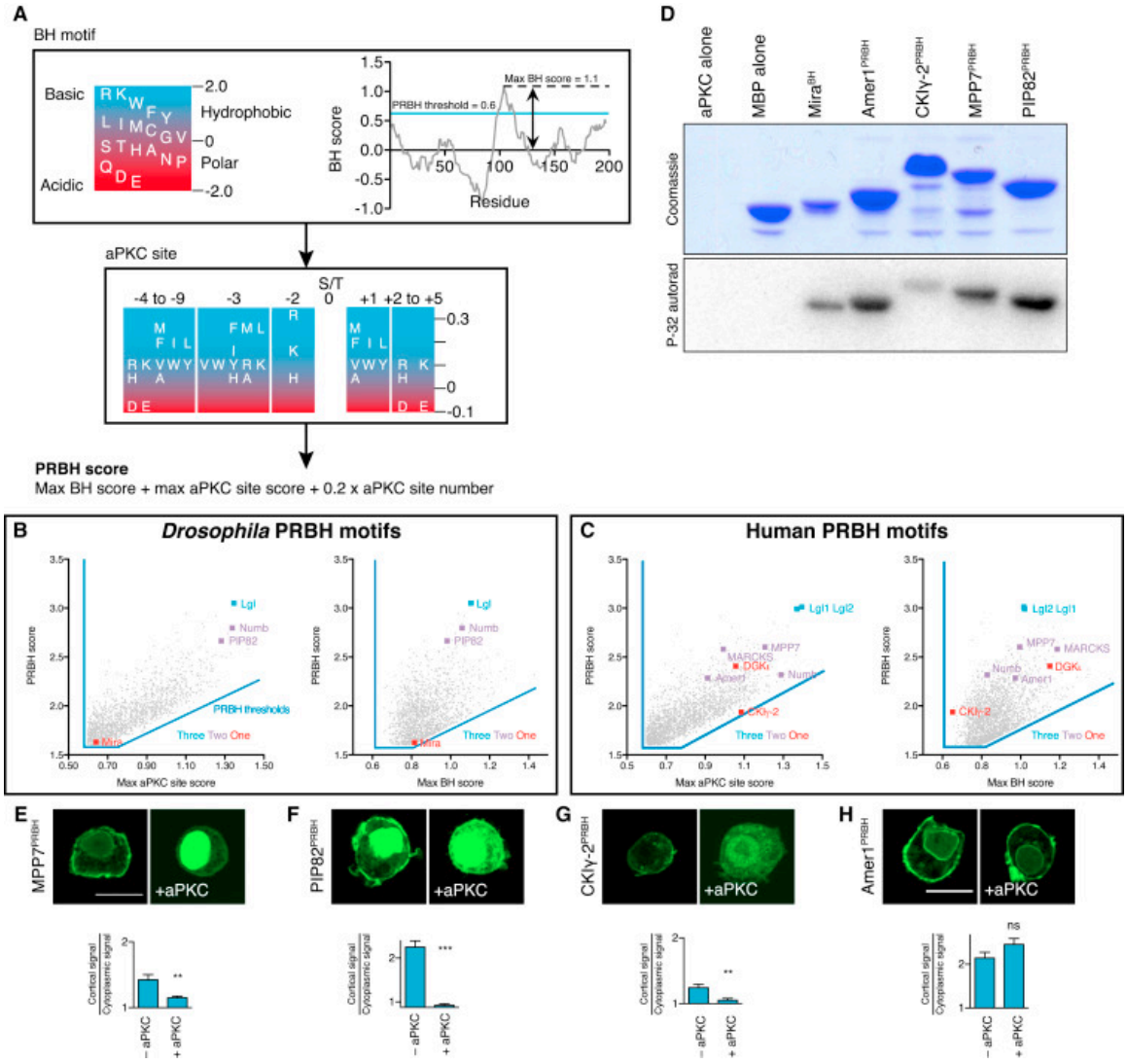

proteomes of human, fly, worm, and sponge, demonstrating that its charge and phosphosites are conserved in metazoan (Figures 2-10B-C, Supplemental Figure 4). The algorithm also identified Numb and Mira, although with lower PRBH scores. It is important to note that for two reasons Par-polarized proteins likely represent a subset of PRBH-containing proteins. First, polarity is only one cellular process for which phosphorylation regulated membrane association is important. Second, as many kinases have overlapping specificity it is unlikely that all the identified PRBH motifs are solely aPKC substrates (especially those with low aPKC site scores). For example, two bona fide PRBH proteins regulated by the conventional PKC were identified: MARCKS and diacylglycerol kinase (DGK) (Luo et al., 2003; Topham et al., 1998; Überall et al., 1997). Finally, aPKC functions in other processes besides polarity (Farese et al., 2014; Standaert et al., 2001). While these effects increase the false positive rate for identifying polarity proteins, they also suggest that the algorithm will have utility outside of polarity.

To validate the algorithm, we selected several candidate PRBH motifs to determine if they are bona fide regulated membrane association elements. We selected candidates from the fly and human proteomes with a range of PRBH scores, aPKC site scores, and maximum BH scores (Figures 10B-C) to examine how well PRBH score correlates with activity. For each candidate, we tested if they can be phosphorylated by aPKC in vitro, whether they associate with the cortex in S2 cells, and whether aPKC can displace them into the cytoplasm. We found that each protein was indeed phosphorylated by aPKC in an *in vitro* kinase assay (Figure 10D). Membrane-associated guanylate kinase (MAGUK) p55 subfamily member 7 (MPP7) regulates tight junction formation (Stucke et al., 2007) and has a single, highly scored putative PRBH motif that includes two predicted aPKC

phosphosites (Figures 10C and 10E). The candidate MPP7 PRBH was highly enriched at the cell cortex and aPKC expression inhibited cortical localization (Figure 10E). PIP82, a *Drosophila* protein involved in signal transduction downstream of photoreceptors (Suri et al., 1998), similarly contains two PRBH motifs, the stronger of which has high BH character and two predicted aPKC sites (Figures 10B and 10F). We observed that the PIP82 candidate PRBH sequence also localized to the S2 cell cortex and this localization was antagonized by aPKC (Figure 10F).

We also examined several lower scoring PRBH motifs to determine if they function as aPKC regulated cortical localization motifs. The putative PRBH motif on human casein kinase I γ (CKIγ-2) contains a strongly predicted aPKC site rated similar to MPP7, but has weak basic character as demonstrated by a low maximum BH height (Figures 2-8C and 2-8G). To our knowledge, its localization remain uncharacterized in polarized cells, but the Casein Kinase-associated protein Lrp6 localizes basolaterally in the *Xenopus* neuroectoderm (Davidson et al., 2005; Huang and Niehrs, 2014). CKIγ-2 PRBH localizes weakly to the cell cortex and has punctate localization suggesting it localizes to endomembrane organelles, as seen previously for Casein kinase (Tomishige et al., 2009). Expression of aPKC reduced the cortical localization of the CKIγ-2 candidate PRBH and did not alter the distribution of CKIγ-2 between the cortex and cytoplasm (Figure 10G). The human tumor suppressor Adenomatous polyposis coli membrane recruitment protein (Amer1, also known as WTX) represses WNT/β-catenin signaling (Grohmann et al., 2007; Rivera et al., 2007; Tanneberger et al., 2011); it contains a strong BH signal but a weak aPKC phosphosite score (Figures 10C and 10H). Correspondingly, we found that the Amer1 PRBH is targeted to the cell cortex, but aPKC

expression does not reduce its cortical localization (Figure 10H). However, the number of potential phospho-accepting residues within Amer1's PRBH makes it a prime candidate for regulation by another kinase. We conclude that the PRBH algorithm is a good predictor of aPKC-regulated cortical association, with higher scoring motifs more likely to exhibit this behavior. Furthermore, a more precise assessment of PRBH character can be made be directly comparing BH motif area, the number of aPKC phosphosites, etc.

DISCUSSION

The organization of the animal cell cortex by the Par complex involves two key steps (Goehring, 2014; Goldstein and Macara, 2007; Knoblich, 2010; Prehoda, 2009). The first involves the specification of the Par domain by upstream components such as the Rho GTPase Cdc42. In the second, diverse proteins must "plug into" Par polarity by occupying cortical areas that lack the Par complex. We have examined how the key output of the Par complex, aPKC activity, leads to cortical exclusion of the diverse array of Par-polarized proteins. Our approach was to examine the cortical interactions of three Par substrates that had no described sequence or domain similarities and to determine how aPKC phosphorylation modulates their cortical binding. Although these Par substrates do not have clear sequence homology, they each contain a "phospho-regulated BH" motif that couples aPKC phosphorylation to membrane affinity. This coupling is a direct consequence of the overlap of BH and aPKC phosphorylation sites in the PRBH motif as this allows phosphorylation to have a significant effect on the electrostatic character of the sequence. Using this defining feature, we developed a computational approach for identifying candidate PRBH motifs, which we validated that aPKC regulates

cortical association of several hits from the human and fly proteomes. We expect this technique will be useful for identifying candidate polarity proteins and proteins involved in other cellular processes where regulated membrane association is important.

Multivalent interactions mediate Par substrate cortical localization

We have found that Par substrate BH motifs localize to the cortex, but it is important to note that robust targeting requires elements outside of the BH sequence. While our data suggest that PRBH motifs are key regulatory elements for polarity, the requirement of additional interactions for high-affinity cortical interactions means that they are unlikely to lead to substrate polarity on their own. Similar "multivalent" interaction mechanisms has been observed with other BH motif-containing proteins that are regulated by phosphorylation and utilize accessory interactions to enhance their cortical targeting, including the yeast pheromone signaling protein Ste5 (Pryciak and Huntress, 1998; Winters et al., 2005) and the actin filament crosslinker MARCKS (Hartwig et al., 1992; McLaughlin and Murray, 2005; Thelen et al., 1991). In Ste5, protein-protein interactions provide additional cortex affinity, whereas MARCKS contains a myristoyl modification that works with its BH motif (George and Blackshear, 1992). The multivalent nature of protein-phospholipid interactions mediated by BH motifs may explain why protein-protein interactions are important to polarize some Par substrates. For example, Lgl interacts with non-muscle myosin II (Betschinger et al., 2005), and this interaction may cooperate with BH-phospholipid binding to yield the increased cortical interaction of full-length Lgl compared to its BH alone. Phospholipid binding by the BH motif and the PTB domain may robustly target Numb to the cell cortex (Dho et al., 1999). However, in

order for cortical localization to be regulated, the accessory interactions must not be stable enough to mediate cortical targeting on their own, or alternatively they must themselves be regulated by phosphorylation (McLaughlin and Murray, 2005; Strickfaden et al., 2007). Future studies of candidate PRBH-containing proteins will determine which regulated interactions are used for Par-mediate polarity and how factors such as cortical binding affinities, multiple PRBH motifs, and cortical mobility cooperate to mediate substrate polarization.

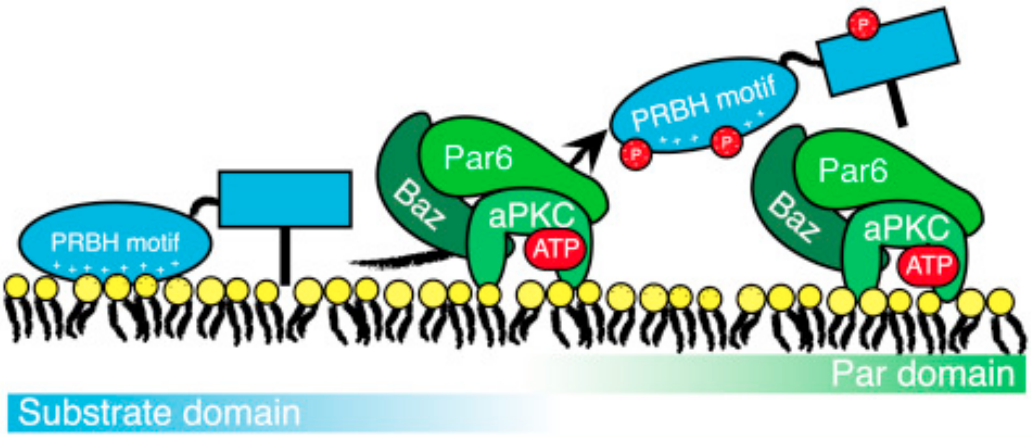

Figure 11. Model for Par Polarization by Phosphoregulated BH Motifs. PRBH motifs mediate localization to regions of the cell cortex opposite the Par complex. The box detail shows the molecular interactions occurring at the interface between the Par and substrate domains. Par substrates will localize to the cortex by electrostatic interactions with phospholipids until they encounter aPKC and become phosphorylated. Phosphorylation reduces their membrane affinity. Weak accessory interactions mediate localization to the cell cortex but they must allow the substrate to dissociate from the cell cortex, when the BH motif is phosphorylated.

PRBH: A mechanism for convergent evolution of Par-mediated polarity?

Phosphorylation can regulate protein activity by several means, including allostery and conformational changes (Cohen, 2000; Johnson and Barford, 1993; Serber and Ferrell, 2007). In this type of regulation, phosphate attachment to a specific side chain alters protein structural features and/or dynamics that are important for catalytic or binding activity (Barford et al., 1991). This coupling requires a connection between the phosphorylation site and the native state energy landscape, such that the phosphorylation site sequence is typically highly conserved (Holt et al., 2009). Allosteric effects or conformational changes may induce the polarization of substrates that lack PRBH motifs (e.g., Baz/Par-3 and Par-1) (Hurov et al., 2004; Morais-de-Sá et al., 2010; Sotillos, 2004; Suzuki et al., 2004). In contrast to complex mechanisms like these, phosphorylation of many Par substrates alters activity by changing the bulk electrostatics of the phospholipid binding sequence (Serber and Ferrell, 2007). Here, phosphorylation must occur close to the binding sequence but does not have to be coupled to structural or dynamic changes in the protein (Holt et al., 2009). Because many sequences satisfy the requirements of (1) an electrostatic character sufficient for binding negatively charged phospholipids, and (2) one or more aPKC phosphorylation sites, we propose that the sequence path for convergent evolution of PRBH motifs could be fairly simple. An existing motif, either BH or aPKC phosphosite is likely to require a small number of mutations to retain existing function while causing a gain of the missing function. For example, a protein that is advantageously targeted to the membrane via a BH motif could require only a small

number of mutations to become polarized with the introduction of one or more aPKC phosphosites.

Functions of candidate PRBH-containing proteins

We identified several proteins whose cortical localization is regulated by aPKC: MPP7 and PIP82 and CKIγ-2. In epithelial cells, MPP7 localizes to the lateral cortex and mediates tight junction formation (Stucke et al., 2007). While previous work has not implicated aPKC in its regulation, its localization and aPKC's inhibition of cortical localization make it a strong candidate Par-polarized substrate. The localization of several Casein kinase paralogs that lack predicted PRBH motifs have been described (Davidson et al., 2005; Gross et al., 1997), although the localization of the PRBH-containing CKIγ-2 in a polarized in vivo context is uncharacterized to our knowledge. However, recent work demonstrated that the CKIγ-associated protein Lrp6 localizes to the basolateral cortex in the neuroepithelium (Davidson et al., 2005; Huang and Niehrs, 2014), suggesting that CKIγ-2 may also exhibit this pattern of localization. Future work will need to address if aPKC indeed regulates CKIγ-2 localization in vivo. The localization and molecular function of PIP82 in *Drosophila* photoreceptor cells has not been described, but it is intriguing that light exposure causes it to be dephosphorylated (Suri et al., 1998). If the PIP82 PRBH is dephosphorylated during this process, it would be a mechanism for coupling cortical localization to light exposure. While we have identified many putative aPKC-regulated PRBH motifs, future work will need to address how this regulatory sequence is used cellular processes besides polarity. One particularly enticing PRBH protein is the retromer component Vps26 as it has been implicated in Par- and Scribble-

mediated endosomal trafficking (de Vreede et al., 2014). Characterization of Vps26 and other PRBH proteins will likely emphasize the diverse functions of aPKC phosphorylation.

A model for protein polarization directed by the Par complex

From these studies, we propose a model for Par complex function (Figure 11). In this model, Par-polarized substrates localize to the cortex via direct interactions between their BH motifs and membrane phospholipids. When a substrate enters the Par domain, either from the cytoplasm or by diffusion along the membrane, it becomes phosphorylated by aPKC. Addition of phosphates alters the electrostatics of the PRBH motif to reduce its affinity for phospholipids causing it to be displaced into the cytoplasm. Future work will be required to complete the "life cycle" of these substrates to understand the fate of Par substrates once displaced into the cytoplasm. Phosphorylation may be coupled to inactivation, degradation, or phosphatase-mediated re-association to the cortex.

EXPERIMENTAL PROCEDURES

Sequence analysis and computational work

BH motifs were initially identified using BH-search: a computational algorithm described in Brzeska et al. (2010) and is available online (http://helixweb.nih.gov/bhsearch/). Domain analyses were performed using SMART (Letunic et al., 2012; Schultz et al., 1998). Figures were assembled using the Adobe Creative Suite.

Molecular cloning and cell culture

All molecular cloning was performed as previously described (Graybill et al., 2012). Please see the Supplemental Experimental Procedures for details. Cell culture was performed as previously described (Lu and Prehoda, 2013). Briefly, cells were grown according to manufacturer's protocol, transiently transfected with Effectene (QIAGEN). Transfected cells were fixed and immunostained as previously described (Lu and Prehoda, 2013) and imaged with the following confocal microscopes: Olympus Fluoview FV1000 BX61 with a PlanApo N 60×/1.42 oil and a Leica SP2 confocal microscope with a 63×/1.40–0.60 oil CS objective. All proteins were tagged at their NH_2 terminus. Image analysis was performed with ImageJ.

Protein expression and purification

Protein expression was performed as previously described (Graybill et al., 2012). aPKC was purified from HEK293F cells transiently transfected with 293fectin transfection reagent (Life Technology). MBP-fusion proteins were expressed and purified from BL21 (DE3) cells, as previously described (Graybill et al., 2012). Cells were lysed by sonication, pelleted by centrifugation at 15,000 rpm, 30 min, 4°C in a JA-20 rotor and the soluble fraction was bound to amylose resin (New England BioLabs) for 45 min, 4°C. The resin was washed with MBP lysis buffer (20 mM Tris-HCl, pH 7.5, 200 mM NaCl, 1 mM EDTA, 1 mM DTT), then eluted with MBP elution buffer (20 mM Tris-HCl, pH 7.5, 200 mM NaCl, 1 mM EDTA, 1 mM DTT, 5 mM maltose). Elutions were pooled for dialysis in storage buffer (20 mM HEPES, pH 7.5, 50 mM NaCl, 1 mM DTT) overnight at 4°C and concentrated with a 10 kDa molecular weight cut-off Vivaspin 20

concentrator (GE Healthcare). Purified proteins were frozen with liquid nitrogen and stored at -80°C.

All His_6:aPKC$^{259-606}$ (kinase domain) constructs were expressed in HEK293F cells by transient transfection using 293fectin transfection reagent (Life Technology). Transfections were performed according to manufacturer's protocols. Expressions and protein purification of aPKC was performed as previously described (Graybill et al., 2012). Briefly, cells were cultured at 37°C, 8% CO_2, 125 rpm in Freestyle HEK293-F media (Invitrogen). Cells were cotransfected with pCMV His6-aPKC$^{259-606}$ (wild type or K293W mutant) and pCMV GST:PDK$^{161-500}$ (kinase domain) at ~1.0×10^6 cells/mL. Cells were harvested 24 hours post-transfection by centrifugation, resuspended in Ni^{2+} lysis buffer (50 mM NaH_3PO_4, 300 mM NaCl, 10 mM imidazole, pH adjusted to 8.0 with NaOH), then stored at -80°C. Cells were lysed by sonication, then lysates were pelleted by centrifugation at 15,000 rps, 30 min, 4°C in a JA-20 rotor. The supernatant was incubated with ammonium sulfate at a concentration of 45% (w/v) for 30 min, 4°C. Then, the solution was centrifuged at 15,000 rpm, 30 min, 4°C in a JA-20 rotor, the pellet was collected and resuspended in Ni^{2+} lysis buffer, then it was incubated with Ni^{2+}-nitrilotriacetic acid resin (Qiagen) for 45 min, 4°C. Resin were washed with Ni^{2+} lysis buffer, then protein was eluted with Ni^{2+} elution buffer (50 mM NaH_3PO_4, 300 mM NaCl, 250 mM imidazole, pH adjusted to 8.0 with NaOH). The eluted sample was dialyzed for 4 hours in storage buffer (20 mM Tris-HCl, pH 7.5, 50 mM NaCl, 1 mM DTT) using the SnakeSkin dialysis membrane (Thermo Scientific). Dialyzed proteins were clarified by centrifugation at 3,000 rpm, 30 min, 4°C. Clarified samples were

concentrated using a 10 kDa molecular weight cut-off Vivaspin 20 concentrator (GE Healthcare). Purified proteins were frozen with liquid nitrogen and stored at -80°C.

Biochemical assays

Lipids from the following sources were purchased from Avanti Polar Lipids: 1,2-dioleoyl- *sn*-glycero-3-phosphocholine, 1,2-Dioleoyl-*sn*-Glycero-3-[Phospho-L-Serine], L- (Egg, Chicken), L-α-Phosphatidylinositol-4-phosphate (Brain, Porcine), L-a-α-Phosphatidic acid (Egg, chicken), Phosphatidlyinositol-4,5-bisphosphate (Brain, Porcine), and 1,2- dioleoyl-*sn*-glycero-3-[phosphoinositol-3,4,5-trisphosphate]. Giant unilamellar vesicles were prepared as described (Winters et al., 2005). Briefly, lipids were added to chloroform at the molar ratios specified, chloroform was removed by rotovap and placing under vacuum for 15 min. Giant unilamellar vesicles were formed by resuspending in 0.2 M sucrose at 0.5 mg/mL total lipid by incubation at 50°C for 4 hours or overnight. Vesicles were stored at 4°C and used within 3 days of generation.

Pelleting assays were performed as previously described (Prehoda et al., 2000). For pelleting assay without aPKC, proteins were pre-spun to clarify in TLA-100 rotor, 65,000 rpm, 20 min, 4°C. All lipid binding cosedimentation assays contained 1-6 μM MBP- tagged protein and 0.23 mg/mL total lipid in assay buffer (20 mM HEPES, pH 7.5, 50 mM NaCl, 1 mM DTT). After incubating proteins and vesicles at 30°C for 30 min, samples were pelleted by ultracentrifugation in a TLA-100 rotor at 65,000 rpm, 60 min, 4°C. The supernatants were removed, the pellets were washed, then the pellets were resuspended in a volume equal to the reaction volume. All samples were run on a 12.5% SDS-PAGE gel and stained with Coomassie Brilliant Blue for analysis.

Gels were imaged using a scanner or the LiCOR. The band intensities were quantified using LiCOR ImageStudio and ImageJ. Gel images were processed with ImageJ and the Adobe Suite. All pelleting assays containing aPKC were performed essentially as described above with the changes noted below. Reactions contained 0.1-0.5 μM MBP-tagged proteins and 0.034 μM aPKC in reaction buffer (500 mM Tris-HCl, pH 7.5, 100 mM NaCl, 100 μM ATP, 100 μM $MgCl_2$). Immunoblotting was performed to detect protein using mouse anti- MBP (1:1000, Santa Cruz Biotechnologies) and IRDye 800 CW goat anti-mouse (1:10,000, LiCOR). Membranes were blocked with TBS-T with 3% milk. Membranes were imaged with using a LiCOR and images were processed with the Adobe Suite. Band intensities were quantified with LiCOR ImageStudio and band intensity data was analyzed using Prism.

Kinase assays were performed as previously described (Atwood and Prehoda, 2009; Graybill et al., 2012). Briefly, aPKC and substrates were incubated in assay buffer (50 mM Tris-HCl, pH 7.5, 100 mM NaCl, 10 mM $MgCl_2$) at 30°C for 5 min before addition of 1 mM ATP doped with [γ-^{32}P]ATP (~1.0 X 10^5/nmol of ATP). The kinase reaction proceeded for 30 minutes before it was quenched by SDS loading dye. Samples were run on a 12.5% acrylamide SDS-PAGE gel, were dried, and exposed to a phosphor screen (Molecular Dynamics). The phosphor screen was imaged with a Storm 860. Images from the Storm 860 Molecular Imager were processed with ImageJ and the Adobe Suite.

Sequence IDs and residue numbers

The following sequences were characterized in this study: Lethal giant larvae:

Species, *Drosophila melanogaster;* Symbol, Lethal (2) giant larvae; FlyBase ID, FBgn0002121; Isoform, PA (length 1161 residues). Lgl BH motif constructs include residues 647-681. Lgl ΔBH motif constructs deletes residues 647-681. Miranda: Species, *Drosophila melanogaster;* Symbol, Mira; FlyBase ID, FBgn0021776; Isoform, PA (length 829 residues). Mira BH constructs include residues 71-110 and the BH motif deletion construct removes residues 72-110. Numb: Species, *Drosophila melanogaster;* FlyBase ID, FBgn0002973; Isoform, PA (length 556 residues). Numb BH constructs include residues 15-86 and the BH motif deletion construct removes residues 24-56. Neuralized: Species, *Drosophila melanogaster;* Symbol, Neur; Flybase ID, FBgn0002932; Isoform, PA (length 754 residues); BH motif, residues 68-88. Amer1: Species, *Homo sapiens;* NCBI reference sequence, NP_689637.3; PRBH, residues 154-199. Casein Kinase I gamma 2: Species, *Homo sapiens;* Symbol, CKIγ-2; NCBI reference sequence, GenBank ID, AAB88627.1. PRBH motif, 369-415. MAGUK p55 subfamily member 7: Species, *Homo sapiens;* Symbol, MPP7; NCBI Reference Sequence, NP_775767.2. PRBH, residues 289-383. PIP82: Species, *Drosophila melanogaster*; FlyBase ID, FGgn0024943. PRBH motif, residues 400-450.

Cell culture and localization assays

Cell culture was performed as previously described (Lu and Prehoda, 2013). S2 cells were grown at 30°C in Schneider's media (Sigma-Aldrich) with 10% fetal bovine serum. S2 cells were transiently transfected with Effectene (QIAGEN) according to the manufacturer's protocol. Cells were seeded at ~2×10^6 cells/well in a 6-well plate and transfected 24 hours later with 0.5 μg plasmid. 24 hours after transfection, protein

expression was induced for all pMT-transfected cells by addition of 0.5 mM $CuSO_4$. 24 hours post-induction, or 48 hours post-transfection for cells transfected with pTub plasmids, cells were plated on 12 mm glass coverslips in a 24-well plate for immunostaining and imaging.

For immunohistochemistry, cells were washed with PBS, and then fixed with 4% paraformaldehyde in PBS. Cells were washed with PBS with 0.1% saponin, washed three times with block [PBS, 0.1% saponin, and 1% bovine serum albumin (BSA)], and then blocked for 30 minutes with block. Primary antibody incubations were performed for either 1-2 hours at room temperature or overnight at 4°C. Cells were washed three times after immunostaining and between antibody staining steps. The following antibody dilutions were used: mouse anti-HA 1:1000 (Covance), rabbit anti-PKCζ 1:1000 (Santa Cruz Biotechnology), DyLight 488 Donkey anti-mouse 1:500 (Jackson Immunoresearch) and DyLight Donkey 649 anti-rabbit (Jackson Immunoresearch). The cell cortex was stained with Alexa Fluor 555-Phalloidin (1:500, Invitrogen). Coverslips were mounted using Vectashield Hardset Mounting Medium (Vector Laboratories). An Olympus Fluoview FV1000 BX61 with a PlanApo N 60×/1.42 oil and a Leica SP2 confocal microscope with a 63×/1.40-0.60 oil CS objective was used to acquire all images. The cortical-to-cytoplasmic intensities were quantified in ImageJ using the free-hand line tool and freehand selection tool to determine the average fluorescence intensities in each cellular area. Prism was used for statistical analysis of quantified localization data. Images were processed with ImageJ and the Adobe Suite.

Computational identification of PRBH motifs

The PRBH algorithm was implemented using the Python programming language with standard Python libraries including numpy and matplotlib. EMBL-EBI reference proteome files from *Homo sapiens, D. melanogaster, C. elegans,* and *S. cerevisiae*. The BH scoring algorithm used the previously described scores for BH character (Brzeska et al., 2010): A, -0.17; C, 0.24; D, -1.23; E, -2.02; F, 1.13; G, -0.01; H, -0.17; I, 0.31; K, 2; L, 0.56; M, 0.23; N, -0.42; P, -0.45; Q, -0.58; R, 2; S, -0.13; T, -0.14; V, -0.07; W, 1.85; Y, 0.94. Each amino acid residue was assigned a BH score for over a 19 residue BH window (i.e. the amino acid and its 9 NH_2- and COOH-terminal neighbors; unless specified otherwise). Sequences of adjacent residues with BH scores over a BH threshold of 0.6 were identified as peaks. The amino acid sequence of the peak, as well as, the maximum BH score and area over the BH threshold were compiled in a peak list. For human Numb and CKIγ-2, the BH window was reduced to 15 residues such that BH motifs at the extreme NH2- and COOH-terminus were identified. BH scores for residues 9 residues or less from the NH2- or COOH-terminus cannot be scored. Reducing the BH window allows residues closer to the NH2- or COOH-terminus to be scored.

aPKC consensus sequences were identified by scoring the residues flanking S/T residues. The positional scoring was based on the previously described aPKC consensus sequence (Wang et al., 2012). This scoring metric does not strictly follow the consensus sequence from Wang and coworkers such that Ser 96, a verified aPKC phosphosites on Mira, fit the consensus. Hydrophobic residues were score as follows, except where noted otherwise: A, 0.05; F, 0.2; I, 0.2; L, 0.2; M, 0.25; V, 0.1; W, 0.1; Y, 0.1. Basic residues were score as follows, except where noted otherwise: R, 0.1; K, 0.07; H, 0.04; D, -0.06;

E, -0.06. Residues in the +2 position were scored as follows: R, 0.35; K, 0.15; H, 0.05. Residues in the +3 position were scored as follows: F, 0.25; L, 0.25; M, 0.25; I, 0.15; V, 0.1; W, 0.1; Y, 0.1; A, 0.05; R, 0.1; K, 0.1; H, 0.05. The +1 position was scored using the hydrophobic residue metric, and a penalty of -0.4 was given for residues that were not hydrophobic. Points were awarded for basic or hydrophobic residues from the -9 to the -4 position. Sequences with aPKC scores above the aPKC threshold of 0.6 were compiled in an aPKC site list. For proteins with multiple aPKC sites, each was included in the aPKC site list with its corresponding site score.

The aPKC site list and the BH site list were compared, and the PRBH algorithm analyzed sequences occurring in both lists. A PRBH score was computed for sequences occurring in both lists by using the following calculation: 'Maximum BH score' + 'Maximum aPKC site score' + 0.2 * 'aPKC site number in the PRBH motif'. Three additional tests were performed on PRBH sequences: first, the area of the BH motif must be less than 400X the number of aPKC phosphosites. This eliminated many highly basic sequences with few candidate sites. Such sequences were not desired, as phosphorylation is not likely to alter BH character dramatically. Second, when a BH window size of 19 was used, BH motifs with areas less than 90 were discarded. This parameter was not used for identification of PRBH motifs at a protein's NH2- or COOH- terminus because the BH scoring metric reduces the BH signal for these peaks due to the scoring process. Third, PRBH scores less than the PRBH threshold of 1.6 were discarded. Sequences that passed these criteria were compiled in a PRBH sequence list that included the following: protein names, PRBH score, the PRBH sequence, maximum BH score, BH area, aPKC site scores, and aPKC site sequences. The full Python script is available online with the

Supplemental Information available with the manuscript online.

ACKNOWLEDGEMENTS

Plasmids were generously provided by Roland Le Borgne (Numb), Gabrielle Boulianne (Neuralized), Kentaro Hanada (CKIγ-2), and Jürgen Behrens (Amer1). Thanks to Robert Lyle McPherson for his assistance with cell culture and protein purification. We would like to thank Michael Drummond, Chiharu Graybill, Ryan Holly, Kimberly Jones, Robert Lyle McPherson, and Brett Wee for useful discussions, and J. Andy Berglund and Raghuveer Parthasarathy for equipment use. Thanks to Tom Stevens, Brad Nolen, and Chris Doe for comments on the manuscript and to Peter Pryciak for useful discussions about this work. This work was supported by the NIH Predoctoral Training grant GM007759 (M.J.B.) and NIH grant GM068032 (K.E.P.).

BRIDGE TO CHAPTER III

This chapter demonstrated that aPKC phosphorylation of phospholipid binding sites is a crucial step in Par substrate polarization. This work suggested that aPKC-regulated PRBH motifs can function as a "polarization module" on substrates with an optimal set of interactions with the cell cortex, and that aPKC may polarize additional substrates by PRBH motif phosphorylation. The following chapter tests this PRBH-centric model of Par substrate polarization by assessing if the Par complex polarizes other proteins by PRBH motif phosphorylation. In this chapter, I perform a screen of polarized proteins to assess if aPKC regulates their localization to the cortex of cultured cells, aPKC is sufficient for polarization in cultured cells, and whether they are aPKC

substrates. I identify crossveinless-c, a Rho GTPase activating protein that is essential for morphogenesis, to be an aPKC substrate that is polarized by PRBH phosphorylation.

CHAPTER III

THE PAR COMPLEX POLARIZES THE RHOGAP CROSSVEINLESS-C BY PHOSPHORYLATION

This chapter contains unpublished co-authored material with K.E. Prehoda. I performed all experimental work, designed the study, analyzed the data, and wrote the manuscript. Kenneth E. Prehoda supervised the project and contributed to project design.

SUMMARY

The Par complex polarizes many cell types by polarizes specific effectors. A key output of the Par complex is the kinase activity of atypical protein kinase C (aPKC), as phosphorylation induces the polarization of many aPKC substrates. Previously, we demonstrated that the Par complex polarizes several substrates by phosphorylation of a phospholipid binding site, which disrupts localization to the plasma membrane. Here we perform a screen for additional aPKC substrates that are polarized by this mechanism. We find that aPKC regulates cortical association for crossveinless-c (Cv-c), a Rho GTPase activating protein (GAP), by site-specific phosphorylation. Using a reconstituted polarity assay, we find that aPKC is sufficient to polarize Cv-c to cortical domains that lack aPKC. Given the essential role of Cv-c in morphogenesis, this work suggests that aPKC polarization of Cv-c might be an essential process in *Drosophila* development.

INTRODUCTION

A surprisingly small number of proteins establish and maintain the architecture of cells as morphologically divergent as epithelia, migratory cells, and neurons (Etienne-Manneville and Hall, 2001; Joberty et al., 2000; Knust and Bossinger, 2002; Lin et al., 2000; Shi et al., 2003; Solecki et al., 2004; Welchman et al., 2007). A key feature of these cell types is that they are polarized, meaning they have specific molecular contents unequally distributed across the cell. The Partitioning-defective (Par) complex has an essential role in establishing and maintaining cell polarity by regulating the formation of membrane-associated domains (Goehring, 2014; Goldstein and Macara, 2007; Knoblich, 2010; Overeem et al., 2015; Tepass, 2012). To understand the mechanisms of Par polarity, we need to know how the Par complex polarizes its downstream effectors.

The Par complex consists of the Rho GTPase Cdc42, the adaptor Par6, and the atypical protein kinase C (aPKC) (Joberty et al., 2000; Lin et al., 2000; Wodarz et al., 2000). Cdc42, Bazooka (Baz, mammalian Par-3), and other genetically upstream proteins localize aPKC/Par6 to the cell cortex where they establish the apical domain (in epithelia and neural stem cells, or neuroblasts) by polarizing downstream proteins (Rolls, 2003; Watts et al., 1996). A key step in polarizing a cell is the targeting of proteins to the basal or basolateral domain. Several studies have found that aPKC phosphorylates Lethal (2) giant larvae (Lgl), Miranda (Mira), Numb, Par1, and PAR-2, thereby inhibiting the localization of these substrates from the apical domain, or anterior domain in the case of PAR-2 (Atwood and Prehoda, 2009; Betschinger et al., 2003; Hao et al., 2006; Hurov et al., 2004; Smith et al., 2007; Suzuki et al., 2001). Recently, work by us and others found that Lgl, Mira, Numb, and PAR-2 bind to membrane phospholipids and that aPKC

phosphorylation inhibits phospholipid binding, which prevents colocalization with the Par complex (Bailey and Prehoda, 2015; Dong et al., 2015; Motegi et al., 2011; Visco et al., 2016). The commonalities in polarization mechanisms between these proteins led us to hypothesize that the Par complex polarizes its substrates by a common mechanism, wherein phosphorylation inhibits phospholipid binding and cortical targeting to the Par cortical domain.

Phospholipid binding and cortical targeting of Lgl, Mira, Numb, and PAR-2 involves basic and hydrophobic (BH) residues interacting with phospholipids, targeting the protein to the plasma membrane (Bailey and Prehoda, 2015; Dong et al., 2015; Motegi et al., 2011; Visco et al., 2016). We developed a computational tool to assist in the identification of BH motifs that contain an aPKC consensus sequence (i.e. a Phospho-Regulated BH motif) (Bailey and Prehoda, 2015). With this tool, we found that these sequences are common in the proteome of metazoa. We also found that aPKC could inhibit targeting of cortical targeting of candidate PRBH motifs in a Schneider 2 (S2) cell over-expression system. However, a thorough evaluation of this algorithm has yet to be performed to assess whether it has predictive capabilities in the identification of polarized Par substrates. Here, we describe a screen of polarized PRBH motif-containing proteins to determine if they are polarized by aPKC phosphorylation.

RESULTS

aPKC inhibits cortical targeting of crossveinless-c

Inhibition of cortical localization by aPKC is a characteristic behavior of proteins that the Par complex polarizes by phosphorylation (Atwood and Prehoda, 2009; Betschinger et al., 2003; Hao et al., 2006; Hurov et al., 2004; Smith et al., 2007; Suzuki et al., 2001). To identify novel targets of aPKC, we screened for proteins with aPKC-regulated cortical targeting in S2 cells. We started with four criteria to select candidates: (1) having a putative PRBH motif, (2) polarized subcellular localization terms that do not include cortical regions where the Par complex localizes (e.g. basal/basolateral domain, adherens junctions, or lateral domain), (3) lack of transmembrane (TM) regions, (4) lack of predicted secretion signals, (5) S2 cell localization is not available or indicates that the protein is cortically localized. We searched Flybase subcellular localization terms and identified 18 candidates that fit criteria one and two (Supplemental Data Table 1). We used SMART to assess criteria three and four and a literature search to assess criteria five (Letunic et al., 2015). This left us with a list of seven candidates, and these candidates have a range of BH character and aPKC consensus sequence qualities (Figure 12B). These candidates included α-catenin (α-cat), CG42748, crossveinless-c (Cv-c), coracle (Cora), Nullo, p21-activated kinase (Pak), varicose (Vari) (Fehon et al., 1994; Hunter and Wieschaus, 2000; Lye et al., 2014; Moyer and Jacobs, 2008; Simões et al., 2006; Wang et al., 2006).

We cloned all seven candidates and assessed their localization in S2 cells. Each protein was transiently transfected, and its localization was characterized by an NH2-terminal hemagglutinin (HA) epitope tag (Figure 12A). In this over-expression system,

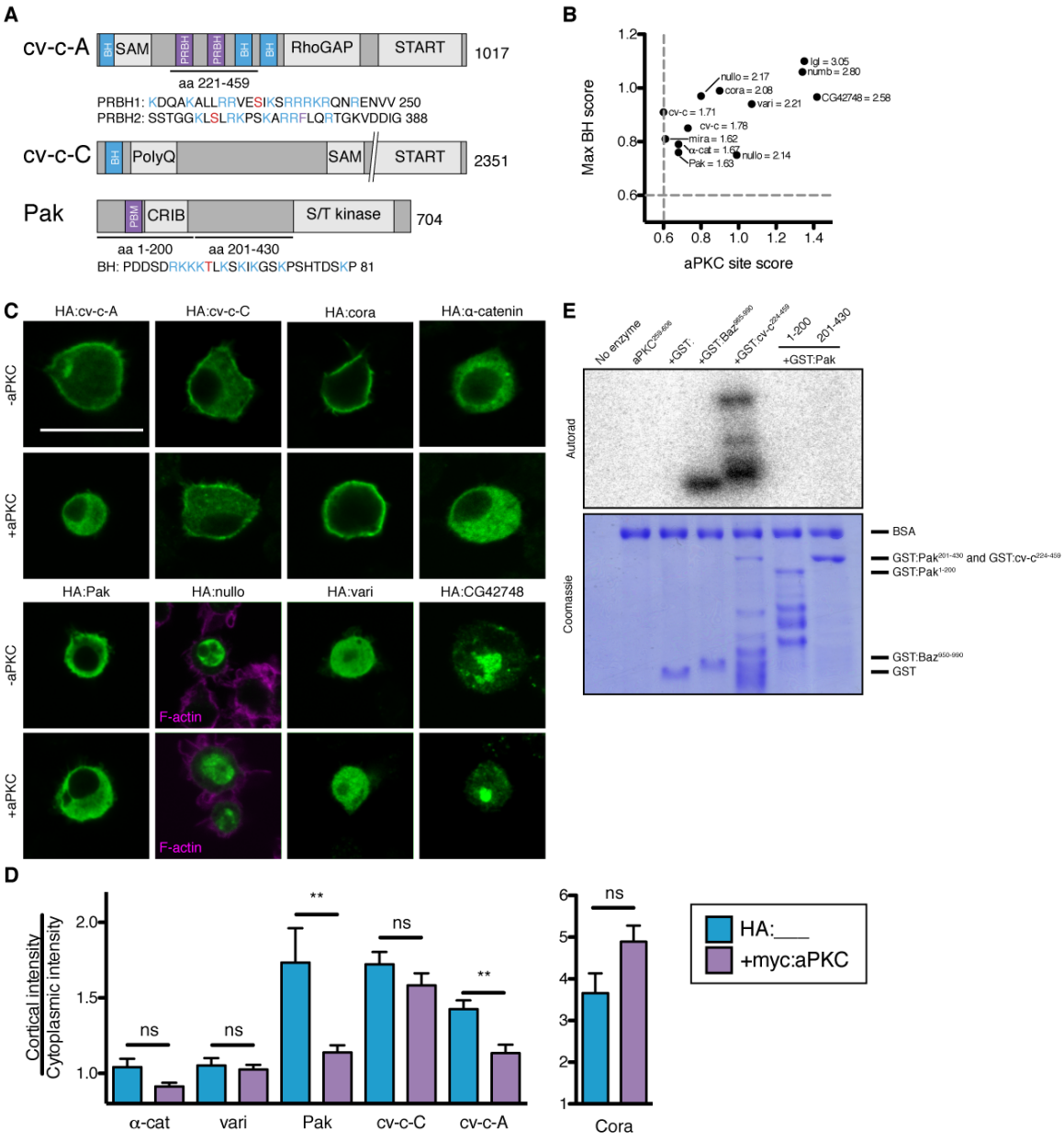

Figure 12. aPKC regulates cortical targeting of its substrate Cv-c. (A) Proposed domain architecture. Abbreviations: CRIB, Cdc42/Rac Interactive Binding domain; PBM, polybasic motif; StAR and phosphatidylcholine transfer protein; SAM, sterile alpha motif. (B) Rating of PRBH, BH, and aPKC site scores for candidates. The PRBH score follows the protein name. (C) aPKC regulates Cv-c-A and Pak cortical targeting. Representative images of S2 cells overexpressing NH2-terminally HA-tagged proteins with or without myc:aPKC. Scale bar, 10 µm. (D) Quantification of cortical-to-cytoplasmic intensities for HA-tagged proteins in the specified conditions. Student's t-test (two-tailed, 95% confidence interval), where ns, not significant; *p < 0.05, **p < 0.01. (E) aPKC phosphorylates Cv-c. *In vitro* kinase assay on GST-tagged Pak and Cv-c deletion constructs. The autorad and Coomassie-stained loading control gel are shown. $Baz^{965-990}$ was included as a positive control.

we observed cortical enrichment (as measured from a cortical-to-cytoplasmic intensity ratio) for Cora, Cv-c and Pak (Figure 12C-D). Next we assessed the localization of these candidates when S2 cells were cotransfected with myc:aPKC full length (FL). We observed reduced cortical localization of Cv-c isoform A (Cv-c-A) and Pak upon co-transfection with myc:aPKC FL (Figure 12C). Interestingly, we did not observe a change in Cv-c isoform C (Cv-c-C) cortical localization upon aPKC over-expression (Figure 12D). The C and A isoforms have different NH2-termini, which likely explains differences in cortical recruitment (Figure 12A). The literature provides few clues regarding the observed localization differences for Cv-c isoforms, as previous studies on Cv-c subcellular localization have focused on isoform A, which is basolateral localization in embryonic spiracle and salivary cells when overexpressed as a UAS transgene (Simões et al., 2006; Sotillos et al., 2013).

aPKC had no effect on the subcellular localization of other candidates. Cora was enriched at the cell cortex regardless of whether aPKC was contransfected. We found α-cat and Vari to have diffuse, cytoplasmic localization that was not regulated by aPKC (Figure 12C-D). Nullo localized to the nucleus regardless of whether singly transfected or cotransfected with myc:aPKC FL (Figure 12C). CG42748 expression was low and localized to puncta regardless of aPKC coexpression. The localization of α-cat, Vari, and Nullo suggests that cortical targeting might require additional protein binding partners that are not highly expressed in S2 cells.

Cv-c is an aPKC substrate

Many proteins that the Par complex polarizes are direct aPKC substrates. To assess if Pak and Cv-c are aPKC substrates, we performed an *in vitro* kinase assay. We used this assay to identify regions of Pak and Cv-c-A that aPKC might phosphorylate (Figure 12A). The central linker region of Cv-c was purified as a GST fusion. We focused on this region of Cv-c as its human homolog Deleted in liver cancer 1 (DLC1) is phosphorylated at multiple residues within this region (Ko and Ping Yam, 2014; Ko et al., 2010; Liao et al., 2007). In an *in vitro* kinase assay, we found that aPKC phosphorylated this region of Cv-c (Figure 12E). We also purified two deletion products of Pak to assess if it was an aPKC substrate: the NH2-terminal 200 amino acids that contain the polybasic motif (PBM) and Cdc42/Rac Interactive Binding (CRIB) domain, and residues 201 to 430. aPKC phosphorylated neither fragment of Pak suggesting that it is not an aPKC substrate (Figure 12E). This suggests that aPKC is unlikely to regulate phospholipid binding at Pak PBM. Also, these data suggest that aPKC regulation of Pak cortical targeting in S2 cells is likely to occur by a phosphorylation-independent mechanism, perhaps as an indirect mechanism through regulation of Cdc42 (Harden et al., 1996). Together these data suggest that Cv-c is an aPKC substrate and a potential downstream effector.

Cv-c is basal in epithelial cells undergoing morphogenesis

The subcellular localization of Cv-c has only been characterized when it is over-expressed as a UAS transgene. We wanted to assess the endogenous localization of Cv-c to verify that it is polarized *in vivo*. Antibodies for Cv-c are not currently available,

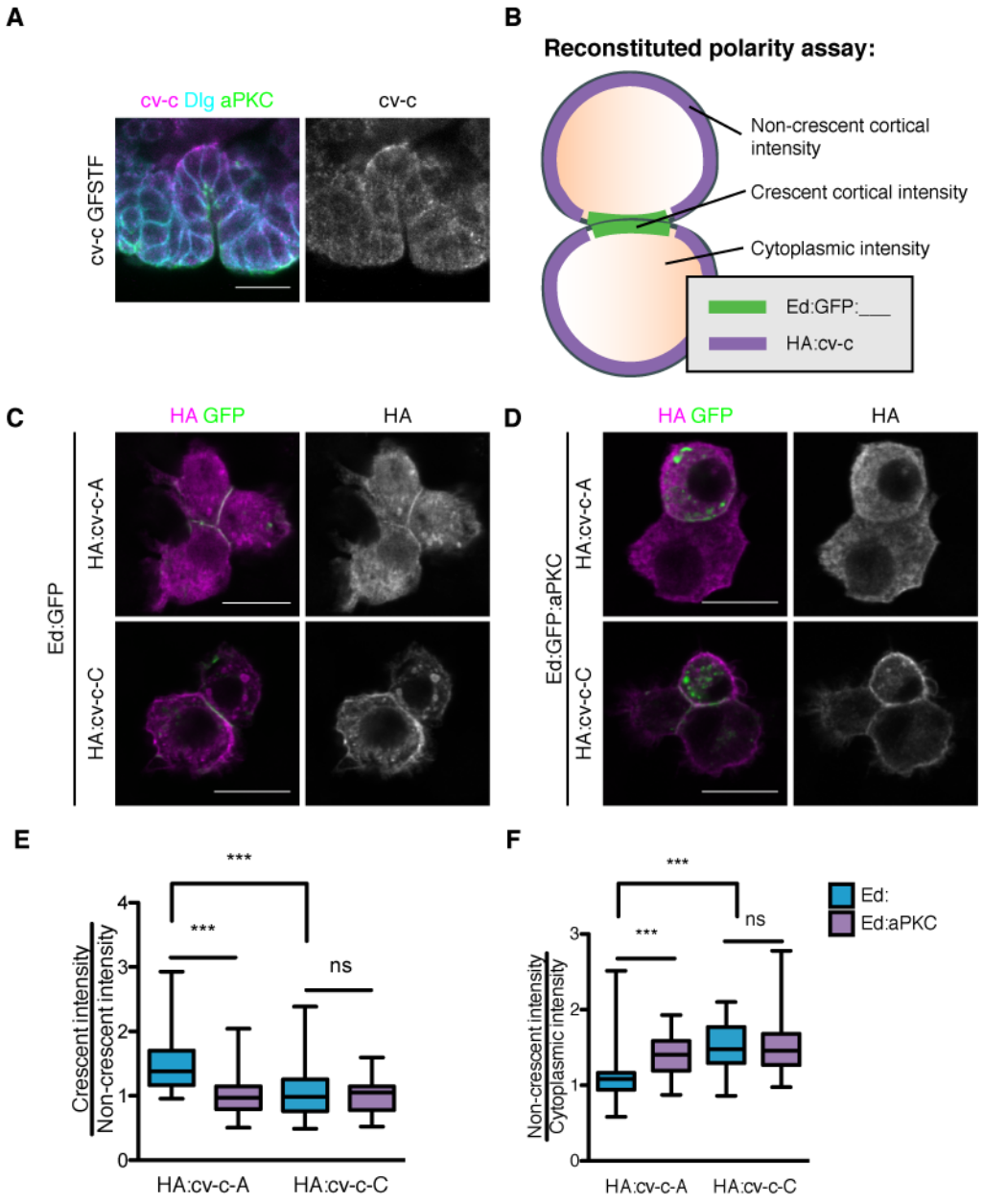

Figure 13. aPKC is sufficient to polarize Cv-c in a reconstituted polarity assay. (A) Cv-c is basal in embryonic epithelia during salivary gland formation. Immunostaining was performed on GFP (Cv-c, magenta), Dlg (cyan), aPKC (green). (B) Cartoon of the Ed assay. Ed concentrates at cell-cell contacts (green) and aPKC can be fused to its intracellular domain. We measured the average intensity at each of the following cellular regions: the Ed-containing cell-cell contacts (crescent intensity), the Ed-free cell cortex (non-crescent cortical intensity), and the cytoplasm. (C-D) Ed:aPKC polarizes Cv-c-A to cortical regions lacking aPKC. Representative images of S2 cells transiently transfected with Ed:GFP: constructs and HA:Cv-c isoforms. (E-F) Ed:aPKC polarizes Cv-c in S2 cells. Quantification of intensity ratios from Ed assay. Students t-test (two tailed, 95% confidence interval), where ns, not significant; ***$p < 0.001$. Scale bar, 10 µm.

but we could assess the endogenous localization of Cv-c with a "protein trap" line (i.e. Cv-c GFSTF) that endogenously tags Cv-c-C with GFP and several epitope tags (Nagarkar-Jaiswal et al., 2015a; Venken et al., 2011). Cv-c has a described role in embryonic morphogenesis, during apical constriction of epithelial cells during tube formation for the salivary gland, spiracles, and Malpighian tubules (Denholm et al., 2005). During salivary gland morphogenesis, Cv-c localizes to the basal region of the apically constricted epithelia (Figure 13A). We did not observe colocalization of Cv-c and aPKC, suggesting that it is not localized to the apical domain. The observed localization is similar to what has been previously reported for Cv-c transgenes (Simões et al., 2006), suggesting that these transgenes accurately report Cv-c subcellular localization in the spiracles. Thus, endogenous Cv-c localizes to the basolateral domain of epithelia.

aPKC is sufficient to polarize Cv-c in a reconstituted polarity assay

A prediction of a Par polarity model is that aPKC is sufficient to polarize its substrates by inhibiting their accumulation at aPKC-containing cortical domains (Prehoda, 2009). Previously, aPKC was shown to be sufficient to polarize Mira when aPKC was fused to the intracellular domain of the cell adhesion protein Echinoid (Ed), which concentrates at cell-cell contacts between S2 cells (Johnston et al., 2009). Exclusion of Mira from cell-cell contacts was not observed in the Ed control. We used this reconstituted polarity assay to assess whether Ed:aPKC is sufficient to polarize Cv-c

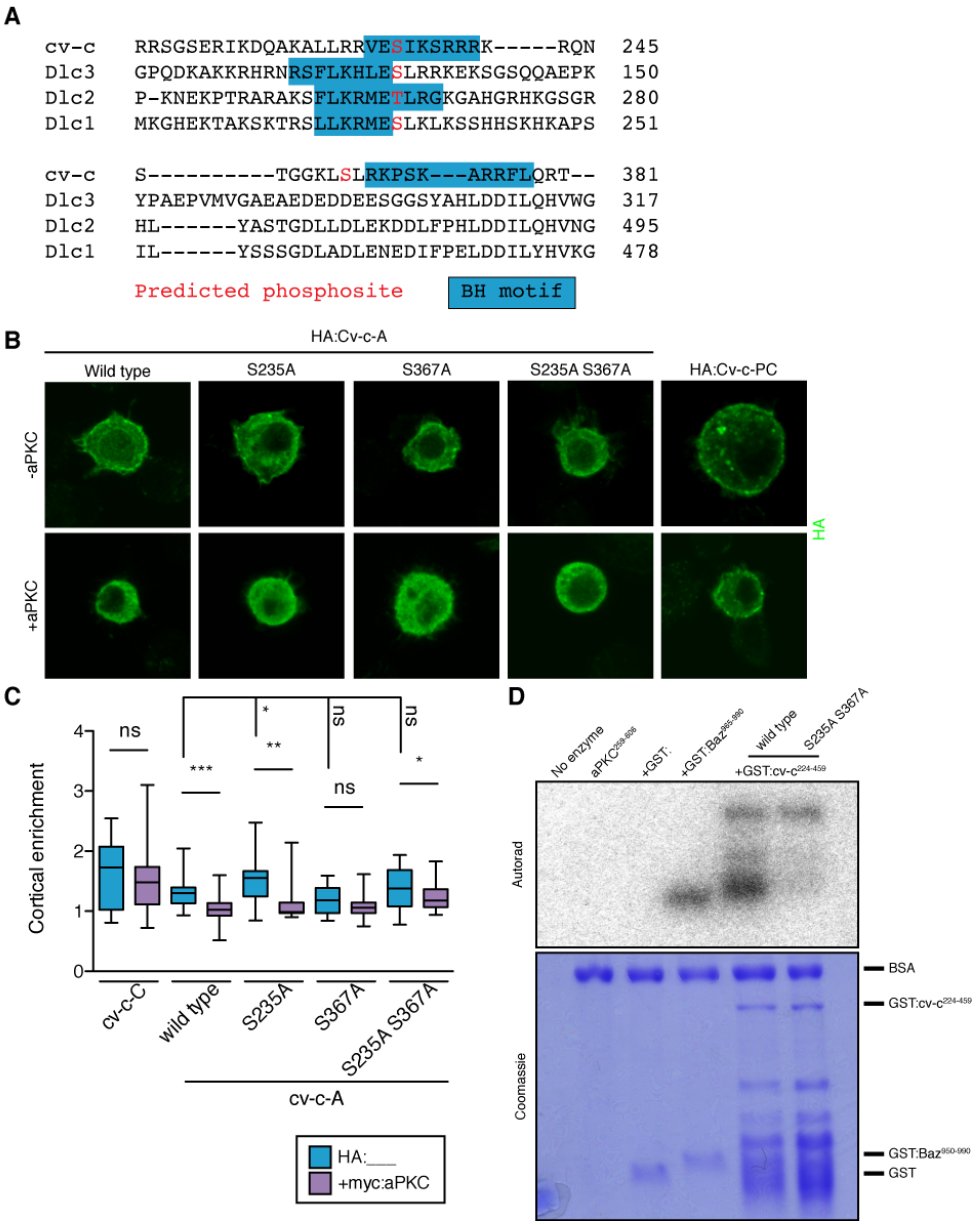

Figure 14. Site-specific phosphorylation mediates Cv-c cortical targeting. (A) Sequence of Cv-c PRBH motifs aligned to the sequence from its human orthologs. Predicted phosphosites are highlighted in red and BH motifs are highlighted in blue. (B) Cv-c mutants remain cortically enriched in the presence of aPKC. Representative images of S2 cells transiently transfected with HA:Cv-c mutants when singly transfected or cotransfected with myc:aPKC FL. (C) Quantification of cortical enrichment for HA:Cv-c mutants ± myc:aPKC FL. Student's t-test to compare transfections ± aPKC (two-tailed, 95% confidence interval), where ns, not significant; *p < 0.05, **p < 0.01, ***p < 0.001. Mutants were compared to their wild type control in single transfections by One-way ANOVA (two tailed, 95% confidence interval, Dunnet), where ns, not significant; *p < 0.05. (D) aPKC phosphorylates Cv-c phosphosite mutants. *In vitro* kinase assay with $aPKC^{259-606}$. GST: and $GST:Baz^{965-990}$ were included as negative and positive controls, respectively.

isoforms (Figure 13B). We observed enrichment of Cv-c-A at cell-cell contacts with the Ed control, quantified as a cortical intensity ratio of Ed-crescents vs cortical regions lacking Ed (Figure 13C and 13E). In cells transfected with Ed:aPKC, we found that Cv-c-A localization to Ed:aPKC-containing cell-cell contacts was significantly reduced (Figure 13D-E). In some cells Cv-c-A was polarized to cortical domains where aPKC was absent, suggesting that aPKC is sufficient to polarize Cv-c-A (Figure 13D and 13F). In both Ed controls and Ed:aPKC conditions Cv-c-C had equal enrichment to cortical regions with and without Ed, suggesting that aPKC is not sufficient to polarize Cv-c-C (Figure 13E-F). These data suggest that aPKC is sufficient to polarize Cv-c-A, but not Cv-c-C, in a reconstituted polarity assay.

Site-specific phosphorylation mediates Cv-c cortical displacement

We next sought to identify which residues may be involved in aPKC regulation of Cv-c subcellular localization. We first chose to mutate the S/T residues that we previously predicted to be putative aPKC phosphosites and contained within the predicted PRBH motifs (Figure 14A) (Bailey and Prehoda, 2015; Brzeska et al., 2010). We generated a series of S/T-to-A point mutants for Cv-c-A and assessed whether aPKC regulates their cortical localization. When overexpressed in S2 cells, these mutants localized to the S2 cell cortex similar to wild type, although S235A had a slight increase in cortical localization (Figure 14B-C). However, these mutants varied from wild type in their response to aPKC. While Cv-c-A lost cortical enrichment when myc:aPKC FL was cotransfected, the S/T-to-A mutants had a smaller loss in cortical enrichment (Figure

14B-C). aPKC failed to alter the cortical enrichment of Cv-c-A S367A, suggesting that this residue is important in regulating cortical targeting. We tested the ability of aPKC to phosphorylate several point mutants with reduced response to aPKC with the *in vitro* kinase assay. We observed little change in the amount of GST:Cv-c-A 224-459 phosphorylated by aPKC (Figure 14D), suggesting that aPKC phosphorylates Cv-c-A at many sites; but many phosphorylation sites do not influence cortical localization.

Site-specific phosphorylation regulates Cv-c polarization

Since aPKC does not inhibit cortical targeting of Cv-c mutants, we wanted to ask whether aPKC could polarize these mutants. We tested whether Cv-c was polarized by Ed:GFP or Ed:GFP:aPKC FL in our reconstituted polarity assay. We found that Ed:aPKC FL has a reduced ability to polarize Cv-c phosphosite mutants (Figure 15A). For Cv-c-A S235A S367A we found no statistically significant difference between Ed:GFP and Ed:GFP:aPKC FL in either of the following cortical intensity rations: non-crescent intensity-to-cytoplasmic intensity or crescent intensity-to-non-crescent intensity (Figure 15B-C). aPKC was still able to polarize Cv-c-A S367A as there were differences between Ed:GFP and Ed:GFP:aPKC FL for its localization to Ed-containing cell-cell contacts and Ed-free cortical regions (Figure 15B-C). These data suggest that phosphorylation of S235 and S367 mediate polarization of Cv-c.

DISCUSSION

The Par complex has an essential role in polarizing multiple proteins by phosphorylation (Goldstein and Macara, 2007). However, the mechanism by which phosphorylation

induces substrate polarization remains uncharacterized for multiple Par substrates. We previously found that the Par complex polarizes several substrates by phosphorylation of phospholipid binding sites that contain multiple basic and hydrophobic residues (Bailey and Prehoda, 2015). From this work, we hypothesized that the Par complex polarizes

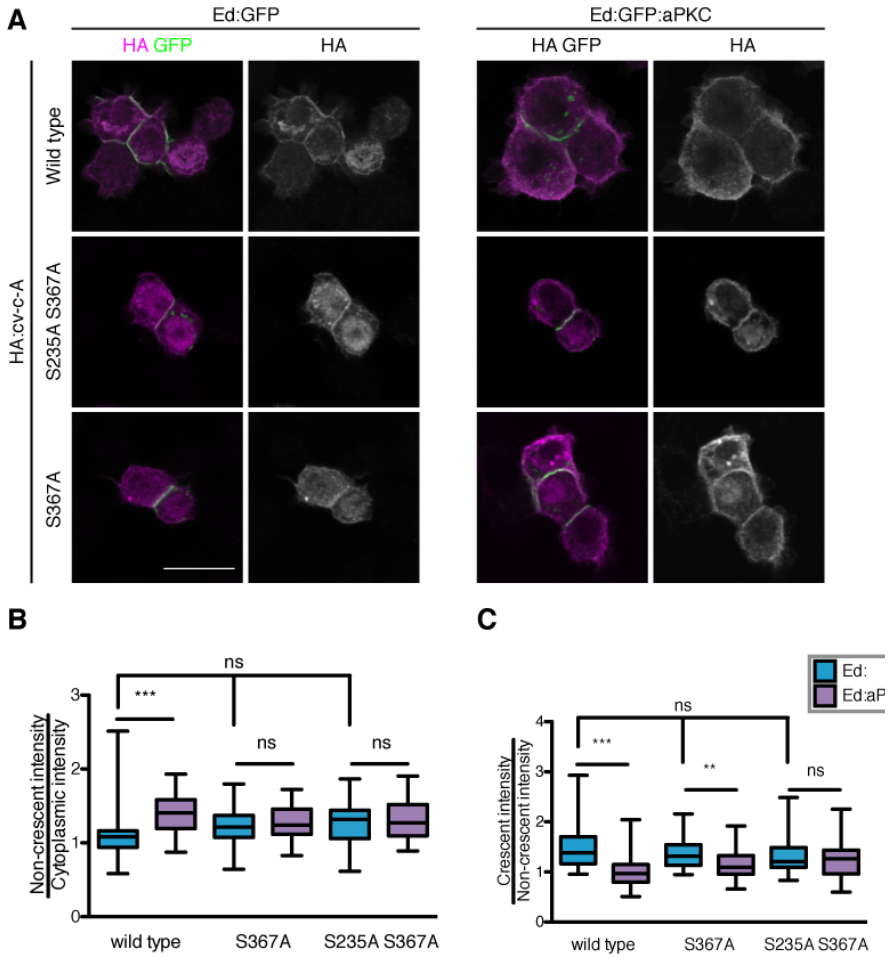

Figure 15. aPKC does not polarize Cv-c phosphosite mutants in a reconstituted polarity assay. (A) Representative images from S2 cells transiently transfected with HA:Cv-c constructs and Ed:GFP constructs. Scale bar, 10 µm. (B-C) Quantification of average intensity ratios for non-crescent vs cytoplasm and crescent vs non-crescent. Student's t-test to compare transfections ± aPKC (two-tailed, 95% confidence interval), where ns, not significant; ***$p < 0.001$. Mutants were compared to their wild type control in single transfections by One-way ANOVA (two tailed, 95% confidence interval, Dunnet), where ns, indicates $p > 0.05$.

other substrates by this mechanism. Here, we find that aPKC regulates cortical targeting and induces the polarization of Cv-c by PRBH motif phosphorylation. Although this polarization mechanism needs to be tested *in vivo*, this study identified an additional Par substrate with a phospho-regulated phospholipid binding-based polarization mechanism.

Cv-c regulates *Drosophila* morphogenesis by spatially inactivating Rho

Cv-c is a Rho GAP that regulates morphogenesis in *Drosophila* (Denholm et al., 2005). Cv-c is a downstream effector of Hox genes, and its transcription is activated in specific cells of the embryonic epithelium to initiate apical constriction and epithelial invagination (Lovegrove et al., 2006). Several null alleles of Cv-c are embryonic lethal due to abnormal embryonic morphogenesis including defects in dorsal closure. Previous work demonstrated that Cv-c is enriched in the basolateral region of the spiracle cells where it regulates tube formation through inhibition of Rho1 (Rho in *Drosophila*) (Simões et al., 2006). Guanine nucleotide exchange factors (GEFs) activity for Rho1 is apically enriched in these cells, such that Rho1 is specifically activated in the apical domain and influences actin dynamics (Simões et al., 2006). Previous studies have not identified a Cv-c that ectopically localizes to the apical domain. Future work will need to assess whether aPKC polarizes Cv-c *in vivo* and determine the physiological significance of its polarization.

Cv-c as an inhibitor of apical identity in epithelia

Recent work has shown Cv-c and its human orthologs to be potent regulators of epithelial polarity. A previous study characterized the effects of over-expressing Cv-c

transgenes with the Gal4-UAS system in the *Drosophila* embryo (Sotillos et al., 2013). This work found that over-expression of Cv-c in epithelia where Cv-c is not endogenously expressed induces dramatic changes to the epithelium, including a loss of apical polarity components and induction of cell migration. These adverse effects of Cv-c over-expression required Cv-c to have GAP activity, as a catalytically dead mutant transgene did not cause these effects. Interestingly, Cv-c caused a depletion in apical aPKC but did not cause a loss of Dlg cortical enrichment. This could be due to the reported GAP activity of Cv-c towards Cdc42 (Atwood et al., 2007; Denholm et al., 2005; Sato et al., 2010). This study found that co-expression of an aPKC transgene rescued the loss of epithelial polarity induced by Cv-c, suggesting that aPKC and Cv-c act as mutual inhibitors. Previous studies found that mutual inhibitory interactions between aPKC and Lgl are essential for polarity of multiple cell types (Betschinger et al., 2003). Future studies will need to assess whether endogenous Cv-c inhibits the Par complex and if this is of importance to epithelial polarity during morphogenesis. Cv-c could inhibit the Par complex by several mechanisms, such as inhibiting aPKC kinase activity, acting as a GAP towards Cdc42, or by an regulating the stability of adherens junctions (Denholm et al., 2005; Hendrick et al., 2016; Sato et al., 2010; Simões et al., 2006). Future studies will need to investigate the role of Cv-c in epithelial polarity, its potential role as an inhibitor of the Par complex, and whether Cv-c functions as a polarity modulator in morphogenesis.

Conservation of Cv-c function to its human orthologs

Cv-c has three human orthologs, the Deleted in liver cancer (DLC) family of genes (Braun and Olayioye, 2015). Deleted in liver cancer 1 (DLC1) was initially identified as a gene that is in a chromosomal region that is frequently lost, mutated, or epigenetically silenced in many human cancers (Durkin et al., 2007a; Yuan et al., 1998). Subsequent studies found DLC2 and DLC3 (also known as StarD13 and StarD8, respectively) to be associated with other human cancers (Ching et al., 2003; Durkin et al., 2007b; Nagaraja and Kandpal, 2004). Much of the sequence and function of Cv-c is conserved to DLC1-3, including the Rho GAP activity (Braun and Olayioye, 2015). A common function of the DLC proteins is localization to focal adhesions to inhibit Rho and destabilize the focal adhesion. The central linker region that contains the PRBH motifs in Cv-c has the least conservation between *Drosophila* and its human orthologs. Sequence changes in central linker region appear to have importance in sub-functionalizing DLC orthologs for distinct subcellular regions (Braun and Olayioye, 2015). For instance, DLC1 localizes to adherens junctions through interactions with the cadherin/catenin complex using a binding site in its linker region (Tripathi et al., 2012). This region of DLC1 also includes a CTEN and tensin2 binding site that confers localization to focal adhesions (Kawai et al., 2009, 2010; Liao et al., 2007). DLC1 also has a polybasic motif that binds phosphatidylinositol-4,5-bisphosphate (PIP_2) within this region that is necessary for its GAP activity (Erlmann et al., 2009). Alignments suggest that this binding site conserved to *Drosophila* and is not the site where aPKC phosphorylates Cv-c. Interestingly, DLC3 has the best homology to the Cv-c PRBH motif including residue S235, suggesting a potential conservation of an aPKC phosphorylation-

dependent polarization mechanism. Additionally, DLC3 is reported to localize to the adherens junctions of epithelial cells by binding Scribble, which assist in polarizing it to the basolateral region (Hendrick et al., 2016). While the BH character of DLC orthologs is only moderately conserved, the aPKC phosphosite S235A is strictly conserved (Figure 14A). However, it should be noted that the residues that flank this residue deviate from an aPKC consensus sequence most in DLC3. Future studies of DLC proteins should assess whether aPKC has a conserved role in their polarization and if regulation by aPKC is of importance to human cancer.

EXPERIMENTAL PROCEDURES

Molecular cloning

Molecular cloning was performed with traditional restriction enzyme-based methods and by Gibson assembly (New England Biolabs Gibson Assembly cloning kit) (Gibson et al., 2009). Briefly, PCR was performed with Q5 High-Fidelity DNA Polymerase (New England Biolabs). Briefly, Pak (isoform C, 704 amino acids (aa)), nullo (isoform B, 213 aa) and CG42748 (isoform C, 1710 aa) were cloned from the following DGRC clones: LD20767, RE47733, and GH01875, respectively. Varicose (isoform C, 469 aa), coracle (isoform B, 889 aa), and Cv-c (isoform C, 2351 aa; isoform A, 1017 aa) were cloned from a larval stage 3 (L3) cDNA library prepared from OregonR. Point mutations were generated by mutagenesis PCR or cloning from a synthetic gBlock (Integrated DNA Technologies). Plasmids were sequenced and sequence analysis was performed with ApE (Citation). Wandering OregonR L3 larvae were picked and homogenized and total RNA was isolated using Life Technologies

TRIZOL per the manufacturer's protocol. cDNA was generated using the Invitrogen SuperScript III First-Strand Synthesis System according to manufacturer's protocol for the oligo(dT)20 primer.

Cell culture

S2 cells were cultured according as previously described. Cells were grown at 27˚C in Schneider's media (Sigma-Aldrich) supplemented with 10% fetal bovine serum (Corning). Cells were transfected with the Qiagen Effectine Transfection Reagent per manufacturer's protocol. Cells were transfected with pMT plasmids that NH2-terminally tagged the protein of interest, unless noted otherwise. aPKC was transfected as pMT myc:aPKC FL (aa 1-606) and pMT Ed:GFP (with or without aPKC FL). Immunostaining was performed using standard methods (Bailey and Prehoda, 2015). Antibodies were used at the following dilutions: 1:1000 rat αHA (Roche 3F10), 1:100 mouse αmyc (Developmental Studies Hybridoma Bank, 9E10-c, (Evan et al., 1985)), 1:500 Cy3 αrat (Jackson ImmunoResearch), 1:500 Alexa 488 αrat (Jackson ImmunoResearch), 1:500 Alexa 647 αmouse (Jackson ImmunoResearch), and 555-Phalloidin (Thermo Fisher Scientific). The Ed assay was performed as previously described (Johnston et al., 2009). Briefly, cells were placed on an orbital shaker for 30 min at ~150 rpm, mixed by pipetting up and down, then allowed to settle on coverslips for 90 minutes.

Cells were imaged by using an Olympus Fluoview FV1000 BX61 with a PlanApo N 60x/1.4 oil objective. Images were analyzed with FIJI and the HA channel was extracted for quantification (Schindelin et al., 2012). All images were quantified blind for cortical to cytoplasmic intensity ratios, which were taken using both the line and freehand

selection tools to determine the mean values. Intensity ratios were calculated using Microsoft Excel, graphs were prepared by GraphPad Prism and statistical tests were performed with GraphPad Prism.

In vitro biochemistry

Proteins were cloned onto pGEX-4T1, then expressed in BL21 (DE3) cells as previously described (Bailey and Prehoda, 2015). Proteins were purified by affinity chromatography according to protocol for Pierce Glutathione Agarose (ThermoFisher Scientific), then dialyzed into 20 mM HEPES, pH 6.8, 100 mM NaCl, 1 mM DTT. Proteins were concentrated with a GE Vivaspin concentrator, 30 kDa molecular weight cut off. Kinase assays were performed as previously described (Bailey and Prehoda, 2015), with the following buffers: reaction buffer (20 mM HEPES, pH 6.8, 100 mM NaCl), enzyme dilution buffer (20 mM HEPES, pH 7.5, 100 mM NaCl, 1 μg/μL BSA, 1 mM DTT, 5 mM $MgCl_2$, and ATP dilution buffer (10 mM HEPES, pH 7.0).

Immunostaining *Drosophila* embryos

The following line was analyzed in this study: Bloomington 61805, y[1] w[*]; Mi{PT-GFSTF.0}Cv-c[MI00245-GFSTF.0]/TM6C, Sb[1] Tb[1]. Embryos were collected on standard Apple juice caps for 12 hours at 20˚C, then fix and immunostained as previously described (Kaczynski and Gunawardena, 2010; Lai and Doe, 2014). Briefly, embryos were bleached in 50% bleach for 3 minutes with gentle swirling and tapping, rinsed thoroughly with deionized water, dried briefly, then transferred to fix in a microfuge tube (500 μL of 4% paraformaldehyde in PBS, 500 μL of heptane) for 25-30

minutes while nutating. The heptane/formaldehyde mix was removed, then 700 µL heptane and 500 µL methanol were added. Immediately after adding methanol, tubes were vigorously smacked on the counter for one minute. The heptane/methanol mix was removed, and embryos were washed four times with methanol. Methanol was removed, and embryos were washed five times with embryo PBSBT (1xPBS, 1% BSA, 0.3% Trixon X-100). Embryo were blocked with PBSBT for 30 minutes at room temperature, then incubated with primary antibody for 16 hours at 4˚C. Primary antibody in PBSBT was removed, embryos were rinsed three times with PBSBT, then washed with PBSBT for 60 minutes. Embryos were incubated with secondary antibody in PBSBT for 90 minutes at room temperature, then given six ten minute washes with PBSBT. All PBSBT was removed, and embryos were stored in SlowFade Antifade reagent (ThermoFisher) overnight. Embryos were imaged with an Olympus Fluoview FV1000 BX61 with a PlanApo N 40x/1.4 oil objective.

The following antibodies were used for characterizing embryos: 1:5000 Chicken αGFP (Abcam, ab13970), 1:100 Mouse αDlg (Developmental Studies Hybridoma Bank, 4F3-c, (Parnas et al., 2001)), 1:1000 rabbit αPKCζ (Santa Cruz Biotechnology, C-20, sc-216), 1:500 Alexa 488 αchicken (Jackson ImmunoResearch), 1:500 Cy3 αmouse (Jackson ImmunoResearch), 1:500 Alexa 647 αrabbit (Jackson ImmunoResearch).

Data analysis and figure preparation

Data was analyzed with the following programs: Microsoft Office, GraphPad Prism, Adobe Creative Suite, FIJI (Schindelin et al., 2012), ApE. Sequence alignments performed with Clustal Omega (Sievers et al., 2011).

ACKNOWLEDGEMENTS

Thanks to the Prehoda lab for feedback on the project, edits on the manuscript, and useful discussions. Thanks to Ryan Holly for providing some purified proteins. Special thanks to Kate Walsh and the lab of Chris Doe for providing training on immunostaining embryos. This work was supported by the NIH Predoctoral Training grant GM007759 (M.J.B.) and NIH grant GM068032 (K.E.P.).

BRIDGE TO CHAPTER IV

In this chapter, I described a screen for aPKC substrates that are polarized by PRBH motif phosphorylation. I focus on proteins that previous studies found to localize to polarity domains that lack the Par complex. In this study, found that aPKC regulates the localization of Cv-c in S2 cells. Furthermore, I found that aPKC polarizes Cv-c in an *ex vivo* reconstituted polarity assay. This work further validates PRBH motifs to be a sequence element that allows a substrate to be polarized to cortical domains that lack the Par complex. In the next chapter, I describe a screen for basal/basolateral PRBH motif-containing proteins for which the sub-cellular localization has not been described previously. This screen identified a protein product of a *Drosophila* candidate gene to localize to the basolateral domain of epithelial cells, and characterized its cortical targeting mechanism.

CHAPTER IV

DROSOPHILA CG6454 IS A CALCIUM-DEPENDENT BASOLATERAL PROTEIN

This chapter contains unpublished co-authored material with Alaní M. Estrella, K.E. Prehoda. All experimental work was performed by me or A.E. Estrella under my direction. I wrote the manuscript. K.E. Prehoda supervised the project and contributed to project design.

SUMMARY

The Par complex has an essential role in cell polarity through the activity of atypical protein kinase C (aPKC). In this study, we set out to find additional aPKC substrates that are polarized by the Par complex. We performed an *in vivo* screen for polarized proteins in the larval central nervous system of *Drosophila* by characterizing the localization proteins with linear motifs that are both putative phospholipid binding sites and aPKC consensus sequences. This screen identified the protein product of a candidate gene, CG6454, to be basolateral in epithelial cells. We characterized two CG6454 isoforms: a long isoform that contained the putative PRBH motifs and a short isoform lacked the putative PRBH motifs in cultured cells. We found that CG6454 has a Ca^{2+}-dependent C2 domain but that the long isoform remains cytoplasmic upon Ca^{2+} stimulation. Furthermore, this suggested that aPKC is not likely to regulate cortical

targeting of CG6454 by PRBH motif phosphorylation. This study identified CG6454 to be a basolateral protein with Ca^{2+}-dependent cortical targeting.

INTRODUCTION

Animals have many types of polarized cells, which are characterized by the asymmetric distribution of molecular contents within the cell (Goehring, 2014; Goldstein and Macara, 2007; Overeem et al., 2015). The polarization of specific proteins and RNAs can serve functions that include regulation of cell fate changes, directing cell motility, and regulation of nutrient transport across an epithelial sheet. A remarkable finding from the characterization of many different types of polarized cells is that the Partitioning-defective (Par) complex is a key regulator of polarity in neurons, epithelia, neural stem cells (neuroblasts), and migratory cells (Etienne-Manneville and Hall, 2001; Joberty et al., 2000; Knust and Bossinger, 2002; Lin et al., 2000; Shi et al., 2003; Solecki et al., 2004). Many of the downstream effectors of the Par complex are cell-type specific, which suggests that proteins plug into the Par polarity machinery to localizes to a subcellular region where the protein should perform a specific function (Drummond and Prehoda, 2016).

The Par complex includes the RhoGTPase Cdc42, its binding partner Par6, and the serine/threonine protein kinase aPKC (atypical protein kinase C) (Joberty et al., 2000; Lin et al., 2000; Wodarz et al., 2000). A network of interactions ensure that apical localization and activation of the Par complex are tightly coupled (Drummond and Prehoda, 2016). The localized and activated Par complex then regulates the localization of effectors largely through the kinase activity of aPKC. aPKC polarizes several of its

substrates by phosphorylation; which, in the case of the substrates Lethal (2) giant larvae (Lgl), Miranda (Mira), Numb, Par1, and PAR-2, excludes them from the cortical domain occupied by the Par complex (Atwood and Prehoda, 2009; Betschinger et al., 2003; Hao et al., 2006; Hurov et al., 2004; Smith et al., 2007; Suzuki et al., 2004; Zhang et al., 2001a, 2001b).

Recently, work by us and others have found that aPKC phosphorylates a phospholipid binding site on Lgl, Mira, Numb, and PAR-2, thereby inhibiting localization to membrane domains where the Par complex localizes (Bailey and Prehoda, 2015; Dong et al., 2015; Motegi et al., 2011; Visco et al., 2016). We found that aPKC regulates the localization of these proteins through a similar effector sequence that confers phospholipid binding by Basic and Hydrophobic (BH) residues and contains an aPKC phosphosite (Bailey and Prehoda, 2015). The sequence similarities allowed us to design a linear motif prediction program to identify BH motifs that contain an aPKC consensus sequence, and thus, have the potential for Phospho-Regulation (i.e. a PRBH motif). Here, we test whether the phospho-regulation of phospholipid binding is general mechanism of Par substrate polarization by performing a screen for polarized proteins with putative PRBH motifs. This screen identifies a previously uncharacterized basolateral protein CG6454 for which we characterize the localization mechanism.

RESULTS

Identification of a previously uncharacterized basolateral protein

To identify proteins that aPKC polarizes by phosphorylation, we performed a screen for polarized PRBH motif-containing proteins. In our previous work, we identified 1436 proteins with putative PRBH motifs in the *Drosophila* proteome (Bailey and Prehoda, 2015). Few of these proteins have antibodies for characterization of endogenous protein localization. However, endogenous expression and localization of a subset of candidates can easily be assessed by characterizing the localization of GFP in Recombination-Mediated Cassette Exchange (RMCE) lines (Nagarkar-Jaiswal et al., 2015b, 2015a; Venken et al., 2011). RMCE were generated using a transposon-based integration of a cassette at a Minos-Mediated Integration Cassette (MiMIC) site within a gene's intronic region. The cassette includes a sequence for SA-EGFP-FIAsH-StrepII-TEV-3xFLAG-SD (abbreviations as follows: SA, splice acceptor; FIAsH, a site for covalent attachment of dye; StrepII, a streptavidin-like tag for protein purification; SD, splice donor), which allow for analysis of protein expression and subcellular localization.

The larval central nervous system has several types of polarized cell types including epithelia and neuroblasts, making it an excellent tissue to characterize in a screen for novel polarized proteins. We searched Flybase for proteins for which a RMCE line was available, contained a predicted PRBH motif, and is expressed in the larval central nervous system (CNS) at moderate or higher levels. From this list of proteins, we then excluded proteins that contained a transmembrane (TM) regions or signal peptides for secretion. This left us with a list of 14 candidate proteins with a range of PRBH scores (Supplemental Table 1, Supplemental Figure 5A). We characterized the expression and

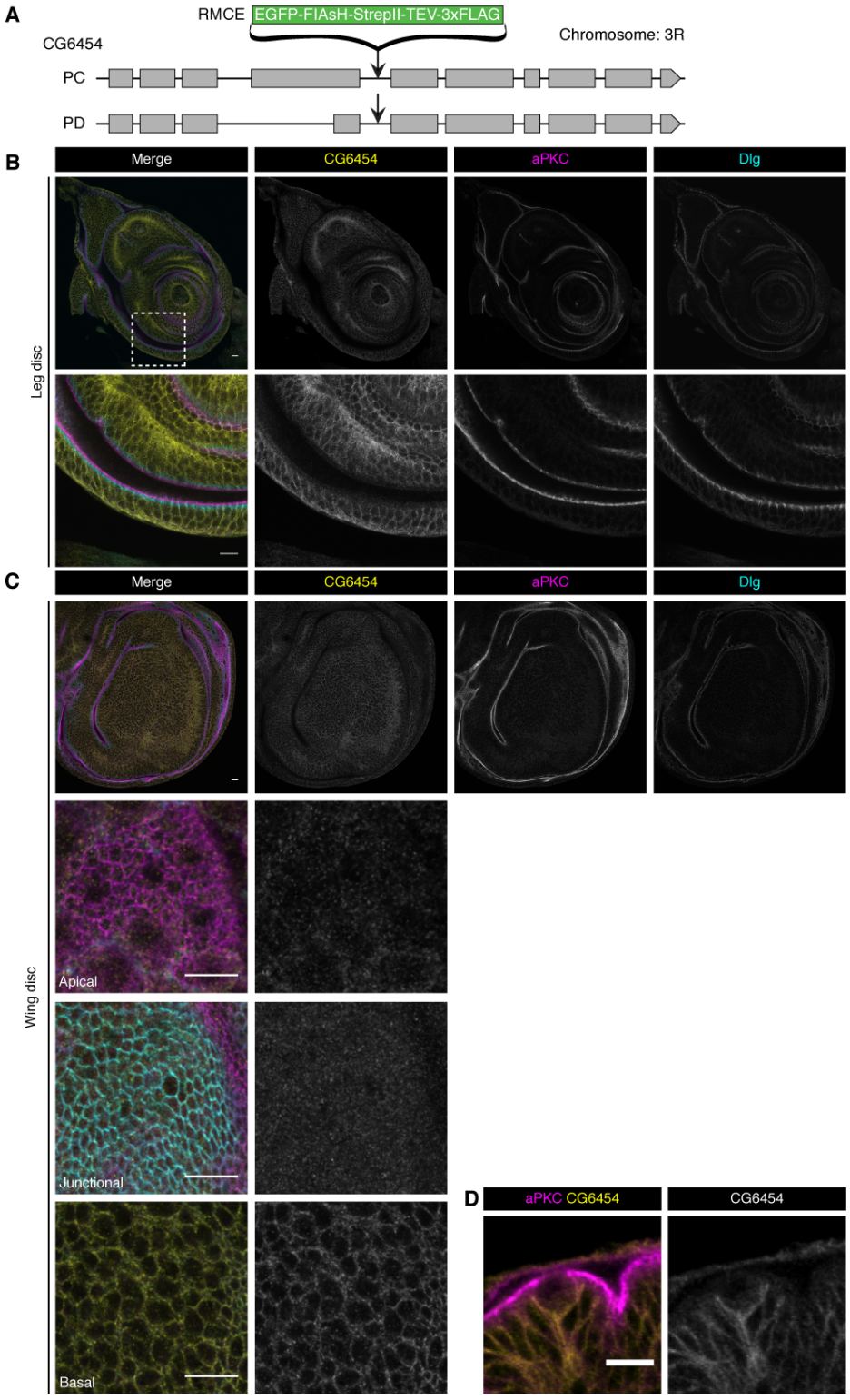

Figure 16. CG6454 is polarized in epithelial cells. (A) Organization of the CG6454 gene region. (B) CG6454 is basolateral in the L3 leg disc. (C) CG6454 is L3 basolateral wing disc, with a z-series to show the apical, junctional, and basal regions of cells in the wing disc. (D) CG6454 retains basolateral localization in mitotic cells in the optic lobe epithelium. Scale bar, 10 µm.

subcellular localization for these proteins with their respective RMCE lines, eleven of which had detectable expression of GFP (Supplemental Figure 5B). Of these, Lgl, alpha-catenin (α-cat) and CG6454 were polarized in cells of the larval brain, including the epithelial cells of the optic lobe. Since Lgl is a well-characterized polarity protein and we have previously shown that aPKC does not regulate α-cat localization in Schneider 2 (S2) cells in an associated manuscript (Figure 12C-D), we chose not to investigate them further here.

We decided to characterize CG6454 subcellular localization further in the imaginal discs, a tissue of proliferative epithelial cells where CG6454 was highly expressed (Aldaz and Escudero, 2010). The protein trap is predicted to label both isoforms (Figured 16A) and RNA-sequencing data indicates that both isoforms are expressed in this tissue (Cherbas et al., 2011). In the epithelial cells of the imaginal discs, CG6454 was basolateral (Figure 16B-D). aPKC and Discs large (Dlg) localize to the apical domain and septate junctions, respectively (Wodarz et al., 2000; Woods et al., 1996). CG6454 does not colocalize with either of these polarity markers, but localizes basal to the septate junction protein Dlg in both the wing and leg antennal discs (Figure 16B-C). Interestingly, CG6454 retains its basolateral localization throughout the cell cycle as it does not colocalize with either aPKC or Dlg in mitotic cells in the imaginal discs (Figure 16D). From these data, we conclude that CG6454 localizes to the basolateral domain of epithelial cells.

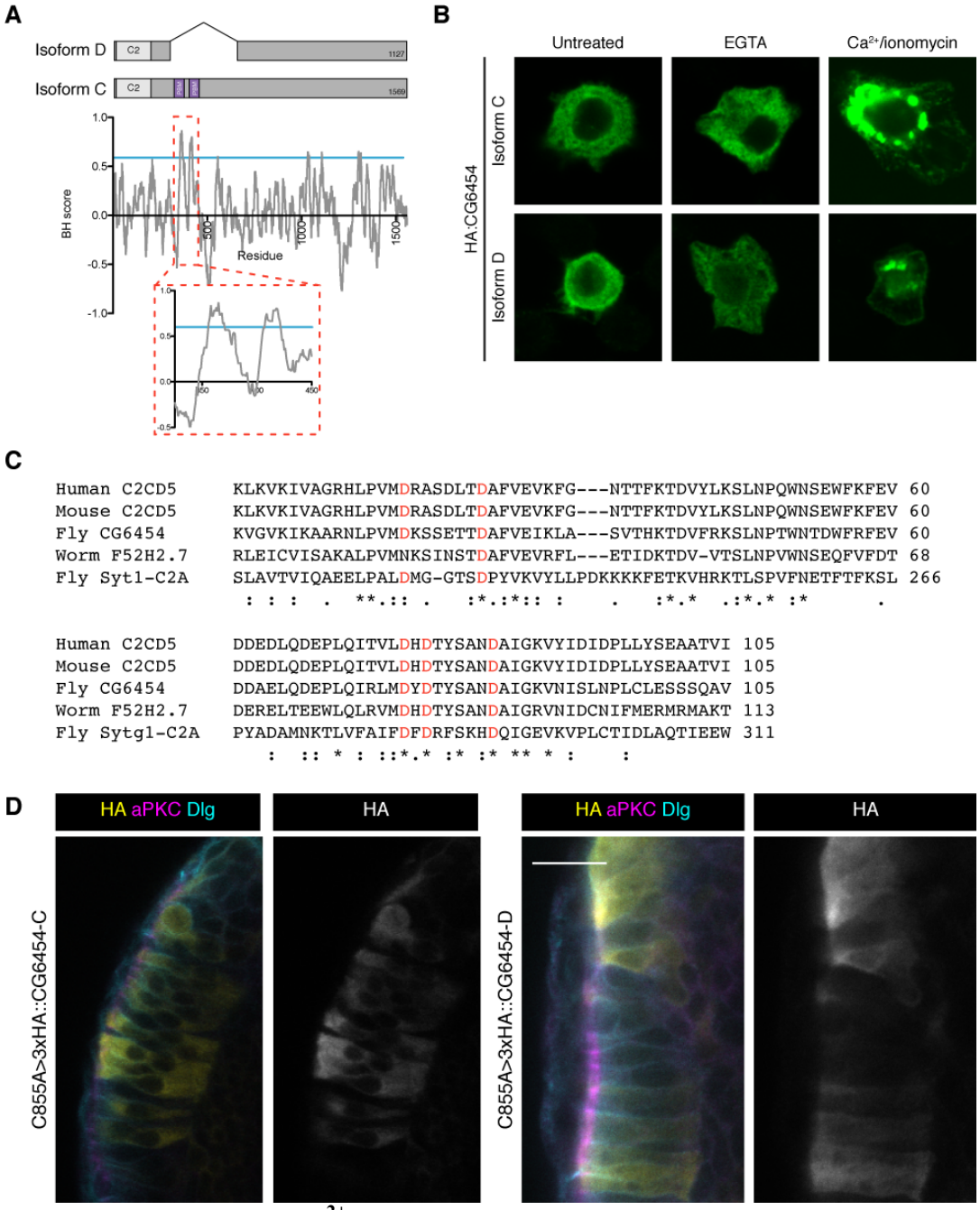

Figure 17. CG6454-D has Ca^{2+}-dependent membrane localization. (A) Domain architecture of CG6454 isoforms highlighting the putative PRBH motifs that are exclusively in the C isoform. (B) Representative images of S2 cells transiently transfected with HA:CG6454 isoforms and treated with either EGTA or Ca^{2+}/ionomycin. (C) Alignment of the C2 domain of CG6454/C2CD5 orthologs (continued from previous page) highlighting the conservation of aspartic acid residues that are important for Ca^{2+}-dependent phospholipids (red). *Drosophila* synaptotagmin 1 (Syt1) has a characterized Ca^{2+}-dependent C2 domain. (D) 3xHA::CG6454 is cytoplasmic when over-expressed in the optic lobe epithelium with the C855A-Gal4 driver. Scale bar, 10 µm.

CG6454 has a Ca^{2+}-dependent C2 domain for membrane targeting

CG6454 is the fly homolog of vertebrate C2 calcium dependent domain containing 5 (C2CD5; also called CDP138 and KIAA0528), which mediates insulin signaling through regulating endocytosis (Xie et al., 2011). *Drosophila* has two isoforms of CG6454, the longer of which (isoform C, CG6454-C) contains an extended fourth exon that is unique to *Drosophila* (Figure 16A and 17A). We cloned both isoforms of CG6454 from a larval cDNA library to determine their localization mechanisms. First, we characterized the localization of CG6454 isoforms in S2 cells (Figure 17B). We predicted that the putative PRBH motifs in CG6454-C would confer stronger cortical localization than isoform D (CG6454-D) because of PRBH motif-mediated cortical targeting (Figure 17A). When transfected into S2 cells, we found CG6454 isoforms to localize to the cytoplasm, similar to the reported localization for human C2CD5 (Figure 17B) (Xie et al., 2011). Previously, C2CD5 was demonstrated to have Ca^{2+}-dependent C2 domain (Xie et al., 2011). The residues involved in Ca^{2+}-dependent phospholipid binding are conserved to *Drosophila* (Figure 4-2C). Since other Ca^{2+}-dependent C2 domains are cytoplasmic when over-expressed in cultured cell unless an increase of intracellular Ca^{2+} is induced (Ananthanarayanan et al., 2002; Stahelin et al., 2003), we tested whether increasing cytosolic Ca^{2+} levels would localize CG6454 to the plasma membrane. We treated S2 cells with either EGTA (negative control) or Ca^{2+} and ionomycin for 1-2 minutes prior to fixing and immunostaining. We found that Ca^{2+} and ionomycin caused CG6454-D to accumulate at the plasma membrane (Figure 17B). Surprisingly Ca^{2+}/ionomycin had a less profound effect on the localization of CG6454-C, as it either

retained diffuse cytoplasmic localization or acquired filamentous and punctate localization in Ca^{2+}-/ionomycin-treated cells (see Figure 17B and Figure 17A). Future studies will need to assess why CG6454-C is unresponsive to Ca^{2+} and how its unique central region inhibits localization to the plasma membrane.

We additionally assessed whether over-expression of CG6454 transgenes recapitulated the localization of the endogenous protein observed in the RMCE line. We over-expressed 3xHA-tagged CG6454 isoforms using the Gal4-UAS system and the epithelial C855A driver (Brand and Perrimon, 1993; Hrdlicka et al., 2002). Surprisingly, we found that both CG6454 isoforms had cytoplasmic localization in the optic lobe epithelium (Figure 17D). CG6454-C localization was diffuse and cytoplasmic while CG6454-D also localized to the nucleus, as was observed in S2 cells (Figure 17D and Figure 18A). Since the RMCE line tags CG6454 in a flexible region and this protein trap is expressed at endogenous levels, we suspect that the CG6454 RMCE more accurately represents the CG6454 localization than the transgene over-expression. Due to the dependence of the C2 domain on intracellular Ca^{2+} for membrane localization, we predict that the over-expressed transgene has ectopic cytoplasmic localization, perhaps due to insufficient intracellular Ca^{2+} levels. Future studies will be needed to dissect the mechanism to polarize CG6454 *in vivo*.

aPKC does not regulate CG6454 localization to the plasma membrane

The polarized localization of CG6454 *in vivo* prompted us to inquire whether aPKC regulates cortical targeting of CG6454 isoforms. We tested this by cotransfecting

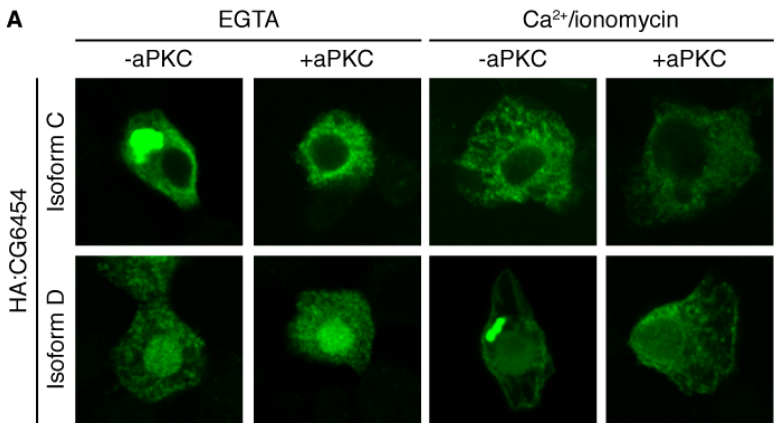

Figure 18. aPKC does not regulate CG6454 localization to the plasma membrane. Representative images from transfections of S2 cells with HA:CG6454 isoforms and myc:aPKC when treated with EGTA or Ca^{2+}/ionomycin for 1-2 minutes.

S2 cells with HA:CG6454 isoforms and myc:aPKC full length (FL), then treating S2 cells with either EGTA or Ca^{2+} and ionomycin. As we observed above, CG6454-C was cytoplasmic in most cells regardless of whether aPKC was cotransfected. CG6454-D localization to the plasma membrane was independent of aPKC in cells transfected with myc:aPKC FL (Figure 18A). Surprisingly, we found an increase in cytoplasmic and punctate localization for CG6454-D when cotransfected with myc:aPKC FL and treated with Ca^{2+}/ionomycin (Figure 18A). However, since we did not observe a localization difference for CG6454-C in cells co-expressing aPKC, we conclude that aPKC is unlikely to polarize CG6454 by PRBH motif phosphorylation.

DISCUSSION

The Par complex has the remarkable ability to polarize many proteins in cells with divergent morphologies (Goehring, 2014; Tepass, 2012). It is still an open question of how the Par complex recognizes proteins to polarize and how it mechanistically induces their polarization. We previously found that the Par complex polarizes several

substrates by phosphorylation of a phospholipid binding site, thereby inhibiting localization to membrane domains where the Par complex resides. In this study, we performed a screen for additional proteins that the Par complex polarizes by this mechanism. We identified *Drosophila* candidate gene CG6454 localizes to the basolateral domain of epithelial cells; however, further characterization of this protein suggests that the Par complex does not directly polarize it by phosphorylation. Future studies will need to determine the minimal region that is sufficient for polarization and how proteins and/or phospholipids target CG6454 to the basolateral domain.

CG6454, the *Drosophila* homolog to C2CD5 is a conserved protein that is expressed in many tissues in *Drosophila*. Our sequence analysis suggests that the long isoform is unique to *Drosophila*. We were unable to determine a physiological function for CG654 in *Drosophila,* and it has few identified binding partners that might provide clues. Additional studies with RNAi and isolation of CG6454 null alleles will be needed to determine its physiological function. The human homolog C2CD5 has been implicated in regulation of insulin signaling by targeting the GLUT4 glucose receptor to the plasma membrane upon insulin signaling (Xie et al., 2011). A second study found that human C2CD5 binds CDK5 and fibroblast intracellular binding protein (FIBP) to regulate cell growth and migration (Xu et al., 2014). In *C. elegans* the C2CD5 homolog, candidate gene F52H2.7, was found to have a dramatically different phenotype as its RNAi led to embryonic lethality due to polar body extrusion defects (Sönnichsen et al., 2005). Further characterization of CG6454 is needed to determine its physiological function in *Drosophila* and whether its function in cell migration, insulin signaling, or meiosis is conserved.

EXPERIMENTAL PROCEDURES

Molecular cloning was performed using standard restriction enzyme based methods. CG6454 was cloned from a larval cDNA library prepared from OregonR. CG6454 isoforms were cloned into pUAST 3xHA attB, and recombined at the attP2 site on chromosome III for experiments with the CG6454 transgenes. S2 cells were transfected with pMT HA:CG6454 isoforms as previously described. S2 cells were fixed and immunostained as previously described (Bailey and Prehoda, 2015). For Ca^{2+}/ionomycin treatments, S2 cells were treated with Ca^{2+}/ionomycin solution (1 mM HEPES, pH 7.4, 2.5 mM $MgCl_2$, 1 mM NaCl, 0.6 mM D-glucose, 6.4 mM sucrose, 10 μM ionomycin, 1 mM $CaCl_2$) or EGTA solution (1 mM HEPES, pH 7.4, 2.5 mM $MgCl_2$, 1 mM NaCl, 0.6 mM D-glucose, 6.4 mM sucrose, 2 mM EGTA) for 1-2 minutes as previously described (Stahelin et al., 2003), then fixed by adding paraformaldehyde solution to a final concentration of 4% in phosphate-buffered saline (PBS).

Antibodies were used at the following dilutions: 1:100 mouse αmyc (Developmental Studies Hybridoma Bank, 9E10-c, (Evan et al., 1985)), 1:3000-1:5000 Chicken αGFP (Abcam, ab13970), 1:100 Mouse αDlg (Developmental Studies Hybridoma Bank, 4F3-c, (Parnas et al., 2001)), 1:1000 rabbit αPKCζ (Santa Cruz Biotechnology, C-20, sc-216), 1:1000 rat αHA (Roche 3F10), 1:500 Alexa 488 αchicken (Jackson ImmunoResearch), 1:500 Alexa 488 αmouse, 1:500 Cy3 αrat (Jackson ImmunoResearch), 1:500 Cy3 αmouse (Jackson ImmunoResearch), 1:500 Alexa 488 αrat (Jackson ImmunoResearch), 1:500 Alexa 647 αmouse (Jackson ImmunoResearch), 1:500 Alexa 647 αrabbit (Jackson ImmunoResearch).

The following RMCE fly lines were used for this study (Nagarkar-Jaiswal et al., 2015b, 2015a; Venken et al., 2011): L(2)gl (Bloomington line 63183), Ask1 (Bloomington line 59799), CG6454 (Bloomington line 60264), Ptpmeg (Bloomington line 61799), PhKgamma (Bloomington line 61784), Nedd4 (Bloomington line 63185), Acsl (Bloomington line 59291), Btk29a (Bloomington line 61656), Rim (Bloomington line 60200), Svp (Bloomington line 63154), α-cat (Bloomington line 59405), Htt (Bloomington line 60215), Hers (Bloomington line 60255), pum (Bloomington line 59818), C855A-Gal4 (Bloomington line 6990), attP2 (Bloomington line 36303). Dissection and immunostaining of tissues was performed with standard methods, as previously described (Daul et al., 2010; Spratford and Kumar, 2014).

Figures were prepared using the Adobe suite. Images were processed with FIJI (Schindelin et al., 2012). Sequence alignment was performed with MUSCLE (Edgar, 2004).

ACKNOWLEDGEMENTS

Thanks to the Prehoda lab for feedback on the project, comments on the manuscript, and useful discussions. Special thanks to Kimberly Jones for training and invaluable discussion on working with *Drosophila.* This work was supported by the NIH Predoctoral Training grant GM007759 (M.J.B.) and NIH grant GM068032 (K.E.P.).

BRIDGE TO CHAPTER V

In this Chapter, I described an *in vivo* screen of putative PRBH motif-containing proteins that attempted to identify proteins that the Par complex polarizes by

phosphorylation. This screen identified a *Drosophila* candidate gene to be basolateral in epithelia but also found that aPKC does not regulate its localization. In the next chapter, I summarize the findings of this dissertation, evaluate screens for polarized PRBH motif-containing proteins, and discuss areas that should be of interest to future studies.

CHAPTER V

THE MECHANISM OF PAR COMPLEX SUBSTRATE POLARIZATION: CONCLUSIONS AND PROSPECTS

SUMMARY

The Par complex has an essential role in the polarization of animal cells that requires it to recognize specific substrates, then localize these substrates to a polarity domain (Goldstein and Macara, 2007). Previous studies have shown that the kinase activity of aPKC is particularly important in the polarization of many substrates including Lethal (2) giant larvae (Lgl), Miranda (Mira), Numb, Par-1, and PAR-2 (Atwood and Prehoda, 2009; Betschinger et al., 2003; Hao et al., 2006; Hurov et al., 2004; Zhang et al., 2001b). Prior to this work, our understanding of the polarization mechanism of Par substrates was limited to PAR-2 (Motegi et al., 2011). The work described here as well as recent work by others shows that the Par complex polarizes Lgl, Mira, and Numb by phosphorylation of a charge-based phospholipid binding site (Bailey and Prehoda, 2015; Dong et al., 2015; Visco et al., 2016). The negative charge of the phosphorylation alters the electrostatics of this phospholipid binding site to reduce the affinity for phospholipids, and disrupts localization to the plasma membrane. The sequence similarities between the phospho-regulated phospholipid binding sites on these proteins suggests that these proteins acquired this sequence convergent evolution.

The similarities in polarization mechanisms for Par substrates made me hypothesize that the Par complex polarizes its substrates by a common mechanism, and that I could identify other polarized Par substrates by having Phospho-Regulated

phospholipid binding sites (or Phospho-Regulated Basic and Hydrophobic motifs, PRBH motifs). To test this hypothesis, I performed two screens for novel Par-polarized substrates. The first screen assessed whether basal/basolateral proteins are aPKC substrates that the Par complex polarizes through phosphorylation. This screen identified crossveinless-c (Cv-c) to be an aPKC substrate that is polarized by site-specific phosphorylation. The second screen characterized the localization of putative PRBH motif-containing proteins in the larval central nervous system of *Drosophila*. This screen identified CG6454 to be basolateral in epithelial cells, however further characterization of this protein using cell culture found that is unlikely to be polarized by an aPKC phosphorylation of a PRBH motif. Further studies will be needed to determine the polarization mechanism of CG6454. Identification of Cv-c as an additional Par-polarized protein provides further evidence that PRBH motifs are important sequences in the polarization of Par substrates.

In the remainder of this chapter, I will discuss several topics related to Par substrate polarization mechanisms. These include a further dissection of PRBH motifs and their potential role in microtubule binding, the role of multivalent interactions with the cell cortex in substrate polarization, an assessment of the screens described in Chapters III and IV, and concluding remarks.

DISCUSSION

Polybasic motifs: phospholipid and/or microtubule binding sites in Par substrate polarization

A string of basic residues, or a polybasic motif, can localize a protein to several different subcellular structures, including the nucleus, membranes, and microtubules. Subtypes of polybasic motifs include Basic and Hydrophobic (BH) motifs, Nuclear localization sequences (NLS), and microtubule binding domains (MTBD). Prediction of the subcellular localization of a protein from a linear motif of basic residues often is difficult because of the similarities between these sequences. Several studies have found that hydrophobic residues adjacent to polybasic motifs (i.e. BH motifs) can repress nuclear localization by inserting into the plasma membrane (Heo et al., 2006; Nakanishi et al., 2004; Takahashi and Pryciak, 2007; Winters et al., 2005). In contrast to a NLS and BH motifs, MTBDs can be permissive of acidic residues, as suggested by the microtubule binding sequence of MAP1B: KKEE and KKEVI (Noble et al., 1989). Additional work should evaluate how these subtypes of polybasic motifs are differentially regulated by phosphorylation.

The sequence similarities between these different subtypes of polybasic motifs suggests that a single BH motif might bind either phospholipids or other molecules depending on upstream signaling. Characterization of the PAR-2 polarization mechanism found this to be the case as its BH motifs bind both phospholipids and microtubules (Motegi et al., 2011). Motegi *et al*. found that PKC-3 (the *C. elegans* aPKC homolog) phosphorylation of PAR-2 dramatically inhibited phospholipid binding but caused only a minor reduction in microtubule binding. Furthermore, this study found that microtubule

binding reduced the ability of PKC-3 to phosphorylate PAR-2. The interplay between microtubules, PKC-3, PAR-1, and PAR-2 were all necessary for posterior localization of PAR-2 in the *C. elegans* zygote. This study provides a fascinating model for BH motifs being a multifaceted localization tool that uses the mitotic spindle as a potential sink for phosphorylated PAR-2. Future studies will need to assess whether microtubule-localized phosphatases assist in recycling PAR-2 to the posterior cortex. Additionally, these studies will need to determine if this mechanism can be generalized to other BH motif-containing aPKC substrates. Mira is an excellent candidate as it ectopically localizes to the mitotic spindle in specific cellular contexts and several mutant backgrounds (Albertson and Doe, 2003; Mollinari et al., 2002). Future studies should assess if an interaction between microtubules and PRBH motifs polarize other Par substrates and whether asymmetry in the mitotic spindle can rescue substrate polarization at telophase (Derivery et al., 2015).

Multivalent interactions in protein polarization

Many polarity proteins have a modular domain architecture for interactions with multiple proteins and/or lipids at the cell cortex. These domains often function in targeting a polarity protein to the membrane, as in the case of aPKC C1 domain, or to a specific polarity domain, as in Numb PTB domain's interaction with Pon (Lu et al., 1998). Determining the mechanism of basal protein targeting was particularly difficult for Par substrates because each substrate has unique domains for binding proteins and/or lipids at the cell cortex. Identification of PRBH motifs in Lgl, Mira, Numb, and Cv-c provides clues regarding a general mechanism for Par substrate polarization.

We propose that these Par substrates have a domain for general cortical targeting and a PRBH motif. The PRBH motif functions as a switch that has either low or high affinity for Par-containing and Par-lacking cortical domains, respectively. Together, the anchoring and switch interactions synergistically could increase cortical binding at non-Par cortical domains. The additional regions of Par substrates that function is partly characterized. For Lgl, this is likely from interactions between its COOH-terminus and the cytoskeleton (Betschinger et al., 2003). For Mira, this likely involves the coiled-coil region and/or an unidentified cortical targeting site. For Numb, this might involve NH2-terminal myristoylation (Benetka et al., 2008; Knoblich et al., 1997). Based on characterization of its human orthologs (Deleted in liver cancer 1-3, DLC1-3), Cv-c is likely to have interactions with multiple proteins and/or lipids. For instance, the uncharacterized steroidogenic acute regulatory protein-related lipid transfer domain (START) domain is predicted to function in shuttling lipids between membranes (Wirtz, 2006) and DLC proteins localize to adherens junctions and the basolateral region by binding α-catenin and Scribble (Hendrick et al., 2016; Tripathi et al., 2012). It will be interesting to determine whether interactions with these proteins is conserved to *Drosophila* and mediate its polarization. Synthetic biology approaches are likely to provide insights regarding when and why cortical localization modules are interchangeable.

Identification and prediction of Par-polarized proteins

This work identified Phospho-Regulated BH (PRBH) motifs to be a key sequence in the polarization of several Par substrates and used several screening approaches to

identify Par polarized proteins. Here, I assess my screening methods and describe ways that these screening methods could be improved in future studies. My work demonstrated that the PRBH identification computer program can identify Par polarized protein, however, further work is needed to assess this program and improve its accuracy. A key limitation of this program is that most candidates are false positives. This is largely because it is a linear motif predictor and cannot determine when the sequence may be buried in a globular domain. Including a computational tool to assess if a linear motif is predicted to be solvent exposed would be challenging. A second limitation is that it cannot identify transmembrane regions or secretion signals that would prevent a Par complex-dependent polarization mechanism. Adding these screening tools should greatly reduce the number of false positives and provides only a minor technical challenge. Third, the computational method to identify an aPKC consensus was simple and could be refined to limit the number of false positives. Further improvements to this prediction are likely to require machine learning approaches and a larger set of *bona fide* aPKC phosphosites.

Despite these limitations, I used the PRBH identification program to perform two screens for novel Par effectors. In the first screen, I characterized PRBH motif-containing proteins that localize to the polarity domains that did not include the apical (e.g. basal, lateral, basolateral, etc.). Then I tested whether these candidates localized to the cortex of cultured cells and whether this localization was inhibited by aPKC. I found that three of five candidates localized to the cell cortex and that aPKC inhibited cortical targeting for one of these proteins. In my second screen for Par polarized proteins, I performed an *in vivo,* protein trap-based screen to identify putative PRBH motif-containing protein with

polarized localization. This screen identified CG6454, a basolateral protein with Ca^{2+}-dependent membrane localization. However, further characterization of this candidate gene found that its membrane localization was not regulated by aPKC. Due to the sample size in these screens and selection biases (i.e. characterizing polarized proteins in Chapter III, availability of protein trap lines in Chapter IV), it is not currently possible to how many additional proteins the Par complex may polarized by PRBH motif phosphorylation. The identification of Cv-c to be a Par polarized protein does, however, suggest that the screening methods used in Chapter IV should be fruitful if performed on a larger scale. Thus, this work suggests that further screens of putative PRBH motifs are likely to identify additional proteins that the Par complex polarizes by phosphorylation.

CONCLUDING REMARKS

In this work, I set out to determine how the Par complex polarizes its substrate by phosphorylation. I found that the Par complex polarizes its substrates by phosphorylation of a phospholipid binding motif, then I developed computational tools to assist in identification of these sequences from proteomic files. From this proteomic analysis, I performed two screens for polarized proteins and identified several new polarized Par substrates. In these screens, I identified an essential regulator of *Drosophila* morphogenesis to be an aPKC substrate that is polarized by phosphorylation. I hope that this work provides both insights into the mechanisms of Par polarity and strategies for identifying novel effectors of the Par complex.

APPENDIX

APPENDIX A: SUPPLEMENTAL MATERIALS FOR CHAPTER II

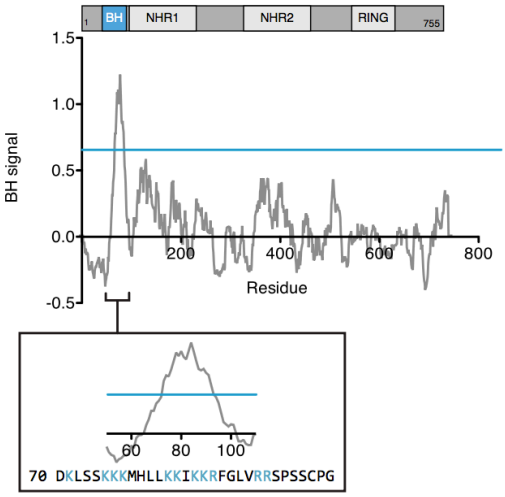

Supplemental Figure 1. Basic-Hydrophobic motif signal of Neur. The BH signal of Neur is plotted aligned to its domain architecture. The inset is a detail of Neur BH with basic residues colored blue. S residues within this region do not fit the aPKC consensus sequence which features a R in the -2 position and a hydrophobic residue in the +1 position, which makes it unlikely to be an aPKC-regulated PRBH motif. (Please see lower for further discussion of this). Abbreviations as follows: NHR, Neur homology region; RING, C_3HC_4 ring zinc finger.

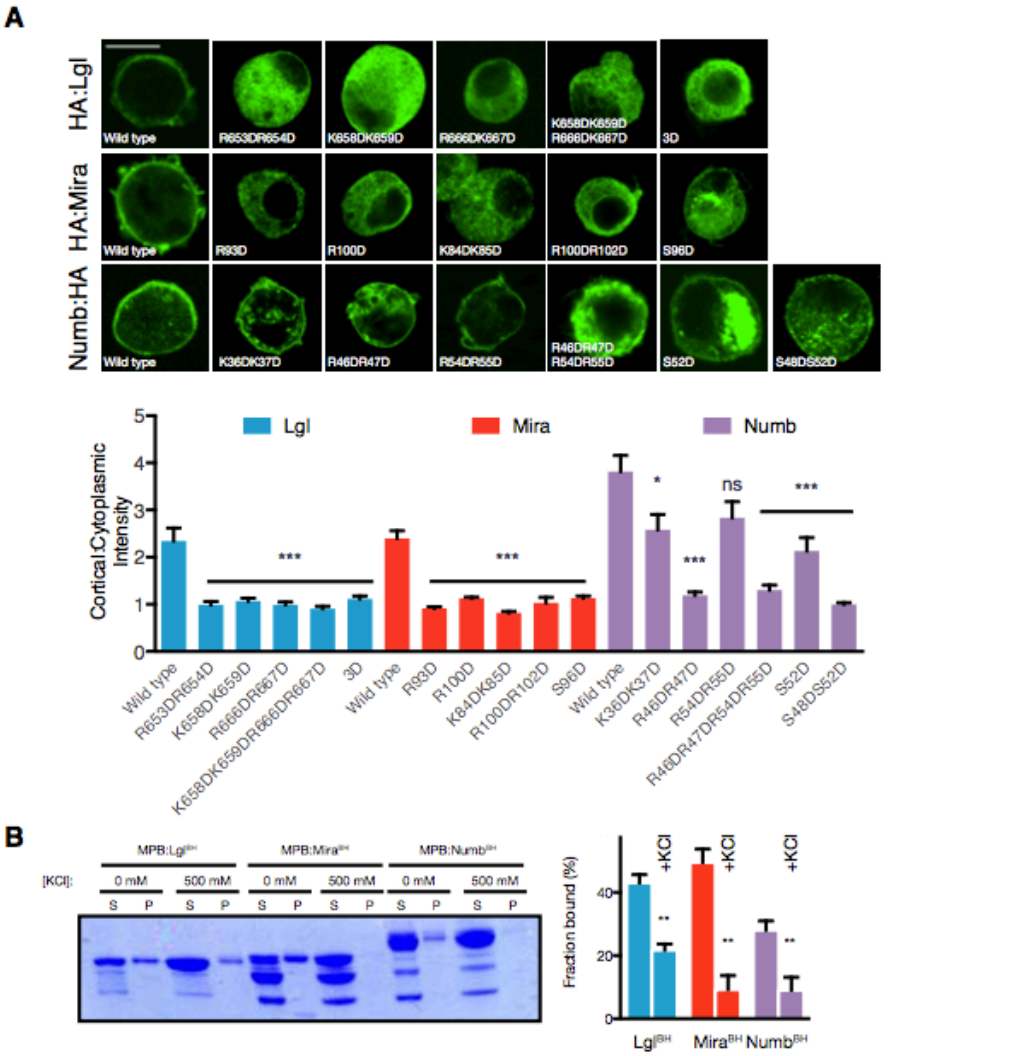

Supplemental Figure 2. Charge mediates cortical targeting and phospholipid binding for Lgl, Mira, and Numb. (A) Mutations to acidic residues reduce cortical localization of full length Lgl, Mira, and Numb. The localization of each full-length protein with point mutations was characterized by immunostaining transiently transfected S2 cells for the HA epitope tag. Localization was quantified as a cortical to cytoplasmic signal intensity ratio for at least 16 cells (mean ± SEM). Statistical testing was performed with t-test to compare the localization of each mutant to the wild type full-length control. A P-value of <0.05 and <0.0001 are marked with one and three asterisks, respectively. No statically significant difference is marked with ns. Scale bar, 10 μm. (B) High ionic strength disrupts BH phospholipid interactions. A Coomassie-stained gel from lipid vesicle-binding cosedimentation assays of vesicles with 4:1 PC:PS plus 10% PIP_2 is shown. Each BH motif was characterized as an MPB-fusion protein. The fraction of protein bound, quantified as the amount of protein in the pellet over total protein, was quantified in triplicate for each vesicle composition. The mean and SEM of the fraction bound are shown. Asterisks indicate $p < 0.01$. Significance was evaluated using a non-parametric t-test relative to low ionic strength.

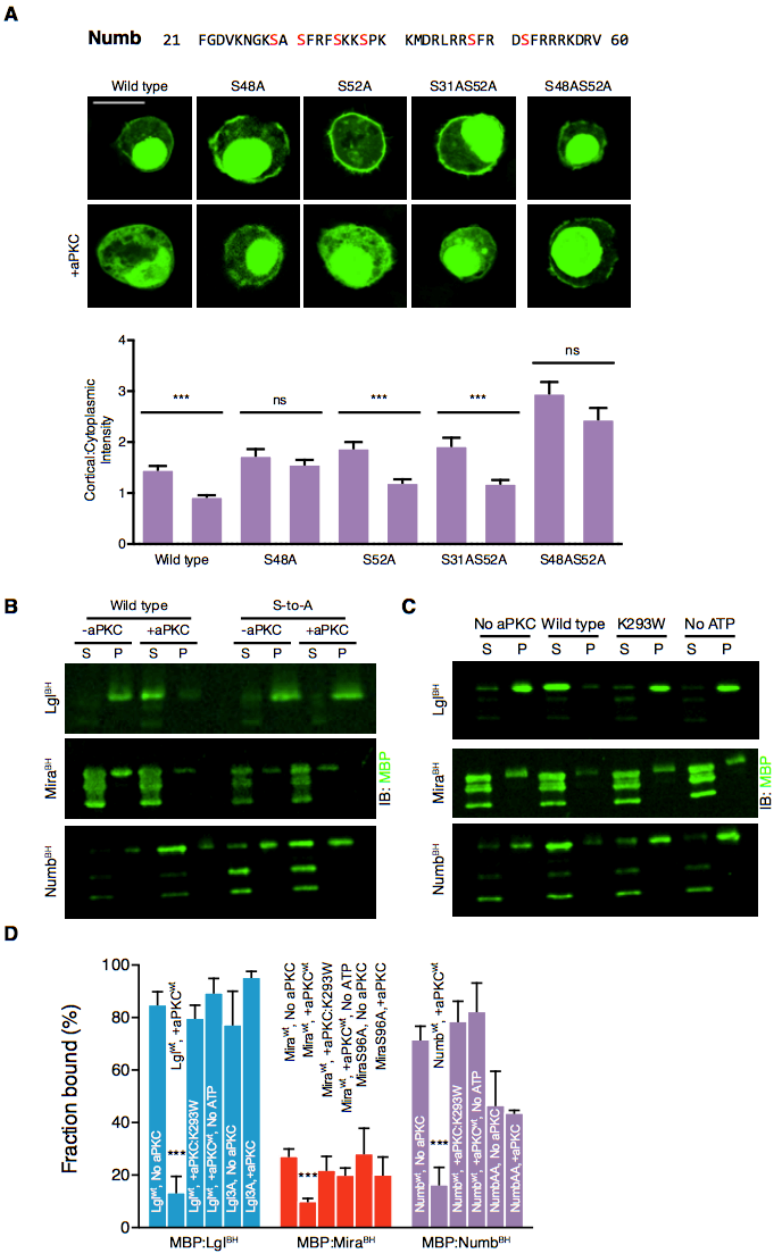

Supplemental Figure 3. aPKC phosphorylation inhibits BH motif lipid binding for Lgl, Mira, and Numb. Related to Figure 2-6. (A) Identification of Numb BH residues involved in regulating aPKC-induced cortical displacement. This figure is related to Figure 4B", but includes a larger collection of Numb S-to-A mutations. The sequence of Numb BH is displayed with potential phosphorylation sites highlighted in red. Representative images from transiently transfected S2 cells in the absence or presence ^{o}f aPKC are displayed. Cells were transfected with EGFP-tagged BH motifs. aPKC expression was verified by immunostaining for PKCζ. The cortical to cytoplasmic intensity ratio was quantified and displayed as the mean ± SEM, and statistical significance was determined by a non- parametric t-test to compare each mutant to its singly transfected control. P values of <0.0001 are marked with three asterisks. No

statistical difference is marked by ns. Scale bar, 10 μm. (B-D) aPKC kinase activity inhibits BH motif phospholipid binding. Images of representative immunoblots to characterize the effect of aPKC on Par substrate BH motif binding to PC/PS/PIP_2 vesicles are presented. Lipid-binding cosedimentation assays were performed in the presence of aPKC and ATP. For C, sample conditions varied as follows: No aPKC, ATP only; wild type, $aPKC^{259\text{-}606}$ and ATP; K293W, aPKC $K293W^{259\text{-}606}$ and ATP; No ATP, $aPKC^{259\text{-}606}$ but no ATP. All samples contained 4:1 PC:PS plus 10% PIP_2 and all BH motifs had the wild type sequence. Samples were analyzed by immunoblotting for the MBP tag. S marks the supernatant and P marks the pellet. The "S-to-A" mutations are: Lgl3A, MiraS96A and NumbS48AS52A. Quantification of aPKC's effect on BH motif vesicle binding displayed in A-B. The fraction of protein bound, quantified as the amount of protein in the pellet over total protein, was quantified in triplicate for each vesicle composition. The mean and SEM of the fraction bound are shown. Asterisks indicate $p < 0.0001$. Significance was evaluated using a non- parametric t-test relative to binding in the absence of aPKC.

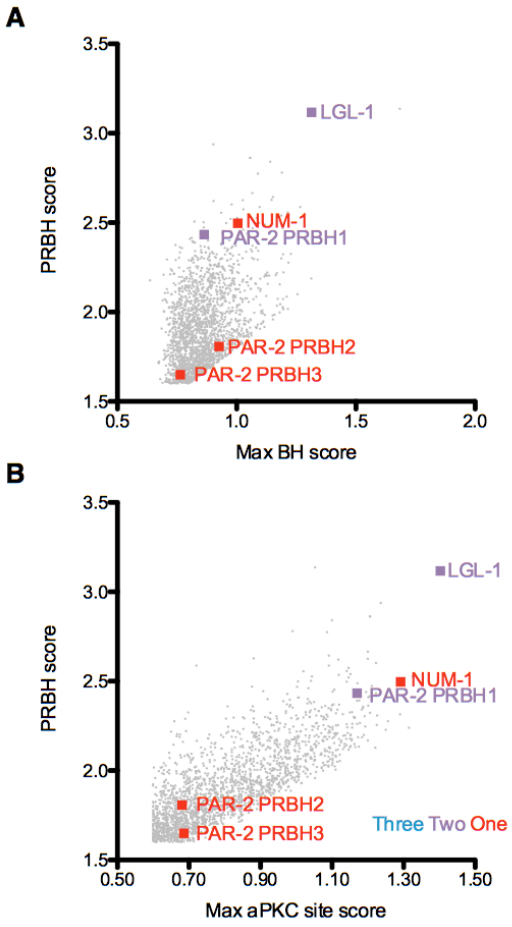

Supplemental Figure 4. Distribution of PRBH scores in the *C. elegans* proteome. PRBH scores, maximum BH score, and the highest aPKC site score are displayed from *C. elegans* proteome. Each point marks a single putative PRBH motif and all identified PRBH motifs are displayed. Blue lines mark the PRBH threshold values. Sequences with scores less than these values are not candidate PRBH motifs. See also Supplemental Data Table 1 with the online version of the text.

APPENDIX

APPENDIX B: SUPPLEMENTAL MATERIALS FOR CHAPTER III

Supplemental Table 1. Identification of polarized putative PRBH proteins.

Gene	Reported localization	Apical localization	TM or extra-cellular PRBH	S2 cell localization	Candidate
CadN	Adherens junction	No	Yes		
CG42748	Lateral plasma membrane	No	No		Yes
cora	Basolateral, septate junction	No	No	Cortically enriched (Fehon Lab)	Yes
cv-c	Basolateral	No	No	Not characterized	Yes
ine	Basolateral	No	Yes		
jar	Reported as basal but localization data suggests otherwise	Yes?			
kug	Adherens junction, basolateral, basal	No	Yes		
l(2)gl	Basolateral, septate junction	No	No		Verified
Liprin-α	Adherens junction	No	No	Localizes to focal adhesions in S2	No
mira	Basal, basolateral	No	No		Verified
nullo	Adherens junction	No	No	Not characterized	Yes
numb	Basal	No	No		Verified
Pak	Adherens junction	No	No	Not characterized	Yes
par-1	Basolateral	No	No		N/A
rols	Adherens junction	No	No	Punctate in S2 cells (Menon 2005 J Cell Biol)	No
vari	Septate junction	No	No	Not characterized	Yes
warts	Adherens junction	No	No	Cytoplasmic, cortical localization requires Merlin (Yin 2013 Cell)	No
ZnT86D	Basolateral	No	Yes		No

APPENDIX

APPENDIX C: SUPPLEMENTAL MATERIALS FOR CHAPTER IV

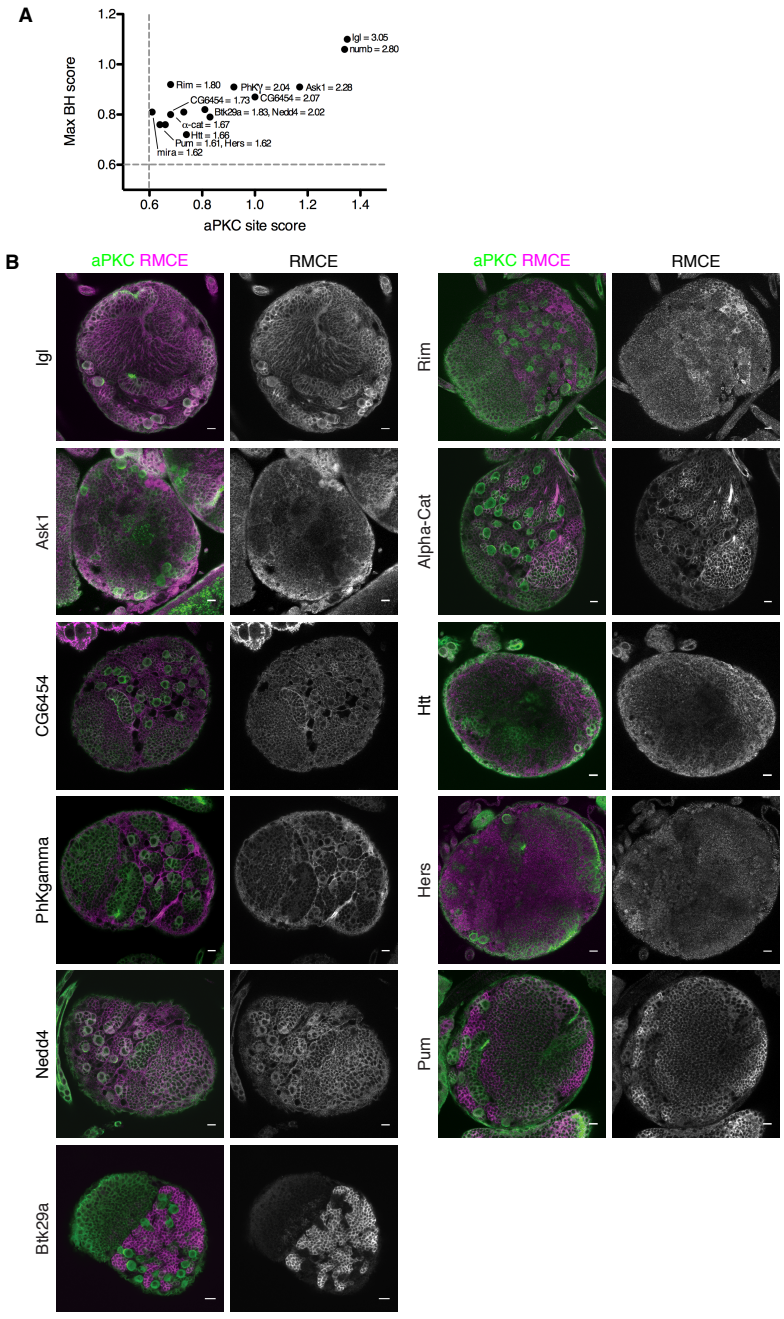

Supplemental Figure 5. RMCE Protein localization in the larval CNS. (A) Scoring of PRBH motifs of analyzed RMCE lines. (B) Protein localization in the CNS of L3 larvae characterized by immunostaining for GFP (RMCE) and aPKC.

Supplemental Table 2. Summary of RMCE screen.

Table 4-1: RMCE Lines with putative PRBH motifs and expression in larval CNS			
Rank	**Gene**	**Expression**	**Subcellular localization**
1	Lgl	NBs, epithelia	Basolateral, cortical, cytoplasmic
119	Pk92B/Ask1	Ubiquitous	Diffuse, punctate
377 and 1246	CG6454	Epithelial, neuronal	Basolateral
404	Ptpmeg	Not detected	N/A
420	PhKgamma	Ubiquitous	Cytoplasmic
470	Nedd4	Ubiquitous	Cytoplasmic
614	Acsl	Not detected	N/A
951	Btk29a	Neurons and epithelia	Cytoplasmic
1021	Rim	Neuronal	Cytoplasmic
1169	Svp	Not detected	N/A
1426	Alpha-Cat	Epitheilia, NBs	Adherens junctions, cortical
1453	Htt	Ubiquitous	Cytoplasmic
1555	Hers	Ubiquitous	Nuclear
1596	pum	Neuronal	Cytoplasmic

REFERENCES CITED

Albertson, R., and Doe, C.Q. (2003). Dlg, Scrib and Lgl regulate neuroblast cell size and mitotic spindle asymmetry. Nat. Cell Biol. *5*, 166–170.

Aldaz, S., and Escudero, L.M. (2010). Imaginal discs. Curr. Biol. *20*, R429–R431.

Ananthanarayanan, B., Das, S., Rhee, S.G., Murray, D., and Cho, W. (2002). Membrane Targeting of C2 Domains of Phospholipase C-δ Isoforms. J. Biol. Chem. *277*, 3568–3575.

Atwood, S.X., and Prehoda, K.E. (2009). aPKC phosphorylates Miranda to polarize fate determinants during neuroblast asymmetric cell division. Curr. Biol. CB *19*, 723–729.

Atwood, S.X., Chabu, C., Penkert, R.R., Doe, C.Q., and Prehoda, K.E. (2007). Cdc42 acts downstream of Bazooka to regulate neuroblast polarity through Par-6–aPKC. J. Cell Sci. *120*, 3200–3206.

Bailey, M.J., and Prehoda, K.E. (2015). Establishment of Par-Polarized Cortical Domains via Phosphoregulated Membrane Motifs. Dev. Cell *35*, 199–210.

Barford, D., Hu, S.H., and Johnson, L.N. (1991). Structural mechanism for glycogen phosphorylase control by phosphorylation and AMP. J. Mol. Biol. *218*, 233–260.

Benetka, W., Mehlmer, N., Maurer-Stroh, S., Sammer, M., Koranda, M., Neumüller, R., Betschinger, J., Knoblich, J.A., Teige, M., and Eisenhaber, F. (2008). Experimental testing of predicted myristoylation targets involved in asymmetric cell division and calcium-dependent signalling. Cell Cycle *7*, 3709–3719.

Betschinger, J., Mechtler, K., and Knoblich, J.A. (2003). The Par complex directs asymmetric cell division by phosphorylating the cytoskeletal protein Lgl. Nature *422*, 326–330.

Betschinger, J., Eisenhaber, F., and Knoblich, J.A. (2005). Phosphorylation-induced autoinhibition regulates the cytoskeletal protein Lethal (2) giant larvae. Curr. Biol. CB *15*, 276–282.

Böhm, H., Brinkmann, V., Drab, M., Henske, A., and Kurzchalia, T.V. (1997). Mammalian homologues of C. elegans PAR-1 are asymmetrically localized in epithelial cells and may influence their polarity. Curr. Biol. *7*, 603–606.

Brand, A.H., and Perrimon, N. (1993). Targeted gene expression as a means of altering cell fates and generating dominant phenotypes. Development *118*, 401–415.

Braun, A.C., and Olayioye, M.A. (2015). Rho regulation: DLC proteins in space and time. Cell. Signal. *27*, 1643–1651.

Brzeska, H., Guag, J., Remmert, K., Chacko, S., and Korn, E.D. (2010). An experimentally based computer search identifies unstructured membrane-binding sites in proteins: application to class I myosins, PAKS, and CARMIL. J. Biol. Chem. *285*, 5738–5747.

Cherbas, L., Willingham, A., Zhang, D., Yang, L., Zou, Y., Eads, B.D., Carlson, J.W., Landolin, J.M., Kapranov, P., Dumais, J., et al. (2011). The transcriptional diversity of 25 Drosophila cell lines. Genome Res. *21*, 301–314.

Ching, Y.-P., Wong, C.-M., Chan, S.-F., Leung, T.H.-Y., Ng, D.C.-H., Jin, D.-Y., and Ng, I.O. (2003). Deleted in Liver Cancer (DLC) 2 Encodes a RhoGAP Protein with Growth Suppressor Function and Is Underexpressed in Hepatocellular Carcinoma. J. Biol. Chem. *278*, 10824–10830.

Cline, E.G., and Nelson, W.J. (2007). Characterization of Mammalian Par 6 as a Dual-Location Protein. Mol. Cell. Biol. *27*, 4431–4443.

Cohen, P. (2000). The regulation of protein function by multisite phosphorylation – a 25 year update. Trends Biochem. Sci. *25*, 596–601.

Cuenca, A.A., Schetter, A., Aceto, D., Kemphues, K., and Seydoux, G. (2003). Polarization of the C. elegans zygote proceeds via distinct establishment and maintenance phases. Dev. Camb. Engl. *130*, 1255–1265.

Daul, A.L., Komori, H., and Lee, C.-Y. (2010). Immunofluorescent Staining of Drosophila Larval Brain Tissue. Cold Spring Harb. Protoc. *2010*, pdb.prot5460.

Davidson, G., Wu, W., Shen, J., Bilic, J., Fenger, U., Stannek, P., Glinka, A., and Niehrs, C. (2005). Casein kinase 1 gamma couples Wnt receptor activation to cytoplasmic signal transduction. Nature *438*, 867–872.

Denholm, B., Brown, S., Ray, R.P., Ruiz-Gómez, M., Skaer, H., and Hombría, J.C.-G. (2005). crossveinless-c is a RhoGAP required for actin reorganisation during morphogenesis. Development *132*, 2389–2400.

Derivery, E., Seum, C., Daeden, A., Loubéry, S., Holtzer, L., Jülicher, F., and Gonzalez-Gaitan, M. (2015). Polarized endosome dynamics by spindle asymmetry during asymmetric cell division. Nature *528*, 280–285.

Dho, S.E., French, M.B., Woods, S.A., and McGlade, C.J. (1999). Characterization of Four Mammalian Numb Protein Isoforms IDENTIFICATION OF CYTOPLASMIC AND MEMBRANE-ASSOCIATED VARIANTS OF THE PHOSPHOTYROSINE BINDING DOMAIN. J. Biol. Chem. *274*, 33097–33104.

Dho, S.E., Trejo, J., Siderovski, D.P., and McGlade, C.J. (2006). Dynamic regulation of mammalian numb by G protein-coupled receptors and protein kinase C activation: Structural determinants of numb association with the cortical membrane. Mol. Biol. Cell *17*, 4142–4155.

Doerflinger, H., Benton, R., Torres, I.L., Zwart, M.F., and Johnston, D.S. (2006). Drosophila Anterior-Posterior Polarity Requires Actin-Dependent PAR-1 Recruitment to the Oocyte Posterior. Curr. Biol. *16*, 1090–1095.

Dong, W., Zhang, X., Liu, W., Chen, Y., Huang, J., Austin, E., Celotto, A.M., Jiang, W.Z., Palladino, M.J., Jiang, Y., et al. (2015). A conserved polybasic domain mediates plasma membrane targeting of Lgl and its regulation by hypoxia. J. Cell Biol. *211*, 273–286.

Drewes, G., Ebneth, A., Preuss, U., Mandelkow, E.-M., and Mandelkow, E. (1997). MARK, a Novel Family of Protein Kinases That Phosphorylate Microtubule-Associated Proteins and Trigger Microtubule Disruption. Cell *89*, 297–308.

Drummond, M.L., and Prehoda, K.E. (2016). Molecular Control of Atypical Protein Kinase C: Tipping the Balance between Self-Renewal and Differentiation. J. Mol. Biol. *428*, 1455–1464.

Durkin, M.E., Yuan, B.-Z., Zhou, X., Zimonjic, D.B., Lowy, D.R., Thorgeirsson, S.S., and Popescu, N.C. (2007a). DLC-1:a Rho GTPase-activating protein and tumour suppressor. J. Cell. Mol. Med. *11*, 1185–1207.

Durkin, M.E., Ullmannova, V., Guan, M., and Popescu, N.C. (2007b). Deleted in liver cancer 3 (DLC-3), a novel Rho GTPase-activating protein, is downregulated in cancer and inhibits tumor cell growth. Oncogene *26*, 4580–4589.

Edgar, R.C. (2004). MUSCLE: multiple sequence alignment with high accuracy and high throughput. Nucleic Acids Res. *32*, 1792–1797.

Engelman, D.M. (2005). Membranes are more mosaic than fluid. Nature *438*, 578–580.

Erlmann, P., Schmid, S., Horenkamp, F.A., Geyer, M., Pomorski, T.G., and Olayioye, M.A. (2009). DLC1 Activation Requires Lipid Interaction through a Polybasic Region Preceding the RhoGAP Domain. Mol. Biol. Cell *20*, 4400–4411.

Etemad-Moghadam, B., Guo, S., and Kemphues, K.J. (1995). Asymmetrically distributed PAR-3 protein contributes to cell polarity and spindle alignment in early C. elegans embryos. Cell *83*, 743–752.

Etienne-Manneville, S., and Hall, A. (2001). Integrin-Mediated Activation of Cdc42 Controls Cell Polarity in Migrating Astrocytes through PKCζ. Cell *106*, 489–498.

Evan, G.I., Lewis, G.K., Ramsay, G., and Bishop, J.M. (1985). Isolation of monoclonal antibodies specific for human c-myc proto-oncogene product. Mol. Cell. Biol. *5*, 3610–3616.

Farese, R.V., Lee, M.C., and Sajan, M.P. (2014). Atypical PKC: a target for treating insulin-resistant disorders of obesity, the metabolic syndrome and type 2 diabetes mellitus. Expert Opin. Ther. Targets *18*, 1163–1175.

Fehon, R.G., Dawson, I.A., and Artavanis-Tsakonas, S. (1994). A Drosophila homologue of membrane-skeleton protein 4.1 is associated with septate junctions and is encoded by the coracle gene. Development *120*, 545–557.

Flores-Benitez, D., and Knust, E. (2016). Dynamics of epithelial cell polarity in Drosophila: how to regulate the regulators? Curr. Opin. Cell Biol. *42*, 13–21.

Frise, E., Knoblich, J.A., Younger-Shepherd, S., Jan, L.Y., and Jan, Y.N. (1996). The Drosophila Numb protein inhibits signaling of the Notch receptor during cell-cell interaction in sensory organ lineage. Proc. Natl. Acad. Sci. *93*, 11925–11932.

Fuerstenberg, S., Peng, C.Y., Alvarez-Ortiz, P., Hor, T., and Doe, C.Q. (1998). Identification of Miranda protein domains regulating asymmetric cortical localization, cargo binding, and cortical release. Mol. Cell. Neurosci. *12*, 325–339.

Fuerstenberg, S., Broadus, J., and Doe, C.Q. (2002). Asymmetry and cell fate in the Drosophila embryonic CNS. Int. J. Dev. Biol. *42*, 379–383.

George, D.J., and Blackshear, P.J. (1992). Membrane association of the myristoylated alanine-rich C kinase substrate (MARCKS) protein appears to involve myristate-dependent binding in the absence of a myristoyl protein receptor. J. Biol. Chem. *267*, 24879–24885.

Gibson, D.G., Young, L., Chuang, R.-Y., Venter, J.C., Hutchison, C.A., and Smith, H.O. (2009). Enzymatic assembly of DNA molecules up to several hundred kilobases. Nat. Methods *6*, 343–345.

Goehring, N.W. (2014). PAR polarity: From complexity to design principles. Exp. Cell Res. *328*, 258–266.

Goldstein, B., and Macara, I.G. (2007). The PAR proteins: fundamental players in animal cell polarization. Dev. Cell *13*, 609–622.

Graybill, C., and Prehoda, K.E. (2014). Ordered multisite phosphorylation of lethal giant larvae by atypical protein kinase C. Biochemistry (Mosc.) *53*, 4931–4937.

Graybill, C., Wee, B., Atwood, S.X., and Prehoda, K.E. (2012). Partitioning-defective Protein 6 (Par-6) Activates Atypical Protein Kinase C (aPKC) by Pseudosubstrate Displacement. J. Biol. Chem. *287*, 21003–21011.

Grohmann, A., Tanneberger, K., Alzner, A., Schneikert, J., and Behrens, J. (2007). AMER1 regulates the distribution of the tumor suppressor APC between microtubules and the plasma membrane. J. Cell Sci. *120*, 3738–3747.

Gross, S.D., Simerly, C., Schatten, G., and Anderson, R.A. (1997). A casein kinase I isoform is required for proper cell cycle progression in the fertilized mouse oocyte. J. Cell Sci. *110 (Pt 24)*, 3083–3090.

Groves, J.T., and Kuriyan, J. (2010). Molecular mechanisms in signal transduction at the membrane. Nat. Struct. Mol. Biol. *17*, 659–665.

Hao, Y., Boyd, L., and Seydoux, G. (2006). Stabilization of cell polarity by the C. elegans RING protein PAR-2. Dev. Cell *10*, 199–208.

Harden, N., Lee, J., Loh, H.Y., Ong, Y.M., Tan, I., Leung, T., Manser, E., and Lim, L. (1996). A Drosophila homolog of the Rac- and Cdc42-activated serine/threonine kinase PAK is a potential focal adhesion and focal complex protein that colocalizes with dynamic actin structures. Mol. Cell. Biol. *16*, 1896–1908.

Harris, T.J.C., and Peifer, M. (2005). The positioning and segregation of apical cues during epithelial polarity establishment in Drosophila. J. Cell Biol. *170*, 813–823.

Hartwig, J.H., Thelen, M., Rosen, A., Janmey, P.A., Nairn, A.C., and Aderem, A. (1992). MARCKS is an actin filament crosslinking protein regulated by protein kinase C and calcium-calmodulin. Nature *356*, 618–622.

Hendrick, J., Franz-Wachtel, M., Moeller, Y., Schmid, S., Macek, B., and Olayioye, M.A. (2016). The polarity protein Scribble positions DLC3 at adherens junctions to regulate Rho signaling. J Cell Sci *129*, 3583–3596.

Heo, W.D., Inoue, T., Park, W.S., Kim, M.L., Park, B.O., Wandless, T.J., and Meyer, T. (2006). PI(3,4,5)P3 and PI(4,5)P2 Lipids Target Proteins with Polybasic Clusters to the Plasma Membrane. Science *314*, 1458–1461.

Holt, L.J., Tuch, B.B., Villén, J., Johnson, A.D., Gygi, S.P., and Morgan, D.O. (2009). Global analysis of Cdk1 substrate phosphorylation sites provides insights into evolution. Science *325*, 1682–1686.

Hrdlicka, L., Gibson, M., Kiger, A., Micchelli, C., Schober, M., Schöck, F., and Perrimon, N. (2002). Analysis of twenty-four Gal4 lines in Drosophila melanogaster. Genesis *34*, 51–57.

Huang, Y.-L., and Niehrs, C. (2014). Polarized Wnt signaling regulates ectodermal cell fate in Xenopus. Dev. Cell *29*, 250–257.

Hunter, C., and Wieschaus, E. (2000). Regulated Expression of nullo Is Required for the Formation of Distinct Apical and Basal Adherens Junctions in the Drosophila Blastoderm. J. Cell Biol. *150*, 391–402.

Hurd, T.W., Gao, L., Roh, M.H., Macara, I.G., and Margolis, B. (2003). Direct interaction of two polarity complexes implicated in epithelial tight junction assembly. Nat. Cell Biol. *5*, 137–142.

Hurov, J.B., Watkins, J.L., and Piwnica-Worms, H. (2004). Atypical PKC phosphorylates PAR-1 kinases to regulate localization and activity. Curr. Biol. CB *14*, 736–741.

Izumi, Y., Hirose, T., Tamai, Y., Hirai, S., Nagashima, Y., Fujimoto, T., Tabuse, Y., Kemphues, K.J., and Ohno, S. (1998). An Atypical PKC Directly Associates and Colocalizes at the Epithelial Tight Junction with ASIP, a Mammalian Homologue of Caenorhabditis elegans Polarity Protein PAR-3. J. Cell Biol. *143*, 95–106.

Joberty, G., Petersen, C., Gao, L., and Macara, I.G. (2000). The cell-polarity protein Par6 links Par3 and atypical protein kinase C to Cdc42. Nat. Cell Biol. *2*, 531–539.

Johnson, L.N., and Barford, D. (1993). The effects of phosphorylation on the structure and function of proteins. Annu. Rev. Biophys. Biomol. Struct. *22*, 199–232.

Johnston, C.A., Hirono, K., Prehoda, K.E., and Doe, C.Q. (2009). Identification of an Aurora-A/PinsLINKER/Dlg spindle orientation pathway using induced cell polarity in S2 cells. Cell *138*, 1150–1163.

Kaczynski, T.J., and Gunawardena, S. (2010). Visualization of the Embryonic Nervous System in Whole-mount Drosophila Embryos. JoVE J. Vis. Exp. e2150–e2150.

Kawai, K., Seike, J., Iino, T., Kiyota, M., Iwamae, Y., Nishitani, H., and Yagisawa, H. (2009). START-GAP2/DLC2 is localized in focal adhesions via its N-terminal region. Biochem. Biophys. Res. Commun. *380*, 736–741.

Kawai, K., Kitamura, S., Maehira, K., Seike, J., and Yagisawa, H. (2010). START-GAP1/DLC1 is localized in focal adhesions through interaction with the PTB domain of tensin2. Adv. Enzyme Regul. *50*, 202–215.

Kemphues, K.J., Priess, J.R., Morton, D.G., and Cheng, N. (1988). Identification of genes required for cytoplasmic localization in early C. elegans embryos. Cell *52*, 311–320.

Knoblich, J.A. (2010). Asymmetric cell division: recent developments and their implications for tumour biology. Nat. Rev. Mol. Cell Biol. *11*, 849–860.

Knoblich, J.A., Jan, L.Y., and Jan, Y.N. (1997). The N terminus of the Drosophila Numb protein directs membrane association and actin-dependent asymmetric localization. Proc. Natl. Acad. Sci. U. S. A. *94*, 13005–13010.

Knust, E., and Bossinger, O. (2002). Composition and Formation of Intercellular Junctions in Epithelial Cells. Science *298*, 1955–1959.

Ko, F.C.F., and Ping Yam, J.W. (2014). Regulation of deleted in liver cancer 1 tumor suppressor by protein–protein interactions and phosphorylation. Int. J. Cancer *135*, 264–269.

Ko, F.C.F., Chan, L., Tung, E.K., Lowe, S.W., Ng, I.O., and Yam, J.W.P. (2010). Akt Phosphorylation of Deleted in Liver Cancer 1 Abrogates Its Suppression of Liver Cancer Tumorigenesis and Metastasis. Gastroenterology *139*, 1397–1407.e6.

Kuchinke, U., Grawe, F., and Knust, E. (1998). Control of spindle orientation in Drosophila by the Par-3-related PDZ-domain protein Bazooka. Curr. Biol. *8*, 1357–1365.

Lai, S.-L., and Doe, C.Q. (2014). Transient nuclear Prospero induces neural progenitor quiescence. eLife *3*, e03363.

Lee, M., and Vasioukhin, V. (2008). Cell polarity and cancer – cell and tissue polarity as a non-canonical tumor suppressor. J. Cell Sci. *121*, 1141–1150.

Lemmon, M.A. (2008). Membrane recognition by phospholipid-binding domains. Nat. Rev. Mol. Cell Biol. *9*, 99–111.

Letunic, I., Doerks, T., and Bork, P. (2012). SMART 7: recent updates to the protein domain annotation resource. Nucleic Acids Res. *40*, D302-305.

Letunic, I., Doerks, T., and Bork, P. (2015). SMART: recent updates, new developments and status in 2015. Nucleic Acids Res. *43*, D257–D260.

Liao, Y.-C., Si, L., White, R.W. deVere, and Lo, S.H. (2007). The phosphotyrosine-independent interaction of DLC-1 and the SH2 domain of cten regulates focal adhesion localization and growth suppression activity of DLC-1. J. Cell Biol. *176*, 43–49.

Lin, D., Edwards, A.S., Fawcett, J.P., Mbamalu, G., Scott, J.D., and Pawson, T. (2000). A mammalian PAR-3–PAR-6 complex implicated in Cdc42/Rac1 and aPKC signalling and cell polarity. Nat. Cell Biol. *2*, 540–547.

Lovegrove, B., Simões, S., Rivas, M.L., Sotillos, S., Johnson, K., Knust, E., Jacinto, A., and Hombría, J.C.-G. (2006). Coordinated Control of Cell Adhesion, Polarity, and Cytoskeleton Underlies Hox-Induced Organogenesis in Drosophila. Curr. Biol. *16*, 2206–2216.

Lu, M.S., and Prehoda, K.E. (2013). A NudE/14-3-3 pathway coordinates dynein and the kinesin Khc73 to position the mitotic spindle. Dev. Cell *26*, 369–380.

Lu, B., Rothenberg, M., Jan, L.Y., and Jan, Y.N. (1998). Partner of Numb Colocalizes with Numb during Mitosis and Directs Numb Asymmetric Localization in Drosophila Neural and Muscle Progenitors. Cell *95*, 225–235.

Luo, B., Prescott, S.M., and Topham, M.K. (2003). Protein kinase C alpha phosphorylates and negatively regulates diacylglycerol kinase zeta. J. Biol. Chem. *278*, 39542–39547.

Lye, C.M., Naylor, H.W., and Sanson, B. (2014). Subcellular localisations of the CPTI collection of YFP-tagged proteins in Drosophila embryos. Development *141*, 4006–4017.

Macara, I.G., and McCaffrey, L. (2013). Cell polarity in morphogenesis and metastasis. Phil Trans R Soc B *368*, 20130012.

Martin-Belmonte, F., Gassama, A., Datta, A., Yu, W., Rescher, U., Gerke, V., and Mostov, K. (2007). PTEN-mediated apical segregation of phosphoinositides controls epithelial morphogenesis through Cdc42. Cell *128*, 383–397.

Matsuzaki, F., Ohshiro, T., Ikeshima-Kataoka, H., and Izumi, H. (1998). miranda localizes staufen and prospero asymmetrically in mitotic neuroblasts and epithelial cells in early Drosophila embryogenesis. Dev. Camb. Engl. *125*, 4089–4098.

Mayor, R., and Etienne-Manneville, S. (2016). The front and rear of collective cell migration. Nat. Rev. Mol. Cell Biol. *17*, 97–109.

McLaughlin, S. (1989). The electrostatic properties of membranes. Annu. Rev. Biophys. Biophys. Chem. *18*, 113–136.

McLaughlin, S., and Murray, D. (2005). Plasma membrane phosphoinositide organization by protein electrostatics. Nature *438*, 605–611.

Mollinari, C., Lange, B., and González, C. (2002). Miranda, a protein involved in neuroblast asymmetric division, is associated with embryonic centrosomes of Drosophila melanogaster. Biol. Cell *94*, 1–13.

Morais-de-Sá, E., Mirouse, V., and St Johnston, D. (2010). aPKC phosphorylation of Bazooka defines the apical/lateral border in Drosophila epithelial cells. Cell *141*, 509–523.

Morone, N., Fujiwara, T., Murase, K., Kasai, R.S., Ike, H., Yuasa, S., Usukura, J., and Kusumi, A. (2006). Three-dimensional reconstruction of the membrane skeleton at the plasma membrane interface by electron tomography. J. Cell Biol. *174*, 851–862.

Motegi, F., Zonies, S., Hao, Y., Cuenca, A.A., Griffin, E., and Seydoux, G. (2011). Microtubules induce self-organization of polarized PAR domains in Caenorhabditis elegans zygotes. Nat. Cell Biol. *13*, 1361–1367.

Moyer, K.E., and Jacobs, J.R. (2008). Varicose: a MAGUK required for the maturation and function of Drosophila septate junctions. BMC Dev. Biol. *8*, 99.

Nagaraja, G.M., and Kandpal, R.P. (2004). Chromosome 13q12 encoded Rho GTPase activating protein suppresses growth of breast carcinoma cells, and yeast two-hybrid screen shows its interaction with several proteins. Biochem. Biophys. Res. Commun. *313*, 654–665.

Nagarkar-Jaiswal, S., Lee, P.-T., Campbell, M.E., Chen, K., Anguiano-Zarate, S., Gutierrez, M.C., Busby, T., Lin, W.-W., He, Y., Schulze, K.L., et al. (2015a). A library of MiMICs allows tagging of genes and reversible, spatial and temporal knockdown of proteins in Drosophila. eLife *4*, e05338.

Nagarkar-Jaiswal, S., DeLuca, S.Z., Lee, P.-T., Lin, W.-W., Pan, H., Zuo, Z., Lv, J., Spradling, A.C., and Bellen, H.J. (2015b). A genetic toolkit for tagging intronic MiMIC containing genes. eLife *4*, e08469.

Nakanishi, H., Santos, P. de los, and Neiman, A.M. (2004). Positive and Negative Regulation of a SNARE Protein by Control of Intracellular Localization. Mol. Biol. Cell *15*, 1802–1815.

Nance, J. (2005). PAR proteins and the establishment of cell polarity during C. elegans development. BioEssays *27*, 126–135.

Noble, M., Lewis, S.A., and Cowan, N.J. (1989). The microtubule binding domain of microtubule-associated protein MAP1B contains a repeated sequence motif unrelated to that of MAP2 and tau. J. Cell Biol. *109*, 3367–3376.

Overeem, A.W., Bryant, D.M., and IJzendoorn, S.C.D. van (2015). Mechanisms of apical–basal axis orientation and epithelial lumen positioning. Trends Cell Biol. *25*, 476–485.

Papayannopoulos, V., Co, C., Prehoda, K.E., Snapper, S., Taunton, J., and Lim, W.A. (2005). A Polybasic Motif Allows N-WASP to Act as a Sensor of PIP2 Density. Mol. Cell *17*, 181–191.

Parnas, D., Haghighi, A.P., Fetter, R.D., Kim, S.W., and Goodman, C.S. (2001). Regulation of Postsynaptic Structure and Protein Localization by the Rho-Type Guanine Nucleotide Exchange Factor dPix. Neuron *32*, 415–424.

Prehoda, K.E. (2009). Polarization of Drosophila neuroblasts during asymmetric division. Cold Spring Harb. Perspect. Biol. *1*, a001388.

Prehoda, K.E., Scott, J.A., Mullins, R.D., and Lim, W.A. (2000). Integration of multiple signals through cooperative regulation of the N-WASP-Arp2/3 complex. Science *290*, 801–806.

Pryciak, P.M., and Huntress, F.A. (1998). Membrane recruitment of the kinase cascade scaffold protein Ste5 by the Gbetagamma complex underlies activation of the yeast pheromone response pathway. Genes Dev. *12*, 2684–2697.

Rivera, M.N., Kim, W.J., Wells, J., Driscoll, D.R., Brannigan, B.W., Han, M., Kim, J.C., Feinberg, A.P., Gerald, W.L., Vargas, S.O., et al. (2007). An X chromosome gene, WTX, is commonly inactivated in Wilms tumor. Science *315*, 642–645.

Rodriguez-Boulan, E., and Macara, I.G. (2014). Organization and execution of the epithelial polarity programme. Nat. Rev. Mol. Cell Biol. *15*, 225–242.

Rohatgi, R., Ho, H.H., and Kirschner, M.W. (2000). Mechanism of N-Wasp Activation by Cdc42 and Phosphatidylinositol 4,5-Bisphosphate. J. Cell Biol. *150*, 1299–1310.

Rolls, M.M. (2003). Drosophila aPKC regulates cell polarity and cell proliferation in neuroblasts and epithelia. J. Cell Biol. *163*, 1089–1098.

van Rossum, G. (2001). The Python Programming Language (Python Software Foundation).

Sato, D., Sugimura, K., Satoh, D., and Uemura, T. (2010). Crossveinless-c, the Drosophila homolog of tumor suppressor DLC1, regulates directional elongation of dendritic branches via down-regulating Rho1 activity. Genes Cells *15*, 485–500.

Schindelin, J., Arganda-Carreras, I., Frise, E., Kaynig, V., Longair, M., Pietzsch, T., Preibisch, S., Rueden, C., Saalfeld, S., Schmid, B., et al. (2012). Fiji: an open-source platform for biological-image analysis. Nat. Methods *9*, 676–682.

Schober, M., Schaefer, M., and Knoblich, J.A. (1999). Bazooka recruits Inscuteable to orient asymmetric cell divisions in Drosophila neuroblasts. Nature *402*, 548–551.

Schultz, J., Milpetz, F., Bork, P., and Ponting, C.P. (1998). SMART, a simple modular architecture research tool: Identification of signaling domains. Proc. Natl. Acad. Sci. *95*, 5857–5864.

Serber, Z., and Ferrell, J.E. (2007). Tuning bulk electrostatics to regulate protein function. Cell *128*, 441–444.

Shen, C.-P., Knoblich, J.A., Chan, Y.-M., Jiang, M.-M., Jan, L.Y., and Jan, Y.N. (1998). Miranda as a multidomain adapter linking apically localized Inscuteable and basally localized Staufen and Prospero during asymmetric cell division inDrosophila. Genes Dev. *12*, 1837–1846.

Shi, S.-H., Jan, L.Y., and Jan, Y.-N. (2003). Hippocampal Neuronal Polarity Specified by Spatially Localized mPar3/mPar6 and PI 3-Kinase Activity. Cell *112*, 63–75.

Sievers, F., Wilm, A., Dineen, D., Gibson, T.J., Karplus, K., Li, W., Lopez, R., McWilliam, H., Remmert, M., Söding, J., et al. (2011). Fast, scalable generation of high-quality protein multiple sequence alignments using Clustal Omega. Mol. Syst. Biol. *7*, 539.

Simões, S., Denholm, B., Azevedo, D., Sotillos, S., Martin, P., Skaer, H., Hombría, J.C.-G., and Jacinto, A. (2006). Compartmentalisation of Rho regulators directs cell invagination during tissue morphogenesis. Development *133*, 4257–4267.

Skwarek, L.C., Garroni, M.K., Commisso, C., and Boulianne, G.L. (2007). Neuralized contains a phosphoinositide-binding motif required downstream of ubiquitination for delta endocytosis and notch signaling. Dev. Cell *13*, 783–795.

Smith, C.A., Lau, K.M., Rahmani, Z., Dho, S.E., Brothers, G., She, Y.M., Berry, D.M., Bonneil, E., Thibault, P., Schweisguth, F., et al. (2007). aPKC-mediated phosphorylation

regulates asymmetric membrane localization of the cell fate determinant Numb. EMBO J. *26*, 468–480.

Solecki, D.J., Model, L., Gaetz, J., Kapoor, T.M., and Hatten, M.E. (2004). Par6α signaling controls glial-guided neuronal migration. Nat. Neurosci. *7*, 1195–1203.

Sönnichsen, B., Koski, L.B., Walsh, A., Marschall, P., Neumann, B., Brehm, M., Alleaume, A.-M., Artelt, J., Bettencourt, P., Cassin, E., et al. (2005). Full-genome RNAi profiling of early embryogenesis in Caenorhabditis elegans. Nature *434*, 462–469.

Sotillos, S. (2004). DaPKC-dependent phosphorylation of Crumbs is required for epithelial cell polarity in Drosophila. J. Cell Biol. *166*, 549–557.

Sotillos, S., Aguilar, M., and Hombría, J.C.-G. (2013). Forces shaping a Hox morphogenetic gene network. Proc. Natl. Acad. Sci. *110*, 4303–4308.

Sousa-Nunes, R., Chia, W., and Somers, W.G. (2009). Protein Phosphatase 4 mediates localization of the Miranda complex during Drosophila neuroblast asymmetric divisions. Genes Dev. *23*, 359–372.

Spratford, C.M., and Kumar, J.P. (2014). Dissection and Immunostaining of Imaginal Discs from Drosophila melanogaster. JoVE J. Vis. Exp. e51792–e51792.

Stahelin, R.V., Rafter, J.D., Das, S., and Cho, W. (2003). The Molecular Basis of Differential Subcellular Localization of C2 Domains of Protein Kinase C-α and Group IVa Cytosolic Phospholipase A2. J. Biol. Chem. *278*, 12452–12460.

Standaert, M.L., Bandyopadhyay, G., Kanoh, Y., Sajan, M.P., and Farese, R.V. (2001). Insulin and PIP3 Activate PKC-ζ by Mechanisms That Are Both Dependent and Independent of Phosphorylation of Activation Loop (T410) and Autophosphorylation (T560) Sites. Biochemistry (Mosc.) *40*, 249–255.

Stein, W. von, Ramrath, A., Grimm, A., Müller-Borg, M., and Wodarz, A. (2005). Direct association of Bazooka/PAR-3 with the lipid phosphatase PTEN reveals a link between the PAR/aPKC complex and phosphoinositide signaling. Development *132*, 1675–1686.

Strand, D., Jakobs, R., Merdes, G., Neumann, B., Kalmes, A., Heid, H.W., Husmann, I., and Mechler, B.M. (1994a). The Drosophila lethal(2)giant larvae tumor suppressor protein forms homo-oligomers and is associated with nonmuscle myosin II heavy chain. J. Cell Biol. *127*, 1361–1373.

Strand, D., Raska, I., and Mechler, B.M. (1994b). The Drosophila lethal(2)giant larvae tumor suppressor protein is a component of the cytoskeleton. J. Cell Biol. *127*, 1345–1360.

Strickfaden, S.C., Winters, M.J., Ben-Ari, G., Lamson, R.E., Tyers, M., and Pryciak, P.M. (2007). A mechanism for cell-cycle regulation of MAP kinase signaling in a yeast differentiation pathway. Cell *128*, 519–531.

Stucke, V.M., Timmerman, E., Vandekerckhove, J., Gevaert, K., and Hall, A. (2007). The MAGUK protein MPP7 binds to the polarity protein hDlg1 and facilitates epithelial tight junction formation. Mol. Biol. Cell *18*, 1744–1755.

Suri, V., Qian, Z., Hall, J.C., and Rosbash, M. (1998). Evidence that the TIM light response is relevant to light-induced phase shifts in Drosophila melanogaster. Neuron *21*, 225–234.

Suzuki, A., Yamanaka, T., Hirose, T., Manabe, N., Mizuno, K., Shimizu, M., Akimoto, K., Izumi, Y., Ohnishi, T., and Ohno, S. (2001). Atypical protein kinase C is involved in the evolutionarily conserved par protein complex and plays a critical role in establishing epithelia-specific junctional structures. J. Cell Biol. *152*, 1183–1196.

Suzuki, A., Hirata, M., Kamimura, K., Maniwa, R., Yamanaka, T., Mizuno, K., Kishikawa, M., Hirose, H., Amano, Y., Izumi, N., et al. (2004). aPKC Acts Upstream of PAR-1b in Both the Establishment and Maintenance of Mammalian Epithelial Polarity. Curr. Biol. *14*, 1425–1435.

Swierczynski, S.L., and Blackshear, P.J. (1996). Myristoylation-dependent and electrostatic interactions exert independent effects on the membrane association of the myristoylated alanine-rich protein kinase C substrate protein in intact cells. J. Biol. Chem. *271*, 23424–23430.

Takahashi, S., and Pryciak, P.M. (2007). Identification of Novel Membrane-binding Domains in Multiple Yeast Cdc42 Effectors. Mol. Biol. Cell *18*, 4945–4956.

Tanneberger, K., Pfister, A.S., Brauburger, K., Schneikert, J., Hadjihannas, M.V., Kriz, V., Schulte, G., Bryja, V., and Behrens, J. (2011). Amer1/WTX couples Wnt-induced formation of PtdIns(4,5)P2 to LRP6 phosphorylation. EMBO J. *30*, 1433–1443.

Tepass, U. (2012). The Apical Polarity Protein Network in Drosophila Epithelial Cells: Regulation of Polarity, Junctions, Morphogenesis, Cell Growth, and Survival. Annu. Rev. Cell Dev. Biol. *28*, 655–685.

Thelen, M., Rosen, A., Nairn, A.C., and Aderem, A. (1991). Regulation by phosphorylation of reversible association of a myristoylated protein kinase C substrate with the plasma membrane. Nature *351*, 320–322.

Tomishige, N., Kumagai, K., Kusuda, J., Nishijima, M., and Hanada, K. (2009). Casein kinase I{gamma}2 down-regulates trafficking of ceramide in the synthesis of sphingomyelin. Mol. Biol. Cell *20*, 348–357.

Topham, M.K., Bunting, M., Zimmerman, G.A., McIntyre, T.M., Blackshear, P.J., and Prescott, S.M. (1998). Protein kinase C regulates the nuclear localization of diacylglycerol kinase-zeta. Nature *394*, 697–700.

Tripathi, V., Popescu, N.C., and Zimonjic, D.B. (2012). DLC1 Interaction with α-Catenin Stabilizes Adherens Junctions and Enhances DLC1 Antioncogenic Activity. Mol. Cell. Biol. *32*, 2145–2159.

Überall, F., Giselbrecht, S., Hellbert, K., Fresser, F., Bauer, B., Gschwendt, M., Grunicke, H.H., and Baier, G. (1997). Conventional PKC-α, Novel PKC-ϵ and PKC-θ, but Not Atypical PKC-λ Are MARCKS Kinases in Intact NIH 3T3 Fibroblasts. J. Biol. Chem. *272*, 4072–4078.

Vaccari, T., Rabouille, C., and Ephrussi, A. (2005). The Drosophila PAR-1 Spacer Domain Is Required for Lateral Membrane Association and for Polarization of Follicular Epithelial Cells. Curr. Biol. *15*, 255–261.

Vasioukhin, V. (2006). Lethal Giant Puzzle of Lgl. Dev. Neurosci. *28*, 13–24.

Venken, K.J.T., Schulze, K.L., Haelterman, N.A., Pan, H., He, Y., Evans-Holm, M., Carlson, J.W., Levis, R.W., Spradling, A.C., Hoskins, R.A., et al. (2011). MiMIC: a highly versatile transposon insertion resource for engineering Drosophila melanogaster genes. Nat. Methods *8*, 737–743.

Visco, I., Hoege, C., Hyman, A.A., and Schwille, P. (2016). In vitro Reconstitution of a Membrane Switch Mechanism for the Polarity Protein LGL. J. Mol. Biol. *428*, 4828–4842.

de Vreede, G., Schoenfeld, J.D., Windler, S.L., Morrison, H., Lu, H., and Bilder, D. (2014). The Scribble module regulates retromer-dependent endocytic trafficking during epithelial polarization. Dev. Camb. Engl. *141*, 2796–2802.

Wang, C., Shang, Y., Yu, J., and Zhang, M. (2012). Substrate recognition mechanism of atypical protein kinase Cs revealed by the structure of PKCι in complex with a substrate peptide from Par-3. Struct. Lond. Engl. 1993 *20*, 791–801.

Wang, H., Singh, S.R., Zheng, Z., Oh, S.-W., Chen, X., Edwards, K., and Hou, S.X. (2006). Rap-GEF Signaling Controls Stem Cell Anchoring to Their Niche through Regulating DE-Cadherin-Mediated Cell Adhesion in the Drosophila Testis. Dev. Cell *10*, 117–126.

Watts, J.L., Etemad-Moghadam, B., Guo, S., Boyd, L., Draper, B.W., Mello, C.C., Priess, J.R., and Kemphues, K.J. (1996). par-6, a gene involved in the establishment of asymmetry in early C. elegans embryos, mediates the asymmetric localization of PAR-3. Development *122*, 3133–3140.

Welchman, D.P., Mathies, L.D., and Ahringer, J. (2007). Similar requirements for CDC-42 and the PAR-3/PAR-6/PKC-3 complex in diverse cell types. Dev. Biol. *305*, 347–357.

Winters, M.J., Lamson, R.E., Nakanishi, H., Neiman, A.M., and Pryciak, P.M. (2005). A membrane binding domain in the ste5 scaffold synergizes with gbetagamma binding to control localization and signaling in pheromone response. Mol. Cell *20*, 21–32.

Wirtz, K.W.A. (2006). Phospholipid transfer proteins in perspective. FEBS Lett. *580*, 5436–5441.

Wirtz-Peitz, F., Nishimura, T., and Knoblich, J.A. (2008). Linking cell cycle to asymmetric division: Aurora-A phosphorylates the Par complex to regulate Numb localization. Cell *135*, 161–173.

Wodarz, A., Ramrath, A., Kuchinke, U., and Knust, E. (1999). Bazooka provides an apical cue for Inscuteable localization in Drosophila neuroblasts. Nature *402*, 544–547.

Wodarz, A., Ramrath, A., Grimm, A., and Knust, E. (2000). Drosophila Atypical Protein Kinase C Associates with Bazooka and Controls Polarity of Epithelia and Neuroblasts. J. Cell Biol. *150*, 1361–1374.

Woods, D.F., Hough, C., Peel, D., Callaini, G., and Bryant, P.J. (1996). Dlg protein is required for junction structure, cell polarity, and proliferation control in Drosophila epithelia. J. Cell Biol. *134*, 1469–1482.

Xie, X., Gong, Z., Mansuy-Aubert, V., Zhou, Q.L., Tatulian, S.A., Sehrt, D., Gnad, F., Brill, L.M., Motamedchaboki, K., Chen, Y., et al. (2011). C2 Domain-Containing Phosphoprotein CDP138 Regulates GLUT4 Insertion into the Plasma Membrane. Cell Metab. *14*, 378–389.

Xu, S., Li, X., Gong, Z., Wang, W., Li, Y., Nair, B.C., Piao, H., Yang, K., Wu, G., and Chen, J. (2014). Proteomic Analysis of the Human Cyclin-dependent Kinase Family Reveals a Novel CDK5 Complex Involved in Cell Growth and Migration. Mol. Cell. Proteomics *13*, 2986–3000.

Yuan, B.-Z., Miller, M.J., Keck, C.L., Zimonjic, D.B., Thorgeirsson, S.S., and Popescu, N.C. (1998). Cloning, Characterization, and Chromosomal Localization of a Gene Frequently Deleted in Human Liver Cancer (DLC-1) Homologous to Rat RhoGAP. Cancer Res. *58*, 2196–2199.

Zhang, H., and Macara, I.G. (2006). The polarity protein PAR-3 and TIAM1 cooperate in dendritic spine morphogenesis. Nat. Cell Biol. *8*, 227–237.

Zhang, F., Huang, Z.-X., Bao, H., Cong, F., Wang, H., Chai, P.C., Xi, Y., Ge, W., Somers, W.G., Yang, Y., et al. (2015). Phosphotyrosyl phosphatase activator facilitates Miranda localization through dephosphorylation in dividing neuroblasts. Development dev.127233.

Zhang, L., Wu, S.L., and Rubin, C.S. (2001a). A novel adapter protein employs a phosphotyrosine binding domain and exceptionally basic N-terminal domains to capture and localize an atypical protein kinase C: characterization of Caenorhabditis elegans C kinase adapter 1, a protein that avidly binds protein kinase C3. J. Biol. Chem. *276*, 10463–10475.

Zhang, L., Wu, S.L., and Rubin, C.S. (2001b). Structural properties and mechanisms that govern association of C kinase adapter 1 with protein kinase C3 and the cell periphery. J. Biol. Chem. *276*, 10476–10484.

(2003). Cell Polarity and the Cytoskeleton in the Caenorhabditis Elegans Zygote. Annu. Rev. Genet. *37*, 221–249.